NANYANG TECHNOLOGICAL UNIVERSITY

FREQUENCY DOMAIN SIGNAL PROCESSING FOR MULTI-CARRIER MODULATION SYSTEMS

YAN YANXIN

SCHOOL OF ELECTRICAL AND ELECTRONIC ENGINEERING

2015

FREQUENCY DOMAIN SIGNAL PROCESSING FOR MULTI-CARRIER MODULATION SYSTEMS

YAN YANXIN

YAN YANXIN

SCHOOL OF ELECTRICAL AND ELECTRONIC ENGINEERING

A thesis submitted to the Nanyang Technological University
in fulfillment of the requirements for the degree of
Doctor of Philosophy

2015

Acknowledgement

Foremost, I hereby would like to express my deepest sense of gratitude to my advisor, Professor Ma Maode for being my mentor in all respects of education and research. His guidance and support enable me to step into the final stage of pursuing my Ph. D.

I wish to sincerely thank Prof. Gong Yi, for he guided my first step as a Ph. D student and gave me the inspiration during my research work. I wish to thank Dr. Shi Qinghua for the fruitful discussions during my study.

My thanks also extend to Mr. Li Jun for his great support and advice during my work in ROHM Shanghai Design Centre.

Last but not least, I would like to thank my parents and parents-in-law, my wife Hu Xia and my daughter Yan Shijing, my brother and my sisters for their unconditional love and support during the long journey of my Ph. D study.

Table of Contents

Summary

Orthogonal frequency division multiplexing (OFDM) has become a popular technique in wireless and cable transmissions for its robustness against multipath delay spread at high data rate and efficient spectrum utilization. Basically there are two types of OFDM modulations classified by the guard interval between OFDM symbols: cyclic prefix (CP) OFDM and zero padded (ZP) OFDM. CP OFDM has been adopted widely in various communication systems such as digital audio broadcasting (DAB), digital video broadcasting (DVB), IEEE802.11a/g/n, IEEE802.16d/e/m (WiMAX) and Long Term Evolution (LTE) because of its simple implementation. Some literature have demonstrated that the ZP OFDM and CP OFDM can offer similar BER performance if ZP OFDM adopts the traditional overlap-add (OLA) method for receiving. In this case, ZP OFDM will not guarantee that the symbol can be recovered from subchannels with power of zero. Both ZP and CP OFDM systems are sensitive to inter-symbol interference (ISI) and inter-carrier interference (ICI).

Based on OFDM, multi-carrier code division multiple access (CDMA) was proposed inherit the merits of OFDM and CDMA by combining the direct sequence (DS) CDMA and OFDM. The difference between MC-CDMA and OFDM is that MC-CDMA applies DS spreading in frequency domain and transmits a data symbol over all subcarriers; while OFDM directly transmits one data symbol to one subcarrier without spreading. The spreading sequence in MC-CDMA provides multiple access capability, and hence improves the performance at the high signal-to-noise ratio (SNR) level. In substance, MC-CDMA is a type of OFDM system, and is also sensitive to the ISI and ICI.

Firstly this thesis focuses on multi-carrier modulation (MCM) systems such as OFDM system and MC-CDMA system, and proposes the frequency domain oversampling (FDO) technique together with minimum mean square error (MMSE) equalizer to improve the bit error rate (BER)

performance for ZP and CP MCM systems in multiple interference environment including ISI and ICI. In addition, the BER performance of the proposed FDO-based equalizers in CP and ZP based MCM systems are compared.

For ZP OFDM and ZP MC-CDMA systems, the FDO MMSE equalizer oversamples the received signal including the guard interval in frequency domain, which enables the MMSE equalizer to more efficiently exploit channel state information in the high dimensional space and greatly suppress the interference, hence to improve the BER performance over the frequency selective channel. To reduce the complexity of implementation, the FDO diagonal MMSE (FDO-DMMSE) equalizer, the FDO noise fixed DMMSE (FDO-NF) equalizer and the zero-forcing (FDO-ZF) equalizer are derived from the complex FDO MMSE equalizer. These three equalizers do not require the calculation of matrix inverse, hence significantly reduce the complexity. For the channel with long path delay, the ISI from the adjacent symbols will greatly degrade the receiving performance. The symbol reconstruction (SR) method is proposed to form the reconstructed OFDM symbol in order to minimize the ISI based on the initial equalization result. The FDO based equalizers are applied to the reconstructed OFDM symbols to obtain more accurate result. Then additional iterations including SR and FDO based equalizer can be performed to further improve the BER performance. This type of iterative FDO based receiving can be adopted to combat the large ISI and ICI caused by severe multipath, carrier frequency offset and Doppler frequency shift.

For CP OFDM and CP MC-CDMA systems, because the two received adjacent symbols are overlapped in the guard interval, the FDO based equalizers cannot be directly used. However, it is possible to take advantage of the SR method to reconstruct the OFDM symbol to reduce the ISI that caused by the overlapping. Hence, the iterative FDO based receivers can be adopted to combat the large ISI and ICI caused by severe multipath, carrier frequency offset and Doppler frequency shift. In addition, the FDO-MMSE equalizer in CP MCM systems can take advantage of the CP part to improve the BER performance. The simulations show that the proposed iterative FDO based receivers can offer much better BER performance than the conventional zero forcing

(ZF) receiver.

Secondly, the energy detection (ED) algorithm in OFDM systems is studied in the thesis. In the cognitive radio (CR) networks, the OFDM system shall be able to detect the primary user (PU) signals that occupy the same frequency range. ED is a popular spectrum sensing method because of its low implementation complexity and robustness to the unknown fading channel and unknown primary signal. For the OFDM based systems, the narrow-band PU signal is difficult to detect when it straddles the boundaries of two adjacent subcarriers. The thesis analyzes the effect of discrete Fourier transform (DFT) size on detecting narrow-band signals in OFDM systems, and suggests using the large DFT size to improve the probability of detection in frequency domain. However, in some cases, it is difficult to increase the DFT size. The thesis further proposes a novel ED algorithm with noise smoothing method to improve the probability of detection for the OFDM system with fixed DFT size and without increasing the number of DFTs. In the case of the primary signal with roughly known frequency, the digital down-converter is applied to shift the primary signal to zero frequency first and followed by noise smoothing that can be implemented by multiple complex adders. The effect of noise smoothing of the proposed ED method is analyzed. The SNR gains obtained for different subcarriers are different. The close-form solution of probability of detection for OFDM system under quasi-static multipath channel is derived and verified by simulations.

Finally, we conclude our research work and list some potential research points in the future at the end of this thesis.

Table of Figures

List of Abbreviations

AI-BER	Average Instantaneous Bit Error Rate
BER	Bit Error Rate
CDMA	Code Division Multiple Access
CE	Controlled Equalization
CFO	Carrier Frequency Offset
CP	Cyclic Prefix
CR	Cognitive Radio
CSD	Cyclo-Stationary Detection
CU	Cognitive User
DAB	Digital Audio Broadcasting
DMMSE	Diagonal Minimum Mean Square Error
DS	Direct Sequence
DVB-T	Digital Video Broadcasting – Terrestrial
ED	Energy Detection
EGC	Equal Gain Combining
FDE	Frequency Domain Equalizer
FDO	Frequency Domain Oversampling
FDO-DMMSE	FDO based diagonal MMSE equalizer
FDO-MMSE	FDO based Minimum Mean Square Error equalizer
FDO-NF	FDO based Noise Fixed DMMSE equalizer
FDO-ZF	FDO based zero forcing equalizer
FFT	Fast Fourier Transform
FIR	Finite Impulse Response

FS	Fractional Sampling
FSFD	Fractional Spaced Frequency Domain
ICI	Inter-Carrier Interference
IFFT	Inverse Fast Fourier Transform
ISI	Inter-Symbol Interference
IUI	Inter-User Interference
LAN	Local Area Network
LRT	Likelihood Ratio Test
MAI	Multiple Access Interference
MC-CDMA	Multi-Carrier Code Division Multiple Access
MCM	Multi-Carrier Modulation
MF	Matched Filter
MMSE	Minimum Mean Square Error
MRC	Maximum Ratio Combining
MSE	Mean Squared Error
MUD	Multi-User Detection
NF	Noise Fixed
NS	Noise Smoothing
OFDM	Orthogonal Frequency Division Multiplexing
OLA	Overlap-Add
OSF	Oversampling Factor
PAPR	Peak-to-Average Power Ratio
PC	Partial Combining
PD	Probability of Detection
PU	Primary User

SNR	Signal-to-Noise Ratio
SR	Symbol Reconstruction
UWB	Ultra Wideband
WiMAX	Worldwide Interoperability for Microwave Access
WSSUS	Wide-Sense Stationary Uncorrelated Scattering
ZF	Zero Forcing
ZP	Zero Padding

Notation

Generally, the boldface uppercase letters denote matrices and the boldface lower-case letters denote vectors, and italics denote scalars.

$\mathbf{X}^{T}$	Transportation of matrix **X**.
$\mathbf{X}^{H}$	Conjugate transpose of matrix **X**.
$\otimes$	Convolutional operation.
E(X)	Expectation of random variable X.
$(\mathbf{X})^{+}$	Moore-Penrose pseudo-inverse of matrix **X.**
diag{**x**}	The diagonal matrix with the vector **x** on the diagonal.

1 Introduction

Cognitive Radio (CR) was initially introduced in [1] to exploit the unused spectrum and coexist with other wireless services. Traditional fixed spectrum allocation scheme is not suitable for current growing wireless applications. Some wireless applications are operated on specific spectrum band, but they may not be active all time or may not fully use the allocated spectrum. To fully utilize the spectrum, it is a basic requirement that the cognitive user (CU) or secondary user (SU) shall perform spectrum sensing frequently to detect the presence of the primary user (PU) over the specific spectrum. The CU can be active when the PU is not active or the CU can work in the reduced spectrum by excluding the spectrum of PU. This kind of spectrum management requires that the CU is able to select the modulation scheme according to the spectrum sensing result to dynamically adjust the spectrum. With multi-carriers modulation (MCM) transmission and the use of fast Fourier transform (FFT), Orthogonal Frequency Division Multiplexing (OFDM) based modulator such as multi-carrier code-division multiple access (MC-CDMA) is a nature choice for CR systems [2].

OFDM has become a popular technique for wireless transmission and been accepted for various wireless standards such as digital audio broadcast (DAB), digital video broadcast (DVB), IEEE802.11a/g/n, wireless local area network (WLAN), IEEE802.16d/e/m (WiMAX) and Long Term Evolution (LTE) for its robustness against multipath delay spread at high data rate.

OFDM is a type of MCM system which transmits the high data rate signals on a number of subcarriers with low data rate at different frequencies simultaneously. The subcarriers are made orthogonal to each other so that they can be demodulated without any inter-channel or inter-carrier interference (ICI). OFDM systems can be implemented easily in the discrete time by using an inverse discrete Fourier transform (IDFT) to act as a modulator in transmitter side and a discrete Fourier transform (DFT) as a demodulator in receiver side. The transmitted data are distributed over subcarriers in frequency domain and the samples at the output of IDFT are transmitted actually in time domain. The main advantage of OFDM system is its high spectral

efficiency due to the closely packed and overlapped orthogonal subcarriers. Another advantage of OFDM system is that it converts a frequency selective channel into a number of independent flat-faded subchannels which can be individually modulated [3]. In this case, the easily-implemented frequency domain equalizer (FDE) for individual sub-carrier can be used after DFT. Generally, the DFT can be implemented by the FFT, which reduce the computations of the DFT significantly.

The disadvantage of OFDM is that it is sensitive to timing and frequency synchronization errors, which will cause inter-symbol interference (ISI) between the adjacent OFDM symbols and ICI due to loss of orthogonality among the frequency subcarriers. ISI can be greatly reduced by inserting guard interval between the OFDM symbols. If the length of guard interval is larger than the multipath delay spread, ISI can be fully eliminated. Basically there are two types of OFDM classified by the guard interval: one is cyclic prefix (CP) OFDM and the other is zero padded (ZP) OFDM. The advantages of CP OFDM are that CP OFDM can naturally keep the orthogonality of the subcarriers and the implementation of the zero forcing (ZF) equalizer in frequency domain is quite easier, which can provide the same BER performance as the conventional MMSE equalizer. The disadvantage is that the CP OFDM with ZF or MMSE equalizer cannot guarantee the symbol recovery if the power of the subchannel is nearly zero. By contrast, the merits of ZP OFDM system are lower transmission power and guaranteed symbol recovery even there are subchannels with power of zero [4]-[6]. Hence, the BER performance can be improved by using ZP OFDM. However, the disadvantage is that, to benefit from the merit of guaranteed symbol recovery, the complex equalizer is required for the ZP OFDM system.

Based on OFDM, Multi-carrier CDMA (MC-CDMA) was proposed by [7] and [8] in 1993 at first and then studied by many papers. It inherits the merits of OFDM and CDMA by combining DS CDMA and OFDM, and becomes one of the candidate technologies for 4^{th} generation wireless communication systems [9]. The difference between MC-CDMA and OFDM is that MC-CDMA applies DS spreading in the frequency domain and transmits a data symbol over multiple subcarriers; while OFDM directly transmits one data symbol on one subcarrier without spreading. The spreading sequence in MC-CDMA provides multiple access capability, and hence improves the performance at the high signal-to-noise ratio (SNR) level. In MC-CDMA system, the data

symbols from different users are first multiplied by the different *N*-chip spreading code to get the *N*-chip spread data. The *N*-chip spread data of different users are added together and then mapped to *N* subcarriers. In receiver, the demodulated data on each subcarrier are de-spread by multiplying the spreading code of each user.

However, since MC-CDMA system is based on the OFDM technology, it has the same disadvantages as OFDM system. It is also sensitive to the ISI and ICI interference caused by the timing and frequency errors. In addition, it suffers from inter-user interference (IUI) due to the power difference of the different users. The heavy multiple interference such as ISI, ICI and IUI will greatly degrade the performance of MC-CDMA system. Hence, it is quite necessary to design the high performance receivers for OFDM and MC-CDMA system that can tolerate the large combined interference.

Although MCM is extensively adopted in various wireless communication standards due to the excellent spectral efficiency and low implementation complexity, in recent years, single-carrier modulation (SCM) has become another interesting research field. The comparison between the SCM and the MCM has been discussed in an extensive literature, which shows the two modulations have similar performance if the SCM adopts a nonlinear frequency domain equalizer. Compared with the above MCM systems, the SCM system has the advantages of low peak-to-average power ratio (PAPR) and robustness to frequency offset and phase noise. However, the disadvantages are complex equalization required for a comparable performance with the MCM systems and sensitive to a highly frequency selective multipath channel. Therefore, the SCM scheme can serve as a complement to the MCM scheme, but not a potential replacement of it [10]. Although the MCM encounters the high PAPR issue, there are many different methods that can be adopted to reduce the PAPR [11]. In this thesis, we focus on the MCM systems. There are three advantages of using complicated multi-carrier system. Firstly, the multi-carrier modulation is suitable for the cognitive radio network because it can dynamically mask some frequency bands for other services. Secondly, with our proposed equalizers, the BER performance can be further improved. Thirdly, the implementation of our proposed FDO-DMMSE and FDO-ZF equalizers is just slight complex than that of the conventional OFDM receiver. It only needs more FFTs, which

is affordable in many systems.

1.1 Motivation

The motivation of this project is to find a method in frequency domain to combat the large combined interference including frequency-selective multipath fading, carrier frequency offset and Doppler frequency shift for a MCM based system such as OFDM and MC-CDMA. The other motivation is to increase the probability to detect other wireless services in the OFDM systems so that the PU and the CU cannot interfere with each other in the cognitive radio networks.

The major problem in the OFDM based system is the combined interference caused by frequency-selective multipath fading channel, carrier frequency offset, and Doppler frequency shift. MC-CDMA is actually an OFDM based system and thus also highly sensitive to timing and frequency synchronization errors between the transmitter and the receiver. There is an extensive literature that attempt to overcome this problem by proposing many algorithms to estimate the timing and frequency error in an OFDM based receiver, which actually can greatly reduce the ISI and ICI. However, the frequency offset estimation method may not get accurate result over multipath fading channel. The frequency offset cannot be eliminated completely. The residual frequency offset and Doppler frequency shift after compensation may greatly decrease the BER performance. In addition, it is inevitable to encounter Doppler frequency shift for moving device, which will greatly affect the BER performance of the OFDM based system, because Doppler frequency shift is difficult to be eliminated completely. Thus, in the combined large multiple interference environment, the OFDM based system will not obtain the performance as good as expected. There is a high demand to design a receiver for the OFDM based system that can tolerate large combined interference.

In addition, to fully utilize the spectrum, the OFDM system is required to perform spectrum sensing frequently to detect the presence of the PU signal over the specific spectrum. In some radio networks, the cognitive user may have wide bandwidth, but the primary user is narrow-band signal. For example, the subcarrier space of Ultra-Wideband (UWB) system is 4.125 MHz specified in WiMedia standard. The WiMAX device may have the small bandwidth as 1.25 MHZ.

It's very hard for UWB device to detect such narrow-band signals transmitted by WiMAX device if the signals are happen to be located between two subcarriers of a UWB system. In such case, the probability of detection will be greatly reduced. The CU and PU may interfere with each other. However, detecting narrow-band signals is one of the practical difficulties in implementation of spectrum cognition without increasing the implementation complexity. Hence, it is quite meaningful to improve the probability of detection for narrow-band signals in the OFDM based system.

1.2 Objective

The overall objectives of this research are to develop the FDO based MMSE equalizers in OFDM and MC-CDMA systems to combat the heavy multiple interference. The conventional equalizer directly converts the received OFDM or MC-CDMA signals to frequency domain with the subcarriers that are the same as that for data transmitting. This kind of equalizer keeps the orthogonality of the subcarriers and is easily implemented in the receiver. However, if some subcarriers have very low power (nearly zero) due to the deep fading of the subchannels, the data symbols may not be fully recovered. In this case, the BER performance may be degraded to some extent. Our motivation comes from that if the received OFDM signal is oversampled in high dimension frequency domain, even there are some subchannels with power of zero in this frequency domain, it is still possible to recover the data in normal frequency domain with data subcarriers by taking advantage of MMSE method. To reduce the complexity of implementation, we also design the complexity-reduced FDO based receivers for the practical applications based on our proposed FDO-MMSE receiver.

Moreover, the other objective is to propose a novel energy detection (ED) method for narrow-band signal in OFDM systems by using noise smoothing method to improve the SNR of the processed signal and hence to improve the probability of detection for narrow-band PU signal over multipath fading channel.

1.3 Summary of Contributions

The main contributions of the thesis are the FDO based receivers that we proposed for the

OFDM based systems and the improved energy detection method for narrow-band signals in the OFDM systems.

From our investigation, the FDO based MMSE equalizer is only studied for ZP OFDM in some literature. In Chapter 3, we propose the FDO-MMSE equalizer for the both ZP OFDM and ZP MC-CDMA systems. The proposed FDO-MMSE equalizer can achieve much better BER performance than the conventional MMSE/ZF equalizer. However, it is quite difficult to implement. To reduce the complexity of implementation, we propose novel FDO-DMMSE, FDO-NF and FDO-ZF equalizers, which do not require the calculation of matrix inverse. The FDO-DMMSE and FDO-NF equalizers just slightly reduce the BER performance improvement compared with the FDO-MMSE equalizer. However, the BER performance of FDO-ZF equalizer is not as good as that of the above FDO based equalizers even it is better than that of the conventional equalizer. Hence, we propose a method to further improve the BER performance of FDO-ZF equalizer by increasing the oversampling rate. In addition, the expression of solution for the BER performance of FDO based equalizer is developed. For the case that the guard interval is insufficient to avoid ISI, we propose the novel iterative FDO based receivers that combine the SR method and FDO based equalizers.

In Chapter 4, we extend our proposed iterative FDO based receivers (IT-FDO-MMSE, IT-FDO-DMMSE, IT-FDO-NF and IT-FDO-ZF) to CP OFDM and CP MC-CDMA systems, which never occur in other literature. The SR method is proposed for the iterative FDO based receivers to reduce the ISI from the adjacent OFDM symbols. It is the first time for combining the OFDM symbol reconstruction (SR) and FDO method for CP OFDM and CP MC-CDMA systems, which enables the MMSE equalizer to exploit more efficiently the received signal and the channel state information in the high dimensional space and greatly suppress the interference.

In the cognitive radio systems, it is very important to detect the narrow-band PU signal in OFDM systems. The conventional energy detection method is robust and easy to implement. However, it has difficulty to detect the narrow-band signal that is not exactly on the subcarriers of the OFDM systems, and the probability of detection greatly decreases in low SNR level. Hence, we propose increasing the DFT size to improve the probability of detection of the energy

detection. In the case that the DFT size cannot be changed, we propose the noise smoothing method for energy method to achieve high SNR gain compared with the conventional ED under the quasi-static multipath channel. The close-form solution of the probability of detection for our proposed noise smoothing ED is developed and verified by simulations.

In Summary, the main achievements in this dissertation are listed as follows:

- The FDO-MMSE based equalizers for ZP MC-CDMA, CP OFDM and CP MC-CDMA based systems are proposed.
- The easily implemented FDO-DMMSE, FDO-NF and FDO-ZF equalizers for ZP and CP MCM based systems are proposed.
- The iterative FDO based equalizers for ZP OFDM and ZP MC-CDMA systems are proposed when the guard interval is insufficient to avoid ISI.
- The SR method together with the FDO based equalizers are proposed for CP OFDM and CP MC-CDMA systems.
- The expression of solution of BER performance for the FDO based equalizers is developed.
- The effect of the DFT size on the probability of detection of energy detection is analyzed.
- The noise smoothing method to improve the probability of detection of energy detection is proposed for narrow-band PU signals on quasi-static multipath channel.
- The close-form solution of the probability of detection for the improved energy detection with noise smoothing method is derived and verified.

1.4 Thesis Organisation

In general terms, the focus of this dissertation is on the FDO based receivers and the energy detection of narrow-band PU signal in the OFDM based systems. The outline of each chapter is listed as follows.

Chapter 1, the present chapter, gives the motivation, objective, outline, and contributions of this dissertation.

Chapter 2 reviews the existing literature on conventional receivers for OFDM and MC-CDMA

systems, the FDO method and the energy detection method for spectrum sensing.

Chapter 3 considers ZP OFDM and ZP MC-CDMA systems, and proposes the FDO based equalizers including FDO-MMSE, FDO-DMMSE, FDO-NF and FDO-ZF equalizers, and provides the expression of solution for BER calculation of the proposed FDO based equalizers. The effect of the path delay length is analyzed. When the path delay is longer than the guard interval, the BER performance is degraded by the ISI from the adjacent OFDM symbols. This chapter proposes the SR method to reduce the effect of ISI, and the iterative FDO based receiver to improve the system BER performance. The simulations are performed to verify the BER performance of the proposed FDO based receivers and show that the proposed FDO based receivers can offer much better BER performance than the conventional ZF/MMSE receiver in ZP OFDM and ZP MC-CDMA systems. In addition, this chapter compares the BER performance of the proposed FDO based equalizer between ZP OFDM and ZP MC-CDMA systems.

Chapter 4 proposes the iterative FDO based receivers including IT-FDO-MMSE, IT-FDO-DMMSE, IT-FDO-NF and IT-FDO ZF equalizers for CP OFDM and CP MC-CDMA systems and develops the expression of solution for BER calculation. As far as we know, the FDO based equalizers are never adopted for CP OFDM systems because of the ISI. Therefore, it is the first time that the thesis proposes the FDO based receivers together with the SR method for CP OFDM systems. In addition, this chapter compares the BER performance of the proposed FDO equalizers between CP OFDM and ZP OFDM system. It also compares the BER performance of the proposed FDO equalizers between CP OFDM and CP MC-CDMA, and the BER performance between ZP MC-CDMA and CP MC-CDMA system.

Chapter 5 focuses on the energy detection of narrow-band PU signal in OFDM system under multipath fading channel. The effect of DFT size on detecting narrow-band signals in OFDM systems is analyzed, and large DFT size is proposed to improve the probability of detection. In the case that the DFT size cannot be changed, a novel spectrum sensing scheme with noise smoothing technique is proposed to improve the probability of detection without increasing the complexity of implementation. Simulations are performed to verify the proposed schemes.

Chapter 6 summarizes the results of the thesis and presents the future research fields.

2 Literature Survey

The OFDM technique is a method of digital modulation in which a data stream is split and transmitted in parallel by a number of narrow-band channels at different frequencies. There are two types of OFDM techniques classified by the guard interval. One is CP OFDM and the other is ZP OFDM. It has been shown that CP OFDM and ZP OFDM can offer similar BER performance by using conventional equalizer [5].

The MC-CDMA technique is a promising technology because it incorporates the benefits of OFDM and DS-CDMA ([7]-[9]). The authors in [12] indicate that the MC-CDMA system can achieve much better BER performance than the OFDM system as the spreading factor is more than or equal to 8. In [13], the authors have compared the BER performance of the DS-CDMA and MC-CDMA techniques at various modulation levels, and have shown that DS-CDMA and MC-CDMA with full spreading factor and MMSE equalizer have a similar performance as the uncoded systems. However, compared with turbo coded systems, MC-CDMA with smaller spread factor can provide a better performance because it can benefit from the better frequency interleaving that leads to the larger coding gain. Compared to a DS-CDMA system using Rake receiver, MC-CDMA system with maximum likelihood detection and equal gain combining (EGC) equalizer can offer better BER performance [14], [15].

Since MC-CDMA system is actually a type of OFDM system, it has the same disadvantages as OFDM system. Both OFDM and MC-CDMA systems are sensitive to the ISI and ICI interference caused by the timing error, frequency offset and Doppler frequency shift. The heavy multiple interference may greatly degrade the performance of OFDM and MC-CDMA systems. To reduce the effect of timing and frequency error, there are many algorithms proposed to estimate the timing position and frequency offset. For example, [14] presents a joint timing and frequency estimation technique to find the accurate timing position of a frame and large carrier frequency offset at low SNR for slow fading environment, which can also be used for MC-CDMA system. However, the frequency offset cannot be eliminated completely. The residual frequency offset

after compensation may still greatly decrease the BER performance. Hence, it is very important to design high performance equalizers for OFDM and MC-CDMA systems so that they can tolerate large interference. In this chapter, we firstly review the existing literature that introduces equalizers for OFDM and MC-CDMA systems. Then, we review the literature that uses the oversampling technique in frequency-domain, which are different from our proposed FDO method for the design of equalizers in OFDM systems. Finally, we review the spectrum sensing methods that have been studied in the existing literature.

2.1 Equalizers for OFDM Based System

OFDM system transmits the data stream over multiple orthogonal subcarriers, which enables the equalization with low complexity in frequency domain for multipath fading channel [17]. There are numerous literature that have studied the OFDM receiver ([5], [17]-[19],). Although the MMSE receiver can minimize the output error and improve the system performance for most systems, it does not improve the BER performance of a traditional CP OFDM receiver. For CP OFDM system, the CP part is usually removed to avoid ISI. The OFDM symbol without CP can keep it's orthogonality of subcarriers in frequency domain. Thus, the traditional optimal MMSE receiver of CP OFDM can be reduced to a number of scalar MMSE receivers, and the scalar MMSE receiver does not improve the error rate performance ([18] Chapter 6, [19]) compared with the zero-forcing (ZF) receiver. Hence, the most CP OFDM systems adopt the more practical ZF receiver.

Although an additional CP part is transmitted in CP OFDM, it is always removed to eliminate ISI before channel estimation and equalization. The data of CP is not fully utilized. Therefore, the performance of CP OFDM cannot offer better BER performance than that of ZP OFDM with FDO technique. In [20] and [21], the CP reconstruction is employed to restore the cyclicity of the received symbol for multipath channel with large delay (i.e., larger than CP length). The received CP is removed and the virtual CP is reconstructed to remove the ISI after the transmitted symbols are estimated. These methods improve the BER performance by minimizing the ISI. If there is no ISI, the BER performance will not be improved.

In the traditional ZP OFDM receivers, because of the less complexity of implementation, the OLA method is adopted by adding the guard interval to the beginning part of the OFDM symbol in time domain before DFT. In this case, the ZP OFDM with OLA is equivalent to the traditional CP OFDM. The conventional MMSE equalizer is equivalent to the ZF equalizer, and can be reduced to multiple scalar equalizers for each subcarrier [19]. Although the implementation is quite simple, the receiver cannot guarantee that the symbol can be recovered once the channel frequency responses of some subcarriers are close to zero. Hence, the ZP OFDM with OLA receiver is similar to the CP OFDM with ZF receiver and is still sensitive to frequency offset and Doppler frequency shift.

The MC-CDMA technique is a promising technology because it incorporates the benefits of OFDM and DS-CDMA ([8], [9], [22]). In [13], the authors have compared the BER performance of the DS-CDMA and MC-CDMA techniques at various modulation levels, and have shown that the DS-CDMA and MC-CDMA with full spreading factor have a similar performance in the uncoded systems. However, with turbo coding, MC-CDMA with smaller spread factor can provide better performance than DS-CDMA because it can benefit from the better frequency interleaving that leads to larger coding gain.

There are several kinds of combining equalizer that can be used for MC-CDMA system: MMSE combining, equal gain combining (EGC), maximum ratio combining (MRC), controlled equalization (CE), orthogonal restoring combining (ORC) and partial combining (PC) [10], [22]-[25]. EGC technique keeps the orthogonality of the spreading code in MC-CDMA system and consequently can offer good performance in the downlink for a large number of users, which is effective in combating interference in the downlink. MRC weights the received signal with the attenuation of each fading channel and corrects the phase shift of the fading channel. Hence, it can perform better than EGC in the uplink where each user has different channel, and in the downlink with small number of users. Controlled equalization attempts to restore the orthogonality between users. Only when the subchannel attenuation is above a certain threshold, it will be equalized with ZF method (i.e., channel inverse); otherwise, only phase equalization is applied. ORC is actually ZF equalization, which amplifies the noise when SNR is low. PC technique is actually a

combination of EGC, MRC and ORC, where the equalization coefficient depends on a parameter. With different value of this parameter, PC equalizer can be simplified to EGC, MRC or ORC equalizers. The optimization of this parameter requires the estimation of SNR, which cause the complexity of implementation.

Among these combining techniques, the MMSE combining has been demonstrated to have the best BER performance [23]. Hence, in this thesis, we will combine it with the frequency domain oversampling technique to more efficiently exploit the received signal and the channel information for better BER performance.

2.2 Oversampling Techniques for OFDM Based System

There has been some literature that use oversampling in the frequency domain for OFDM. In [26], FDO technique is used to reduce the computational complexity and processing time of inverse FFT (IFFT) for the OFDM wireless local area network transmitters. In [27], an FDO-based receiver is proposed to suppress multiple access interference induced by Doppler frequency shifts and frequency offset for the uplink of MC-CDMA systems, where it oversamples the received signal at the factor of an integer M, and then groups all the samples in M groups to simplify the linear MMSE equalizer. The works in [5] and [28] introduce fractionally spaced frequency-domain (FSFD) MMSE equalization by taking advantage of the whole OFDM symbol including the guard interval for ZP OFDM. However, the proposed MMSE equalizers are quite complex and difficult to implement and can only be used in ZP OFDM system. In [29] and [30], the authors exploit the FDO method for ZP OFDM in underwater acoustic communications. They assume that at least two null subcarriers shall be inserted between the data subcarriers and the pilot subcarriers in [29], and propose the FDO based MMSE and ZF receiver to improve system performance over underwater acoustic channel with large Doppler frequency shifts. In [30] they combine the FDO method and interference subtraction to cancel the inter-block interference caused by asynchronous multiuser transmissions.

The time-domain fractional sampling (FS) method has been studied in many papers ([31] and

[32]), it is quite different from frequency domain oversampling. The comparison of FS and FDO is discussed in [28] and shows that the FDO-MMSE for ZP OFDM can offer better performance. The authors in [33] propose to use oversampling technique in frequency domain to obtain higher frequency components than the useful frequencies for data and remove the unwanted high frequency part to reduce the noise. Hence, the system BER performance can be improved. However, the improvement is quite limited by using this method if the low pass filter has narrow transition band. In [34], the oversampling technique is adopted to calculate the bound for the peak of the continuous envelope of the OFDM signals. It has been shown that the continuous envelop can be tightly bounded by its oversampled sequence with oversampling rate increasing. The authors in [35] propose the oversampling method in time domain to estimate the carrier frequency offset in the OFDM system without pilot symbols. This method explores that the intrinsic phase among the neighboring samples is common among all subcarriers. The authors in [36] study the orthogonality between signal and noise subspaces and develop a subspace based blind estimation method by using frequency domain oversampling, which can be formulated as a minimum eigenvector problem.

From our investigation, we can find that the oversampling technique is used in OFDM system for various purposes, however, the frequency domain oversampling based equalizer is only studied for ZP OFDM and it is difficult to implement due to high complexity.

2.3 Energy Detection in OFDM System

CR was initially introduced in [1] to exploit the unused spectrum and coexist with other wireless services. Traditional fixed spectrum allocation scheme is not suitable for current rapidly growing wireless applications. Some wireless applications are operated in licensed spectrum bands, but they may not be active all time or may not fully use the allocated spectrum. To fully utilize the spectrum, it is a basic requirement that the CU or secondary user shall perform spectrum sensing frequently to detect the presence of the PU over the licensed spectrum. The CU can be active when the PU is inactive or the CU can avoid harmful interference to the PU. In the

case of wideband CU signals and narrowband PU signals, the CU can work in a reduced spectrum by excluding the spectrum of the PU signals after identifying or detecting the PU signals.

Based on the assumptions made to the PU signal, many spectrum sensing methods have been proposed. Among them, matched filter (MF) for known PU signals and likelihood ratio test (LRT) for PU signals with known distribution have demonstrated good performance [37]. Cyclo-stationary detection (CSD) takes advantage of the known cyclic frequency of the primary signal to improve the probability of detection (PD) [38], [39]. Energy detection (ED) is a popular spectrum sensing method for the detection of unknown primary signals over fading channels ([40]-[45]). However, the PD of ED is greatly reduced when SNR is becoming low. The work in [46] modifies the traditional ED method by updating the test statistic dynamically to avoid the effect of instantaneous signal power drop. But the performance improvement is quite limited. The author in [47] proposes a novel spectrum sensing method to improve the SNR of a received signal by using stochastic resonance technique. A kind of discrete overdamped bistable oscillator process is adopted to amplify the SNR. However, it can only detect the signal in time domain without the ability to distinguish which subcarrier is occupied by the PU signals in the OFDM systems. The practical difficulties to implement ED, such as the detection of narrow-band PU signals for multi-carrier based CR systems, are highlighted in [48] without suitable solutions to overcome those difficulties.

In this thesis, we focus on the detection of narrow-band signal in OFDM system and propose a novel energy detection algorithm in frequency domain to improve the probability of detection of conventional ED without increasing the DFT size over the multipath fading channels.

3 Frequency Domain Oversampling for ZP Based MCM Systems

3.1 Introduction

The OFDM technique is a method of digital modulation that transmits the high data rate signals on a number of subcarriers with low data rate simultaneously. There are two types of OFDM techniques classified by the guard interval. One is CP OFDM and the other is ZP OFDM. The advantages of CP OFDM are that CP OFDM can keep the orthogonality of the subcarriers and the implementation of the conventional ZF equalizer in frequency domain is quite easier, which can provide the same BER performance as the conventional MMSE equalizer ([18] and [19]). The disadvantage is that the CP OFDM with the conventional ZF or MMSE equalizer cannot guarantee the symbol recovery if the power of the subchannel is nearly zero. By contrast, the merits of ZP OFDM system are lower transmission power and guaranteed symbol recovery even there are subchannels with power of zero or near zero([4], [5], [6]). However, it requires the complex channel equalizer for guaranteed symbol recovery, which actually takes advantage of the frequency oversampling method.

The MC-CDMA technique is a promising technology because it incorporates the benefits of OFDM and DS-CDMA. The BER of MC-CDMA system reduces more quickly than that of OFDM system as we increase the transmission power [12]. In DS-CDMA system, the Rake receiver is usually adopted for better performance. However, the BER performance is limited by the number of the Rake fingers, i.e., the complexity of implementation. In MC-CDMA system, many kinds of combining methods can be applied in the receiver such as MMSE, EGC, MRC, CE, ORC and PC combining. Among them, MMSE combining can offer the best performance.

In this chapter, we focus on the ZP based MCM systems which include ZP OFDM and ZP MC-CDMA. Although the conventional MMSE equalizer for OFDM system is easily implemented, it cannot guarantee the symbol recovery if the power of the subchannel is nearly zero. Hence, it

does not fully exploit the advantages of ZP OFDM system. On the other hand, both ZP OFDM and ZP MC-CDMA system are sensitive to the long multipath delay, frequency offset and Doppler frequency shift. Therefore, in this chapter, we propose the FDO based equalizers for ZP OFDM and ZP MC-CDMA systems that have the capability to fully take advantage of the merits of ZP systems and to combat the multiple interference environments, and hence improve the BER performance of the systems. For the long multipath delay channel, if the guard interval is insufficient to avoid ISI, we propose the SR method together with the FDO equalizers to minimize the effect of ISI, which is able to improve the BER performance of the system in the heavy combined interference environment.

3.2 System Model for ZP Based MCM system

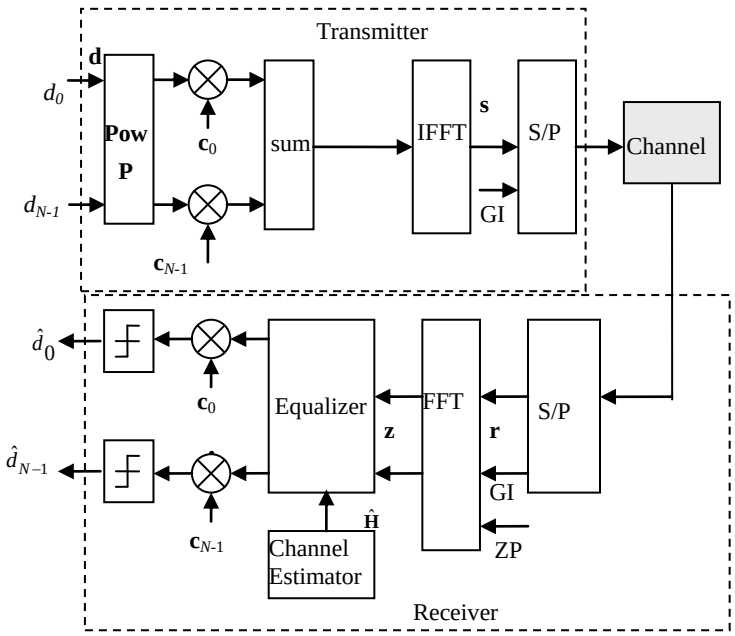

Fig. 3-1. Structure of ZP OFDM/MC-CDMA with FDO based equalizers

In this thesis, MCM systems denote OFDM system and MC-CDMA system. We study a downlink MCM system with N subcarriers and N users, as shown in Fig. 3-1. The OFDM symbol duration is T and a ZP guard interval (GI) with normalized duration length G is appended at the end of each OFDM symbol. It is assumed that the system adopts a synchronous transmission. The transmitted time domain signal of an OFDM symbol $\mathbf{s}=[s_0, s_1, \ldots, s_{N-1},..., s_{N+G-1}]^T$ after sampling

can be expressed as

$$\mathbf{s}=\begin{cases}\mathbf{F}_N^{-1}\mathbf{CPd} & (n=0,1,...,N-1)\\ \mathbf{0} & (n=N,...,N+G-1)\end{cases}, \tag{3.1}$$

where N is the size of inverse discrete Fourier transform (IDFT); G is the size of guard interval; $\mathbf{F}_N^{-1}$ is the IDFT matrix, and the element $F_{n,m}$ of $\mathbf{F}_N^{-1}$ is given by $F_{n,m}=\frac{1}{\sqrt{N}}e^{j2\pi\frac{nm}{N}}$ $(n,m=0,1,...,N-1)$; $\mathbf{C}=[\mathbf{c}_0,\mathbf{c}_1,\ldots,\mathbf{c}_{N-1}]\frac{1}{\sqrt{N}}$ is the normalized spreading code satisfying $\mathbf{C}^{\mathrm{H}}\mathbf{C}=\mathbf{I}_N$, $\mathbf{I}_N$ is the $N\times N$ identity matrix; $\mathbf{d}=[d_0, d_1, \ldots, d_{N-1}]^{\mathrm{T}}$ represents modulated data symbols, and $\mathbf{P}=\mathrm{diag}\{\sqrt{P_0},\sqrt{P_1},...,\sqrt{P_{N-1}}\}$ represents transmission power adjustment for N users. $\mathbf{P}=\mathbf{I}$ means that the transmission power is not adjusted for every user.

Since the MC-CDMA spreads the data of each user over the frequency domain, a high level modulation can be adopted for a high data rate. As long as the spreading codes are orthogonal (i.e., $\mathbf{C}^{\mathrm{H}}\mathbf{C}=\mathbf{I}_N$), the IUI can be fully removed. However, the system imperfections such as a frequency offset and frequency-selective fading will destroy the orthogonality of the subcarriers and the different users, and hence leads to a large IUI for high level modulation. The IUI actually can result in multiple access interference (MAI) in the MC-CDMA system. Hence, the MC-CDMA system is quite sensitive to frequency offset and frequency-selective fading if no advanced multi-user detection (MUD) is employed.

Based on Fig. 3-1 and equation (3.1), if we consider that both **C** and **P** are identity matrix, i.e., each user allocates one subcarrier and is transmitted without power adjustment, we have the ZP OFDM system shown in (3.2).

$$\mathbf{s}=\begin{cases}\mathbf{F}_N^{-1}\mathbf{d} & (n=0,1,...,N-1)\\ \mathbf{0} & (n=N,...,N+G-1)\end{cases}. \tag{3.2}$$

We consider the time varying multipath fading channel described by the wide-sense stationary uncorrelated scattering (WSSUS) model, and assume the number of resolvable paths is Q. The equivalent channel impulse response can be modeled as

$$h(t,\tau)=\sum_{q=0}^{Q-1}h_q(t)\delta(\tau-\tau_q), \tag{3.3}$$

where the channel path $h_q(t)$ of delay τ_q is a complex random process representing the multipath components with different Doppler frequency shifts and $\delta(\tau-\tau_q)$ is Kronecker delta function. The channel can be characterized by a correlation function

$$\mathrm{E}[h_q(t)h_{q+\Delta q}(t+\Delta t)^*]=\sigma_q^2\delta(\Delta q)\mathrm{J}_0(2\pi f_d\Delta t), \tag{3.4}$$

where $\mathrm{J}_0(\ )$ is the zeroth-order Bessel function of the first kind, f_d is the maximum Doppler frequency, and σ_q^2 is the variance of $h_q(t)$. Please note that the channel $h(t,\tau)$ changes with time within an OFDM symbol due to the Doppler frequency shifts. It's difficult to completely compensate the effect of the Doppler frequency shifts. Since the residual Doppler frequency shifts are unknown to the receiver, we can simply assume that the channel is quasi-static frequency-selective fading channel modeled as (3.5) for analysis. The Doppler frequency shift is introduced in simulations for BER performance comparison.

$$h(\tau)=\sum_{q=0}^{Q-1}h_q\delta(\tau-\tau_q), \text{ and } \sum_{q=0}^{Q-1}\mathrm{E}[|h_q|^2]=1, \tag{3.5}$$

and the frequency response of the channel $h(\tau)$ is given by

$$H(f)=\int_0^{\infty}h(\tau)e^{-j2\pi f\tau}d\tau=\sum_{q=0}^{Q-1}h_qe^{-j2\pi f\tau_q}. \tag{3.6}$$

In discrete time domain, it is assumed that the delays $\tau_q = q$ is an integer from 0 to Q-1, which represents a multiple of the sample period in (3.5). Hence, the discrete channel is $\mathbf{h}=[h_0 \ \ldots \ h_{Q-1}]^{\mathrm{T}}$ and the channel length is Q.

The equivalent channel frequency response after frequency-domain oversampling with an oversampling factor (OSF) of M/N at the m-th (m= 0, 1, …, M-1) fractional frequency, where $M = N+Q$ (i.e., the length of the OFDM symbol including the multipath channel delay), can be shown to be

$$H_m = H\left((\frac{m}{M}+\varepsilon)\frac{1}{T}\right) = \sum_{q=0}^{Q-1} h_q e^{-j2\pi(\frac{m}{M}+\varepsilon)\frac{q}{N}}, \tag{3.7}$$

where ε is the frequency offset between the transmitter and the receiver. In time domain, the discrete channel is $\mathbf{h}=[h_0, h_1, \ldots, h_{Q-1}]$. Now we define

$$\mathbf{H} = \text{diag}\{H_0, H_1, \ldots, H_{M-1}\}, \tag{3.8}$$

where H_m denotes the channel frequency response at the m-th fractionally-spaced frequency. The distribution of the complex channel gain is not specified. In the simulation, it is assumed that the power of the paths is linearly decaying.

The received signal $\mathbf{r}=[r_0, r_1, \ldots, r_{M-1}]$ of one OFDM symbol can be written as the convolution of the transmitted signal and the channel impulse response, i.e.,

$$r_n = \sum_{q=0}^{Q-1} h_q s_{n-q} + v, \;\; n = 0,1,\ldots,M-1, \tag{3.9}$$

where v denotes the additive white Gaussian noise with mean zero and variance σ^2 and $M=N+Q$, and $s_n=0$, when $n \geq N$.

The FDO of the received signal is realized by taking M points DFT on the received signal r_n in (3.9). We assume Q is less than the length of ZP guard interval G. If Q is unknown, we can assume $M=N+G$, the whole OFDM symbol including guard interval will be used for linear MMSE equalizer. It is unnecessary to assume a large M (i.e., $M> N+Q$) for MMSE equalizer, because the large M will not improve the BER performance when MMSE equalizer is adopted. The received signal in the fractionally spaced frequency domain can be written as

$$\mathbf{z} = \mathbf{H}\mathbf{F}_{MN}\mathbf{\Lambda}_{\varepsilon}\mathbf{F}_N^{-1}\mathbf{C}\mathbf{P}\mathbf{d} + \mathbf{\eta}, \tag{3.10}$$

where $\mathbf{F}_{MN} = \{ F_{m,n} \}_{M\times N}$ denotes the $M\times N$ zero-padded DFT matrix, which reflects the mapping from N transmitter subcarriers to M received subcarriers. The element $F_{m,n}$ of $\mathbf{F}_{MN}$ is defined as $F_{m,n} = e^{-j2\pi mn/M}/\sqrt{M}$ (l = 1, 2, …, M-1 and n = 0, 1, …, N-1). The diagonal matrix $\mathbf{\Lambda}_{\varepsilon}$ = diag{1, $e^{j2\pi\varepsilon/N}$, $e^{j2\pi\varepsilon 2/N}$, $\cdots$, $e^{j2\pi\varepsilon(N-1)/N}$} represents the effect of the normalized CFO

ε between the transceivers. Similarly, we define $\mathbf{F}_M = \{ F_{m,n} \}_{M\times M}$ where m = 1, 2, …, M-1 and n = 0, 1, …, M-1. Finally, $\boldsymbol{\eta}$ is a colored (due to frequency-domain oversampling) zero-mean Gaussian noise vector with the covariance matrix $\mathrm{E}[\boldsymbol{\eta}\boldsymbol{\eta}^{\mathrm{H}}] = \sigma^2\mathbf{F}_M\mathbf{F}_M^{\mathrm{H}} = \sigma^2\mathbf{I}$. Eqn. (3.10) shows that the transmitted signal can be detected by the received signal with the channel response in the oversampled frequency domain. The detection will benefit from the frequency domain oversampling by using the oversampled channel and subcarrier information.

The conventional ZF equalizer with overlap-add (OLA) method is discussed in [5] and can be expressed by (3.11).

$$\hat{\mathbf{d}} = \mathbf{P}^{-1}\mathbf{C}^{-1}\mathbf{H}^{-1}\mathbf{z} = \mathbf{P}^{-1}\mathbf{C}^{-1}\mathbf{H}^{-1}\mathbf{F}_N([r_0 \quad r_1 \quad \ldots \quad r_{N-1}]+[r_N \quad \ldots \quad r_{N+G-1} \quad 0 \quad \ldots \quad 0])^{\mathrm{T}}. \tag{3.11}$$

3.3 Proposed FDO Receivers for ZP OFDM and ZP MC-CDMA

In this section, we propose the linear FDO MMSE receiver that combines MMSE and FDO techniques to combat the large combined interference, and the FDO diagonal MMSE equalizer and FDO ZF equalizer with low complexity based on the proposed system model.

3.3.1 FDO-MMSE Equalizer

For a linear MMSE receiver, the transmitted symbols **d** can be estimated from the frequency-domain oversampled **z** by multiplying an optimal weight matrix $\mathbf{W}_{\mathrm{FM}}^{\mathrm{H}}$, i.e.,

$$\hat{\mathbf{d}} = \mathbf{W}_{\mathrm{FM}}^{\mathrm{H}}\mathbf{z}. \tag{3.12}$$

According to the orthogonality principle, for an optimal linear estimation, the estimation error $\mathbf{d}-\hat{\mathbf{d}}$ is orthogonal to the known random variable **z**, i.e., $\mathrm{E}[(\mathbf{d}-\hat{\mathbf{d}})\mathbf{z}^{\mathrm{H}}] = 0$. By defining $\boldsymbol{\Phi} = \mathbf{F}_{MN}\boldsymbol{\Lambda}_{\varepsilon}\mathbf{F}_N^{-1}$ and assuming that the users' signals have the same power since we do not know the power information of each transmitted data in the receiver (i.e., $\mathrm{E}\{\mathbf{d}\mathbf{d}^{\mathrm{H}}\} = P_d\mathbf{I}$ and $\mathbf{P} = \mathbf{I}$, where P_d is the average power of the transmitted data), and further assuming that the signals for the inactive users in **d** are set to 0, the proposed FDO-MMSE receiver has the following weight matrix:

$$\mathbf{W}_{\mathrm{FM}}^{\mathrm{H}} = (\mathbf{H\Phi C})^{\mathrm{H}}(\mathbf{H\Phi\Phi}^{\mathrm{H}}\mathbf{H}^{\mathrm{H}} + \gamma\mathbf{I})^{-1}, \tag{3.13}$$

where **H** is the channel information that can be replaced by estimated channel $\hat{\mathbf{H}}$, **Φ** represents the mapping to the oversampled frequency domain. To calculate **Φ**, set ε=0 (i.e., $\mathbf{\Lambda}_{\varepsilon}$=**I**) because the actual frequency offset cannot be accurately estimated, and the residual CFO ε in (3.10) is unknown to the receiver. Simulations have been conducted to evaluate the effect of a nonzero frequency offset. Once the oversampling factor *M*/*N* is selected, the value of **Φ** can be pre-calculated. $\gamma = \sigma^2/P_d = 1/SNR$ denotes the signal and noise information. The matrix inverse operation in $\mathbf{W}_{\mathrm{FM}}^{\mathrm{H}}$ can be replaced with the Moore-Penrose pseudo inverse, because when γ is quite small, the matrix $\mathbf{H\Phi\Phi}^{\mathrm{H}}\mathbf{H}^{\mathrm{H}} + \gamma\mathbf{I}$ is close to singular due to *M*>*N*, the result of matrix inverse may be inaccurate. In order to reduce the computation of matrix inverse, equation (3.13) can be written as the equivalent form in (3.14).

$$\mathbf{W}_{\mathrm{FM}}^{\mathrm{H}} = \mathbf{C}^{\mathrm{H}}(\mathbf{\Phi}^{\mathrm{H}}\mathbf{H}^{\mathrm{H}}\mathbf{H\Phi} + \gamma\mathbf{I})^{-1}(\mathbf{H\Phi})^{\mathrm{H}}, \tag{3.14}$$

which can be verified by using the singular value decomposition of **Φ** in both (3.13) and (3.14). Thus, the dimension of matrix to be inversed is reduced from *M*×*M* to *N*×*N*.

It is obvious that this equalizer can be used for both multi-user and single-user detection in ZP MC-CDMA system as long as the users' spreading codes are known. Note that for single user detection, **C** contains only the intended user's spreading code. For ZP OFDM system, **C** is an identity matrix.

For an MMSE equalizer in the OFDM system, the interference can be greatly suppressed by $\mathbf{W}_{\mathrm{FM}}^{\mathrm{H}}$ due to the minimization of mean square error (MSE) of estimated data $\hat{\mathbf{d}}$. For a conventional receiver without oversampling, *N* subcarriers are orthogonal. The weight matrix $\mathbf{W}_{\mathrm{FM}}^{\mathrm{H}}$ is a diagonal matrix. The optimal estimator can be reduced to *N* scalar MMSE receivers. And the scalar MMSE receiver cannot improve the performance in terms of error rate [18]. By using the FDO method, $\mathbf{W}_{\mathrm{FM}}^{\mathrm{H}}$ is no long diagonal, thus the data on *N* subcarriers can be recovered

from M ($M>N$) sampled subcarriers while the noise can be suppressed when it spreads over M subcarriers.

3.3.2 FDO Diagonal MMSE Equalizer and FDO Noise Fixed Equalizer

The FDO-MMSE equalizer is computationally intensive since there is an inverse operation of matrix in (3.13). It will then be highly desirable to have an equalizer with much lower complexity while the performance degradation is marginal or negligible.

The matrix $\mathbf{F}_{MN}$ in $\mathbf{\Phi}$ is the first N columns of the M-point DFT matrix $\mathbf{F}_M$. The singular value decomposition of $\mathbf{F}_{MN}$ is given by $\mathbf{F}_{MN} = \mathbf{U}\mathbf{I}_{MN}\mathbf{V}$, where $\mathbf{U}$ and $\mathbf{V}$ are $M\times M$ and $N\times N$ orthogonal matrix respectively, and $\mathbf{I}_{MN}$ is an $M\times N$ matrix that is actually the first N columns of the $M\times M$ identity matrix $\mathbf{I}_M$. Thus, $\mathbf{F}_{MN}\,\mathbf{F}_{MN}^{\mathrm{H}} = \mathbf{U}\mathbf{I}_{MN}\mathbf{V}\mathbf{V}^{\mathrm{H}}\mathbf{I}_{MN}^{\mathrm{H}}\mathbf{U}^{\mathrm{H}} = \mathbf{U}\hat{\mathbf{I}}\mathbf{U}^{\mathrm{H}}$, where $\hat{\mathbf{I}}$ is an $M\times M$ diagonal matrix whose first N diagonal elements are ones and other elements are zeros. Since it only has M-N diagonal elements that are different from that of the identity matrix $\mathbf{I}_M$, we can assume $\hat{\mathbf{I}}\approx\mathbf{I}_M$ for simplification. Hence, we have $\mathbf{F}_{MN}\,\mathbf{F}_{MN}^{\mathrm{H}}\approx\mathrm{I}_M$, which leads to the diagonalization of the matrix $\mathbf{\Phi}\mathbf{\Phi}^{\mathrm{H}}$, i.e., $\mathbf{\Phi}\mathbf{\Phi}^{\mathrm{H}}\approx\mathbf{I}_M$.

Let $\mathbf{\Psi}= \mathbf{H}\mathbf{\Phi}\mathbf{\Phi}^{\mathrm{H}}\mathbf{H}^{\mathrm{H}}+\gamma\mathbf{I}$ and use $\mathbf{\Phi}\mathbf{\Phi}^{\mathrm{H}}\approx\mathbf{I}_M$, we have $\mathbf{\Psi}\approx\mathbf{H}\mathbf{H}^{\mathrm{H}}+\gamma\mathbf{I}$, which actually leads to the diagonalization of matrix $\mathbf{\Psi}$. Now the inverse of diagonal matrix $\mathbf{\Psi}$ is much simpler than that of the original non-diagonal matrix. We refer to the obtained equalizer as the FDO Diagonal MMSE equalizer (FDO-DMMSE), the optimal weight matrix $\mathbf{W}_{\mathrm{FD}}^{\mathrm{H}}$ of which can be rewritten as

$$\mathbf{W}_{\mathrm{FD}}^{\mathrm{H}} = (\mathbf{\Phi}\mathbf{C})^{\mathrm{H}}\mathbf{H}^{\mathrm{H}}(\mathbf{H}\mathbf{H}^{\mathrm{H}}+\gamma\mathbf{I})^{-1}. \tag{3.15}$$

The complexity of the simplified FDO-DMMSE equalizer decreases significantly since that the matrix inverse is not needed. The FDO diagonal equalizer is easily to understand. It firstly equalizes the received data on M-subcarriers domain by $\mathbf{H}^{\mathrm{H}}(\mathbf{H}\mathbf{H}^{\mathrm{H}}+\gamma\mathbf{I})^{-1}$, then converts the equalized data to N-subcarriers domain by $(\mathbf{\Phi}\mathbf{C})^{\mathrm{H}}$.

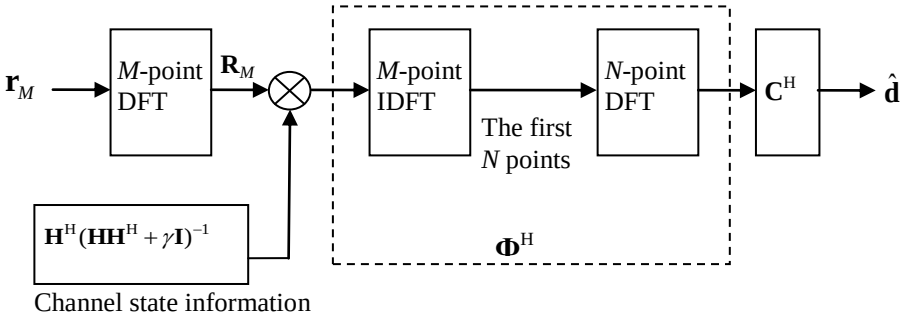

Fig. 3-2. The implementation of FDO-DMMSE equalizer for ZP based MCM systems

The implementation of the FDO-DMMSE is shown in Fig. 3-2. Compared with the conventional ZF equalizer, the FDO-DMMSE only requires an additional *M*-point DFT and *M*-point IDFT, which can be implemented by FFT and IFFT, respectively. In addition, the channel state information in *M*-subcarrier frequency domain shall be calculated and the noise power $\boldsymbol{\gamma}$ shall be estimated. For OFDM system, **C** is set to **I**.

The FDO-DMMSE equalizer needs to estimate the noise power for a better performance, which will cause additional computations. If the noise is forced to a fixed value (i.e., let $\boldsymbol{\gamma} = \boldsymbol{\gamma_0}$), the FDO-DMMSE equalizer can be further simplified to an FDO noise fixed (FDO-NF) equalizer. The FDO-NF equalizer requires only the additional *M*-point IDFT and *M*-point DFT compared to a conventional receiver. It is suitable for the practical applications. $\boldsymbol{\gamma_0}$ can be set based on the expected SNR range in the practical working environment. For example, if we know the rough SNR of the receiver in a working scenario, e.g., around 20 dB, then we can set $\boldsymbol{\gamma_0}$ = 1/(20dB) = 0.01 (we assume P_d=1). Round this SNR, the FDO-NF equalizer can offer a similar BER performance to the FDO-DMMSE equalizer. If the $\boldsymbol{\gamma_0}$ is set to zero, the FDO-NF equalizer becomes an FDO-ZF equalizer.

3.3.3 FDO Zero Forcing Equalizer

The FDO-ZF equalizer for ZP OFDM and ZP MC-CDMA can be obtained from the FDO-MMSE equalizer by ignoring the noise part in (3.13). We use Moore-Penrose pseudo inverse to replace the matrix inverse (3.13). The FDO-ZF can be written as

$$\mathbf{W}_{\mathrm{FZ}}^{\mathrm{H}} = \mathbf{C}^{\mathrm{H}}\mathbf{\Phi}^{\mathrm{H}}(\mathbf{\Phi}\mathbf{\Phi}^{\mathrm{H}})^{+}\mathbf{H}_{M}^{-1} = \mathbf{C}^{\mathrm{H}}\mathbf{\Phi}^{+}\mathbf{H}_{M}^{-1} = \mathbf{C}^{\mathrm{H}}\mathbf{\Phi}^{\mathrm{H}}\mathbf{H}_{M}^{-1}, \tag{3.16}$$

where $\mathbf{\Phi} = \mathbf{F}_{MN}\mathbf{F}_{N}^{-1}$ represents the map from *M*-subcarrier domain to *N*-subcarrier domain.

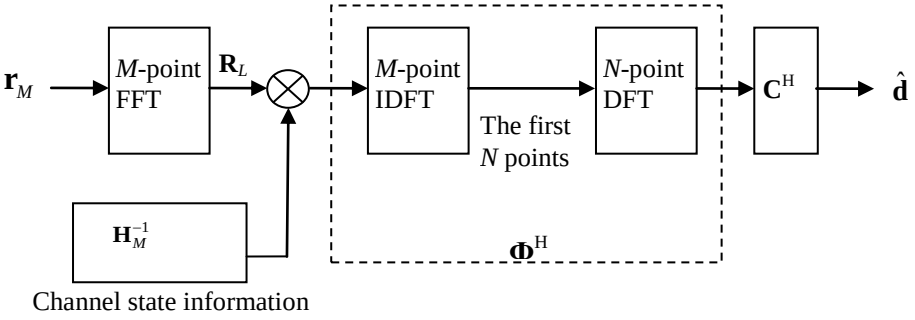

Fig. 3-3. The implementation of FDO-ZF equalizer for ZP based MCM systems

Although the FDO-ZF equalizer in (3.16) cannot offer better BER performance than the MMSE equalizer in (3.13), it is easily implemented because $\mathbf{\Phi}^{\mathrm{H}}$ can be pre-calculated and the inverse of diagonal matrix $\mathbf{H}_M$ can be easily calculated. $\mathbf{\Phi}^{\mathrm{H}}$ actually can be implemented by *M*-point IDFT following by *N*-point DFT shown in Fig. 3-3. Compared with the conventional ZF equalizer for ZF OFDM, the FDO-ZF equalizer only needs one more *M*-point DFT and *M*-point IDFT. There is no need to estimate the noise power γ. For ZP OFDM, $\mathbf{C}$ is set to $\mathbf{I}$.

To improve the BER performance of FDO-ZF equalizer, we can increase the oversampling rate *M/N* for FDO-ZF equalizer (i.e., increase DFT size *M*). In this case, *M* is the DFT size and not equal to *N*+*Q*. The length of received symbol $\mathbf{r}$ is *N*+*Q*. $\mathbf{r}$ shall be padded with zeros to increase its size to *M*, and then be converted to *M*-subcarrier frequency domain by *M*-point DFT. We assume that the channel is perfectly estimated and there is no frequency offset. We replace $\mathbf{W}_{\mathrm{FM}}^{\mathrm{H}}$ in (3.12) with $\mathbf{W}_{\mathrm{FZ}}^{\mathrm{H}}$, and substitute (3.16) and (3.10) into (3.12), we have

$$\hat{\mathbf{d}} = \mathbf{C}^{\mathrm{H}}\mathbf{\Phi}^{+}\mathbf{\Phi}\mathbf{C}\mathbf{d} + \mathbf{\Phi}^{+}\mathbf{H}_{M}^{-1}\mathbf{F}_{M}\bar{\mathbf{v}} = \mathbf{d} + \begin{bmatrix} \mathbf{F}_{N}^{-1} \\ \mathbf{0}_{(M-N)\times N} \end{bmatrix}^{+} \mathbf{F}_{M}^{-1}\mathbf{H}_{M}^{-1}\mathbf{F}_{M}\bar{\mathbf{v}}, \tag{3.17}$$

where $\bar{\mathbf{v}}$ is the noise vector $\mathbf{v}$ padded with [*M*-(*N*+*Q*)] zeros, $\mathbf{0}_{(M-N)\times N}$ is a zero matrix with *M*-*N*

rows and N columns. Please note that $\mathbf{F}_M^{-1}$ and $\mathbf{F}_M$ will not change the power of noise $\mathbf{v}$. When oversampling rate increases, the size of matrix $\mathbf{0}_{(M-N)\times N}$ increases, which will decrease the noise power because more rows of $\mathbf{F}_M^{-1}\mathbf{H}_M^{-1}\mathbf{F}_M$ are truncated by the zero matrix and hence increase the average SNR. However, $\mathbf{H}_M^{-1}$ will increase the noise power given the assumption of quasi-static multipath channel $\sum_{q=0}^{Q-1} \mathrm{E}[|h_q|^2]=1$ (i.e., $\sum_{k=0}^{M-1} \mathrm{E}[|H_k|^2]=1$ in frequency domain). Thus, the increasing of the average SNR is limited by the channel $\mathbf{H}_M^{-1}$. In general, the BER performance of the ZF equalizer can be improved by increasing the oversampling rate M/N (i.e., increasing DFT size M), but the improvement will be limited by the channel attenuation.

Compared with the FDO-based equalizers for ZP OFDM, the FDO-based equalizers for ZP MC-CDMA can achieve better BER performance at high SNR level at the cost of adding spreading code. The orthogonal spreading code is quite simple to implement in the systems. Hence, the FDO-based equalizers for ZP OFDM and for ZP MC-CDMA have the similar complexity of implementation.

3.4 BER Performance of FDO Based Equalizers

Although the close-form BER performance of the FDO-based equalizer is difficult to calculate, it can be estimated by using the average instantaneous BER (AI-BER) with a large amount of OFDM symbols.

For FDO-MMSE equalizer, substituting (3.10) and (3.13) into (3.12), the estimated transmitted data $\hat{\mathbf{d}}$ can be represented by

$$\hat{\mathbf{d}} = \mathbf{W}_{\mathrm{FM}}^{\mathrm{H}}\mathbf{H}\mathbf{F}_{MN}\boldsymbol{\Lambda}_{\varepsilon}\mathbf{F}_N^{-1}\mathbf{C}\mathbf{P}\mathbf{d} + \mathbf{W}_{\mathrm{FM}}^{\mathrm{H}}\mathbf{F}_M\mathbf{v} = \mathbf{B}\mathbf{d} + \mathbf{J}\mathbf{v}, \tag{3.18}$$

where $\mathbf{B} = \mathbf{W}_{\mathrm{FM}}^{\mathrm{H}}\mathbf{H}\mathbf{F}_{MN}\boldsymbol{\Lambda}_{\varepsilon}\mathbf{F}_N^{-1}\mathbf{C}\mathbf{P}$ is an $N\times N$ matrix and $\mathbf{J} = \mathbf{W}_{\mathrm{FM}}^{\mathrm{H}}\mathbf{F}_M$ is an $N\times M$ matrix, $\mathbf{v}$ denotes the zero mean Gaussian noise with variance σ^2.

The estimated data on subcarrier k can be expressed as

$$\hat{d}_k = \sum_{n=0}^{N-1} B_{k,n} d_n + \sum_{m=0}^{M-1} J_{k,m} v_m \quad . \tag{3.19}$$

According to the central limit theorem, when N is large, both $\sum_{n=0}^{N-1} B_{k,n} d_n$ and $\sum_{m=0}^{M-1} J_{k,m} v_m$ approximate to the normal distribution, hence $\hat{d}_k$ approximates to the normal distribution. For quadrature phase shift keying (QPSK) modulation, it is assumed that the mean and the variance of the real and imaginary part of d_n are 0 and 1/2, respectively. Therefore, the instantaneous BER of the x-th OFDM symbol on subcarrier k can be calculated from

$$\beta_k^x = Q\left(\frac{\Re(B_{k,k})}{\sqrt{\sum_{n\neq k} \Re(B_{k,n})^2 + \sum_{n\neq k} \Im(B_{k,n})^2 + \sum_{m=0}^{M-1} \left(\Re(J_m)^2 + \Im(J_m)^2 \right) 2\sigma^2}} \right), \tag{3.20}$$

where $Q(t) = \frac{1}{\sqrt{2\pi}} \int_t^\infty e^{-y^2/2} dy$, $\Re(y)$ and $\Im(y)$ represent the real and imaginary part of y, respectively. $\sum_{n\neq k} \Re(B_{k,n})^2 + \sum_{n\neq k} \Im(B_{k,n})^2$ denotes the inter-carrier interference, and $\sum_{m=0}^{M-1} \left(\Re(J_m)^2 + \Im(J_m)^2 \right) \sigma^2$ denotes the noise suppressed by the equalizers. The average BER of X number of OFDM symbols is given by

$$\beta = \frac{1}{X} \sum_{x=0}^{X-1} \frac{1}{N} \sum_{k=0}^{N-1} \beta_k^x \quad . \tag{3.21}$$

In (3.18), if we replace $\mathbf{W}_{\mathrm{FM}}^{\mathrm{H}}$ with $\mathbf{W}_{\mathrm{FD}}^{\mathrm{H}}$ and $\mathbf{W}_{\mathrm{FZ}}^{\mathrm{H}}$, we can get the BER expressions in the forms of (3.20) and (3.21) for FDO-DMMSE and FDO-ZF, respectively.

3.5 MSE Performance of FDO Based Equalizers

Without loss of generality, we assume that $\mathbf{\Phi} = \mathbf{F}_{MN}\mathbf{F}^{-1}{}_N$, $\mathrm{E}[\mathbf{d}\mathbf{d}^{\mathrm{H}}] = \mathbf{I}_{\mathrm{N}}$, $\mathbf{P} = \mathbf{I}_{\mathrm{N}}$ and $\mathrm{E}[\mathbf{d}\boldsymbol{\eta}^{\mathrm{H}}] = \mathbf{0}$. For a MMSE equalizer, we have $\mathrm{E}[(\mathbf{d} - \hat{\mathbf{d}})\mathbf{z}^{\mathrm{H}}] = \mathbf{0}$. The covariance matrix of the detection error $\mathbf{\Sigma}$,

is given by

$$\mathbf{\Sigma} = \mathrm{E}[(\hat{\mathbf{d}}-\mathbf{d})(\hat{\mathbf{d}}-\mathbf{d})^{\mathrm{H}}] = \mathbf{W}^{\mathrm{H}}\mathbf{\Psi}\mathbf{W} - (\mathbf{H}\mathbf{\Phi}\mathbf{C})^{\mathrm{H}}\mathbf{W} - \mathbf{W}^{\mathrm{H}}\mathbf{H}\mathbf{\Phi}\mathbf{C} + \mathbf{I}_N, \tag{3.22}$$

where $\mathbf{\Psi}=\mathbf{H}\mathbf{F}_{MN}\mathbf{F}_{MN}^{\mathrm{H}}\mathbf{H}^{\mathrm{H}}+\sigma^2$. Considering the cyclic property of trace function Tr(ABC) = Tr(BCA) = Tr(CAB), the average MSE of the FDO-MMSE equalizer can be written as

$$e^2 = \mathrm{Tr}(\mathbf{\Sigma})/N \approx \mathrm{Tr}\left(\mathbf{I}_N - (\mathbf{H}\mathbf{\Phi})^{\mathrm{H}}(\mathbf{H}\mathbf{\Phi}\mathbf{\Phi}^{\mathrm{H}}\mathbf{H}^{\mathrm{H}} + \sigma^2)^{-1}\mathbf{H}\mathbf{\Phi}\right)/N, \tag{3.23}$$

where Tr (·) represents the sum of diagonal elements of a matrix (i.e., trace function).

For the FDO-DMMSE/NF equalizer, subtituting (3.15) to (3.22), the average MSE can be rewritten as

$$\begin{aligned} e^2 \approx\ & \mathrm{Tr}\left(\mathbf{I}_N + (\mathbf{H}\mathbf{\Phi}\mathbf{\Phi}^{\mathrm{H}}\mathbf{H}^{\mathrm{H}} + \sigma^2)(\mathbf{H}\mathbf{H}^{\mathrm{H}} + \sigma^2)^{-1}\mathbf{H}\mathbf{\Phi}\mathbf{\Phi}^{\mathrm{H}}\mathbf{H}^{\mathrm{H}}(\mathbf{H}\mathbf{H}^{\mathrm{H}} + \sigma^2)^{-1}\right)/N \\ & -\mathrm{Tr}\left(2\mathbf{H}\mathbf{\Phi}\mathbf{\Phi}^{\mathrm{H}}\mathbf{H}^{\mathrm{H}}(\mathbf{H}\mathbf{H}^{\mathrm{H}} + \sigma^2)^{-1}\right)/N \end{aligned}. \tag{3.24}$$

For the FDO-ZF equalizer, the average MSE at the receiver can be written as

$$\begin{aligned} e^2 &= \mathrm{Tr}\left((\mathbf{H}\mathbf{\Phi}\mathbf{\Phi}^{\mathrm{H}}\mathbf{H}^{\mathrm{H}} + \sigma^2)\mathbf{H}^{-\mathrm{H}}\mathbf{\Phi}\mathbf{\Phi}^{\mathrm{H}}\mathbf{H}^{-1} - 2\mathbf{\Phi}^{\mathrm{H}}\mathbf{\Phi} + \mathbf{I}_N\right)/N \\ &= \mathrm{Tr}\left((\mathbf{H}\mathbf{\Phi}\mathbf{\Phi}^{\mathrm{H}}\mathbf{H}^{\mathrm{H}} + \sigma^2)\mathbf{H}^{-\mathrm{H}}\mathbf{\Phi}\mathbf{\Phi}^{\mathrm{H}}\mathbf{H}^{-1} - \mathbf{I}_N\right)/N \end{aligned}. \tag{3.25}$$

3.6 Proposed Iterative FDO Receivers for Insufficient Guard Interval

In the case that the guard interval of OFDM is insufficient to avoid ISI, i.e., $G < Q$, the received OFDM symbol is interfered by the adjacent OFDM symbols, which may greatly degrade the BER performance of the receivers. In this section, we design the iterative FDO-based receivers for the ZP OFDM and the ZP MC-CDMA system to minimize the effects of ISI by using the SR method.

3.6.1 Symbol Reconstruction

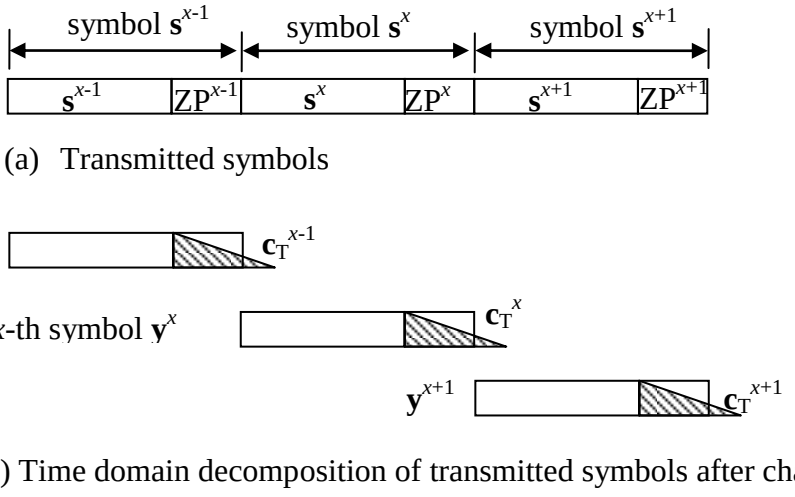

Fig. 3-4. Decomposition for transmitted and received ZP MCM signal

The decomposition of the transmitted and received ZP OFDM and ZP MC-CDMA signal is shown in Fig. 3-4. The multipath channel can be modeled as a finite impulse response (FIR) filter, which filters the transmitted OFDM symbol and output to the receiver. Hence, the filtered OFDM symbol consists two parts: The main body and the tail part. The shadow part in Fig. 3-4 represents the tail of the filtered OFDM symbol that caused by multipath channel. We assume that the x-th filtered OFDM symbol is $\mathbf{y}^x$. $\mathbf{c}_T{}^x$ represents the tail part of the x-th filtered OFDM symbol $\mathbf{y}^x$ after multipath channel. In time domain the adjacent two filtered OFDM symbols $\mathbf{y}^x$ and $\mathbf{y}^{x+1}$ will overlap. Thus, the received x-th OFDM symbol $\mathbf{r}^x$ includes the data from the x-1-th filtered OFDM symbol $\mathbf{y}^{x-1}$ and the x+1-th filtered OFDM symbol $\mathbf{y}^{x+1}$. The x-th filtered OFDM symbol $\mathbf{y}^x$ can be retrieved by

$$y_n^x = \begin{cases} r_n^x - y_{n+N+G}^{x-1}, & 0 \le n < Q-G \\ r_n^x, & Q-G \le n < N+G \\ r_n^x - y_{n-N-G}^{x+1}, & N+G \le n < N+Q \end{cases}. \tag{3.26}$$

However, $\mathbf{y}^{x-1}$ and $\mathbf{y}^{x+1}$ are unknown in current stage. They can only be replaced with the estimated symbol $\hat{\mathbf{r}}^{x}$ and $\hat{\mathbf{r}}^{x+1}$, which can be obtained according to equation (3.27)

$$\hat{\mathbf{r}} = \Xi \mathbf{F}_N^{-1} \mathbf{C} \mathbf{P} \hat{\mathbf{d}}, \tag{3.27}$$

where Ξ is a Toeplitz matrix and the first column of it is $[h_0\ h_1\ \ldots\ h_{Q-1}\ \ldots 0]^{\mathrm{T}}$, which represents the channel information in time domain, and $\hat{\mathbf{d}}$ is the estimated data. Combing (3.26) and (3.27), we can calculate the estimation of symbol $\mathbf{y}^{x}$, i.e., the x-th reconstructed symbol $\tilde{y}^{x}$.

Since $\hat{\mathbf{r}}^{x}$ and $\hat{\mathbf{r}}^{x+1}$ are not accurate, the ISI of the x-th reconstructed symbol $\tilde{y}^{x}$ cannot be fully removed.

The FDO equalizers we proposed in Section 3.3.1, 3.3.2 and 3.3.3 can be adopted for the reconstructed symbol $\tilde{y}^{x}$ to recover the transmitted data.

3.6.2 Iterative FDO Based Receivers

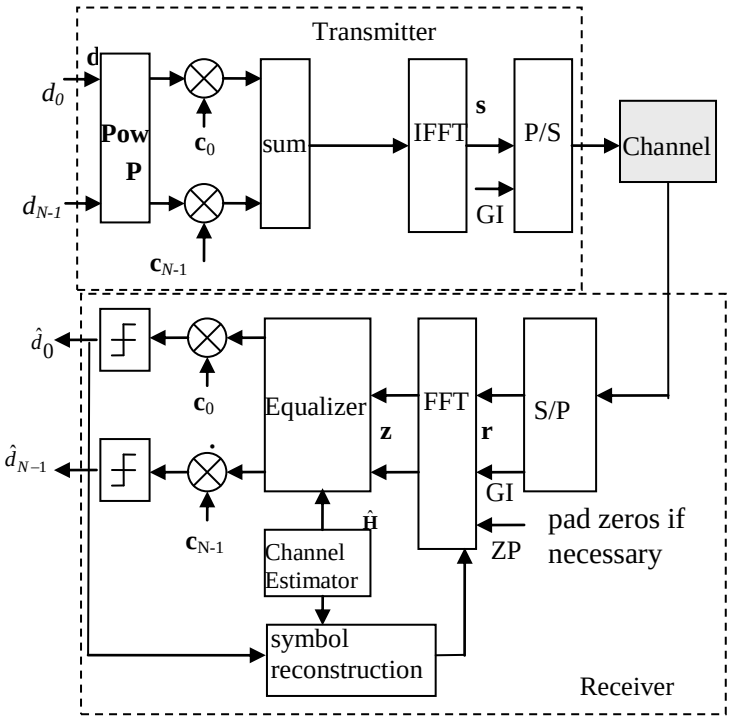

Fig. 3-5. Structure of ZP MCM with iterative FDO based equalizers

In this section, we propose the iterative FDO based equalizers for ZP OFDM and ZP MC-CDMA when the guard interval is not enough to avoid the ISI. The basic structure of the proposed

iterative equalizer is shown in Fig. 3-5. The detailed working procedures are described as follows.

1) Estimate the transmitted data $\hat{\mathbf{d}}$ for the *x*-th OFDM symbol by using the conventional overlap-add (OLA) equalizer. The conventional OLA equalizer is described in (3.11) and [5]. Set the iteration index *I* to 1.

2) Estimate the *x*-th OFDM symbol in time domain by using $\hat{\mathbf{d}}$. In order to achieve a better performance, the equalized data $\hat{\mathbf{d}}$ will be demapped first to get the estimated binary data, and then reversely map the estimated binary data again to the modulated data $\overline{\mathbf{d}}$ to reduce the noise power. According to Section 3.6.1, substituting $\overline{\mathbf{d}}$ for $\hat{\mathbf{d}}$ in (3.27) and (3.9), we have the estimated data of *x*-th symbol in time domain $\hat{\mathbf{r}}^{I,x} = \{\hat{r}_n^{I,x}\}_{n=0}^{N+Q-1}$.

$$\hat{\mathbf{r}}^{I,x} = \Xi \mathbf{F}_N^{-1} \mathbf{C} \mathbf{P} \overline{\mathbf{d}} . \tag{3.28}$$

3) Reconstruct the *x*-th OFDM symbol $\tilde{\mathbf{y}} = \{\tilde{y}_n^{I,x}\}_{n=0}^{N+Q-1}$ to reduce the ISI according to Section 3.6.1.

$$\tilde{y}_n^{I,x} = \begin{cases} r_n^x - \hat{r}_{n+N+G}^{I,x-1}, & 0 \le n < Q-G \\ r_n^x, & Q-G \le n < N+G, \\ r_n^x - \hat{r}_{n-N-G}^{I,x+1}, & N+G \le n < N+Q \end{cases} \tag{3.29}$$

where r_n^x represents the received *x*-th OFDM symbol with ISI.

4) Oversample the new *x*-th reconstructed symbol $\tilde{\mathbf{y}} = \{\tilde{y}_n^{I,x}\}_{n=0}^{N+Q-1}$ in frequency domain by using *M*-point DFT and then retrieve the transmitted data $\hat{\mathbf{d}}$ of the *k*-th OFDM symbol by using the proposed FDO-based equalizers in Section 3.3.1, 3.3.2 and 3.3.3. The retrieved transmitted data $\hat{\mathbf{d}}$ shall be more accurate than the result in step 1).

5) If the iteration number reaches pre-defined maximal number, the FDO-based equalization will be finished. Otherwise, update the iteration index *I*=*I*+1 and go back to step 2) for another iteration.

Since the FDO-based equalizers can greatly suppress the interference, the BER curves of the

proposed receivers can quickly converge after a few iterations.

If the channel delay is shorter than the guard interval (i.e., $Q \leq G$), there is no ISI between two OFDM symbols. Thus, the step 3) is not necessary, and the proposed FDO-based receivers can be simplified to the conventional FDO receivers in Section 3.3.1, 3.3.2 and 3.3.3.

3.7 Simulation Results and Analysis

In this section, we firstly evaluate the performance of our proposed FDO based equalizers for ZP MC-CDMA system. Then we consider the ZP OFDM system by defining **C**=**I** and **P**=**I** and compare the performance of it to the ZP MC-CDMA.

In the simulations, we consider a downlink ZP MC-CDMA system with N=64 subcarriers, 64 users, G = 8, QPSK modulated signals, and Walsh-Hadamard spreading codes. The SNR is defined as P_d/σ^2, where P_d is fixed to 1. We assume that the normalized quasi-static channel has N_q=8 linearly decaying multipath components with delays {0, iT/N, 2iT/N, 3iT/N, 4iT/N, 5iT/N, 6iT/N, 7iT/N} and the total power is normalized to 1 (i.e., the power of each component is {8/36, 7/36, 6/36, 5/36, 4/36, 3/36, 2/36, 1/36}), where i represents the interval between two path components. The maximum path delay (i.e., the channel length) $Q = i(N_q\text{-}1)+1$. Each component follows a complex normal distribution. We assume that the channel coefficients without frequency offset information can be perfectly estimated. The proposed FDO based equalizers in the both uncoded and coded OFDM systems are simulated. In the coded OFDM system, we consider a rate ½ convolutional encoder with constraint-length 7 and generator polynomial [171 133] in transmitter. The receiver adopts a hard-decision Viterbi decoder with a traceback length 32. We compare the four proposed equalizers (FDO-MMSE, FDO-DMMSE, FDO-NF and FDO-ZF) and the conventional ZF equalizer with OLA method.

3.7.1 Sufficient Guard Interval

Firstly we assume that the guard interval is sufficient to avoid ISI, i.e., short multipath delay channel is adapted. In this case, the multipath interval i is set to 1. The maximal path delay is Q=8. The guard interval ZP is long enough to avoid ISI and the OFDM symbol length is M=N+Q=72.

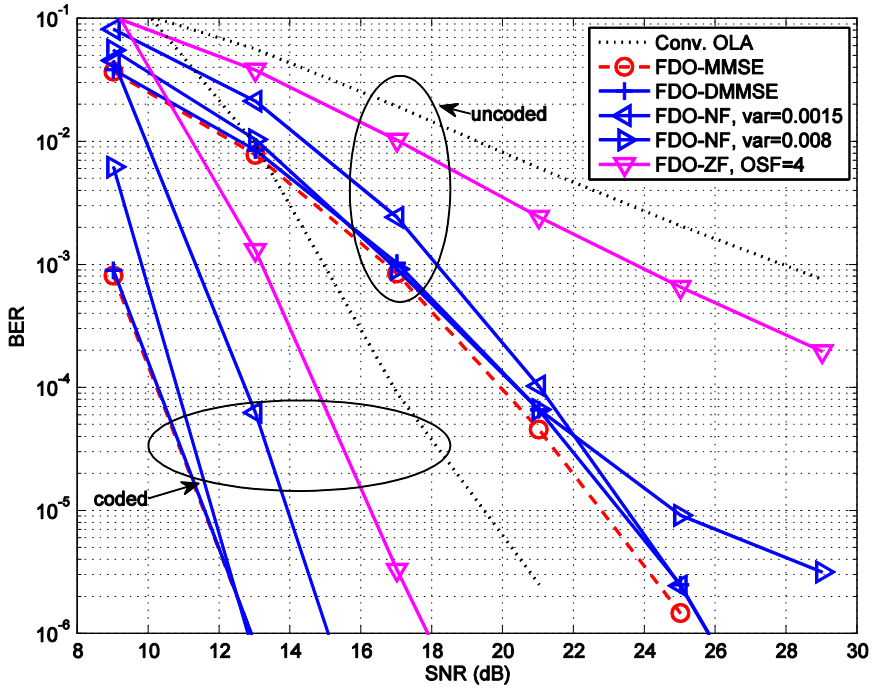

Fig. 3-6. Comparisons for ZP MC-CDMA with sufficient GI

The BER comparison of the various equalizers in the uncoded and coded ZP MC-CDMA systems over a short multipath delay channel is shown in Fig. 3-6. Compared with the conventional OLA equalizer, the FDO-MMSE, FDO-DMMSE and FDO-NF equalizers can significantly improve the BER performance in high SNR level in the coded and uncoded systems. All of them can offer about 9 dB SNR gain at a BER of 1×10^{-6} level in the coded system. The FDO-ZF with OSF=4 can also improve the BER performance obviously in the both coded and uncoded systems. Although the FDO-DMMSE has the lower complexity of implementation than the FDO-MMSE, it still can offer very good BER performance similar to the FDO-MMSE. With properly selected γ in (3.15), the less complex FDO-NF equalizers (e.g., the curve with var=0.008 in Fig. 3-6) can also have very good BER performance that is close to the FDO-MMSE and FDO-DMMSE in the expected SNR range.

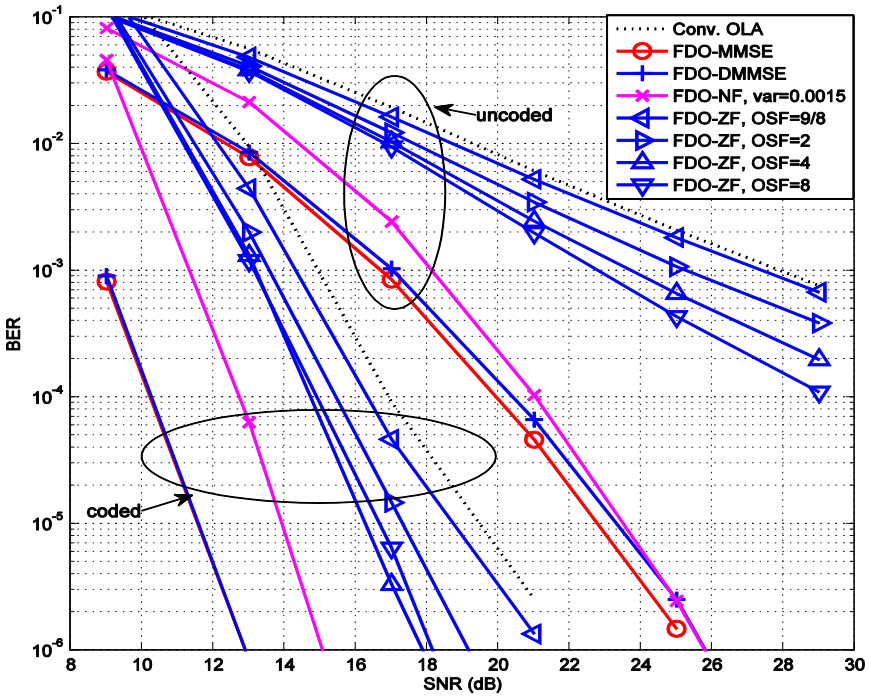

Fig. 3-7. Comparisons of FDO-ZF for ZP MC-CDMA with sufficient GI

The BER performance comparison of the FDO-ZF equalizer with different OSF in the uncoded and coded ZP MC-CDMA systems over a short multipath delay channel is shown in Fig. 3-7. With OSF=9/8, the FDO-ZF equalizer just has slightly better BER performance than the conventional OLA equalizer. However, increasing the OSF can improve the BER performance of FDO-ZF, which matches our analysis in Section 3.3.3. In the uncoded ZP MC-CDMA system, the BER performance can be reduced from 7×10^{-4} to 1.1×10^{-4} at the SNR of 29 dB when OSF increases from 9/8 to 8. In the coded system, the BER performance can be greatly reduced from 2×10^{-5} to 1×10^{-6} at the SNR of 18 dB when OSF increases from 9/8 to 4. However, large OSF requires large DFT size, which increases the complexity of implementation. It is a tradeoff between the BER performance and the complexity.

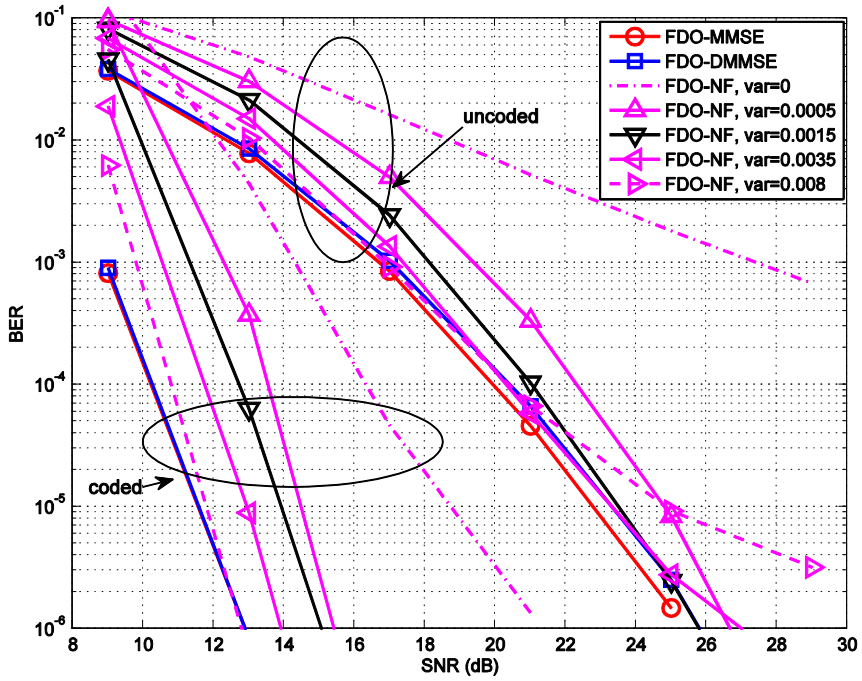

Fig. 3-8. Comparisons of FDO-NF for ZP MC-CDMA with sufficient GI

The BER performance comparison of the FDO-NF equalizers with different fixed noise variances in the uncoded and coded ZP MC-CDMA systems over a short multipath delay channel is shown in Fig. 3-8. The variance choice for the FDO-NF is based on the expected noise variance or SNR in the working environment. For the uncoded system, the FDO-NF with variance 0.0015 (i.e., about 28dB) can have similar BER performance to the FDO-DMMSE around the SNR of 28 dB, but slightly worse when SNR is less than 24 dB. If the actual SNR around 21 dB (i.e., SNR=21dB), a choice of variance =0.008 for FDO-NF can offer similar BER performance to the FDO-DMMSE. For the coded ZP MC-CDMA system, because the channel coding can reduce the SNR requirement, the expected SNR will be lower (e.g., less than 20 dB). Hence, we can choose a large variance (e.g., 0.008) for the FDO-NF equalizer so that the FDO-NF equalizer can have similar BER performance to the FDO-DMMSE equalizer in the expected SNR range.

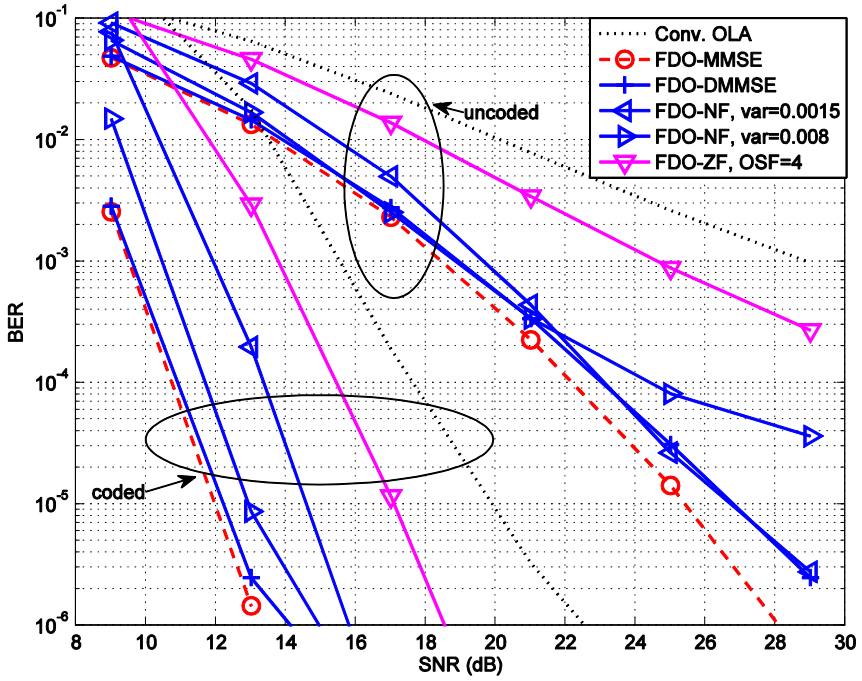

Fig. 3-9. Comparisons of FDO equalizers for ZP MC-CDMA with sufficient GI and ε=5%

The BER performance comparison of the proposed FDO based equalizers in the uncoded and coded ZP MC-CDMA systems over a short multipath delay channel with normalized carrier frequency offset ε=5% (i.e., 5% of the subcarrier spacing) is shown in Fig. 3-9. Compared with the curves in Fig. 3-6, the frequency offset just slightly degrades the BER performance of the FDO based equalizers. In the coded systems, compared to the conventional OLA equalizer, the FDO-MMSE, FDO-DMMSE, FDO-NF (with var=0.008) and FDO-ZF (with OSF=4) equalizers can offer a SNR gain of about 10 dB, 9 dB, 8 dB and 4 dB at the BER of 1×10^{-6}, respectively. In the uncoded system, the BER of the FDO-MMSE, FDO-DMMSE, FDO-NF (with var=0.0015) and FDO-ZF (with OSF=4) equalizers can be significantly reduced from around 1.3×10^{-3} to 3.5×10^{-4}, 5×10^{-6}, 5×10^{-6} and 1×10^{-6} at the SNR of 28 dB, respectively. It means that the proposed FDO based equalizers can tolerate larger frequency offset than the conventional OLA equalizer in the both uncoded and coded systems.

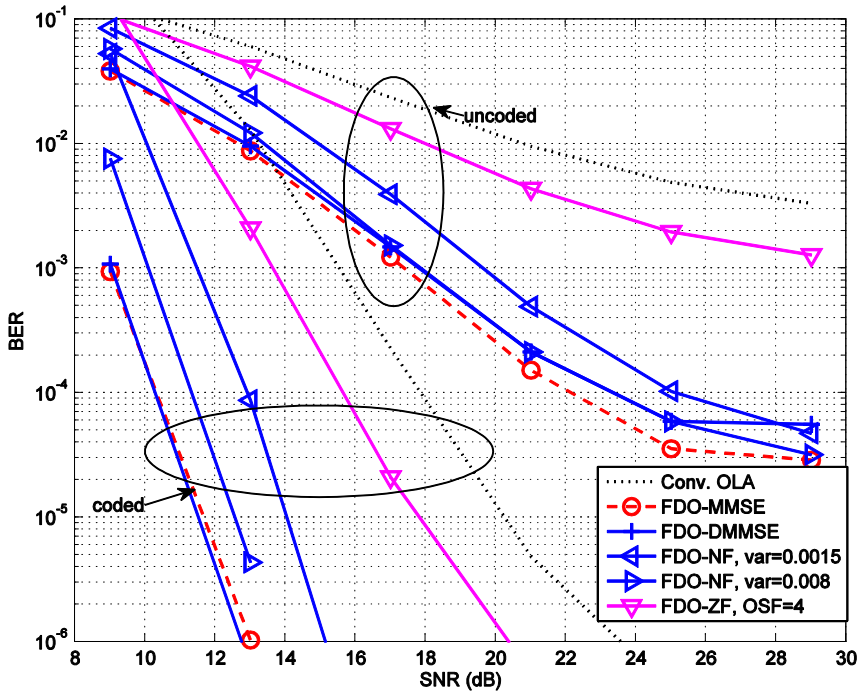

Fig. 3-10. Comparisons of FDO equalizers for ZP MC-CDMA with sufficient GI and f_d=2%

Although our proposed FDO based receivers are designed based on the quasi-static frequency-selective fading channel, they can also work well under a dispersive time-varying fading channel, where the ICI is introduced by Doppler frequency shift. In this case, the channel is varying inside the OFDM symbol, which destroys the orthogonality among the subcarriers. In the simulation, the normalised Doppler frequency shift f_d = 0.02 (i.e. 2% of the symbol rate 1/T) is introduced in the Rayleigh fading channel by using the Matlab function 'rayleighchan'. Since the channel is not fixed for one OFDM symbol, the instantaneous path gain of one sample is adopted as the channel frequency response for the SR, which is obtained from the property 'PathGains' of the Rayleigh channel object. Fig. 3-10 shows that although the FDO based equalizers demonstrate BER floor in high SNR level (e.g., more than 22 dB) in the uncoded system, they can still offer much better BER performance than the conventional OLA equalizer. The FDO-MMSE equalizer can reduce the BER floor from around 4×10^{-3} to 3×10^{-5} level. In the coded system, because the required SNR is low than 22 dB (at BER level of 10^{-6}), the BER performance of the FDO based equalizers are almost not affected by the Doppler frequency shift. Compared with the conventional OLA

equalizer, the FDO-MMSE equalizer can offer SNR gain of 11 dB at a BER of 1×10^{-6}. The FDO-DMMSE and FDO-NF can also offer around 10 dB SNR gain at the BER of 1×10^{-6}. Hence, we can also conclude that the proposed FDO based equalizers can tolerate larger frequency shift than the conventional ZF equalizer.

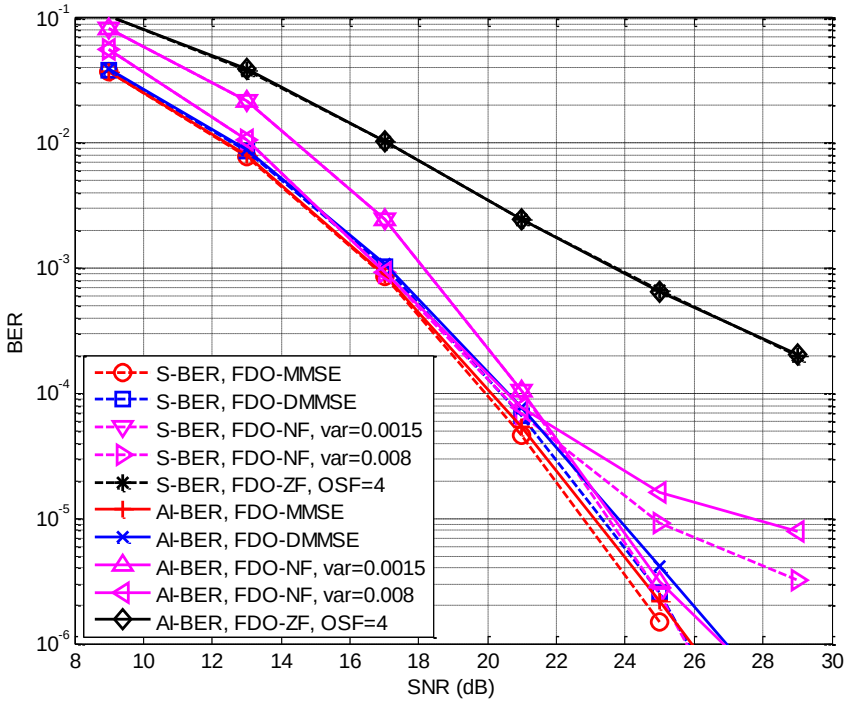

Fig. 3-11. Comparisons between AI-BER and S-BER for uncodedZP MC-CDMA

The BER performance comparison between AI-BER and simulation (i.e., S-BER) for uncoded ZP MC-CDMA system is shown in Fig. 3-11. The AI-BER is calculated based on (3.20) and (3.21). The S-BER is obtained based on the statistics of the number of error bits received in the simulations. We assume that there are no CFO and Doppler frequency shifts for comparison. The curves of AI-BER of all proposed FDO based equalizers are quite close to that counted S-BER from simulations. It means that the AI-BER can represent the performance of the proposed equalizers very well mathematically.

3.7.2 Insufficient Guard Interval

Next, we consider the insufficient guard interval that is insufficient to avoid ISI in long

multipath delay channel. We assume that the multipath interval i is equal to 2. The maximal path delay is Q=15. The guard interval ZP is not enough to avoid ISI and the complete OFDM symbol length is $M=N+Q$=79. In this case, the proposed iterative FDO based equalizers in Section 3.6 shall be adopted. Combing with Section 3.3.1, 3.3.2 and 3.3.3, we have 4 iterative receivers: iterative FDO-MMSE receiver (IT-FDO-MMSE), iterative FDO-DMMSE (IT-FDO-DMMSE), iterative FDO-NF (IT-FDO-NF) and iterative FDO-ZF (IT-FDO-ZF) receivers.

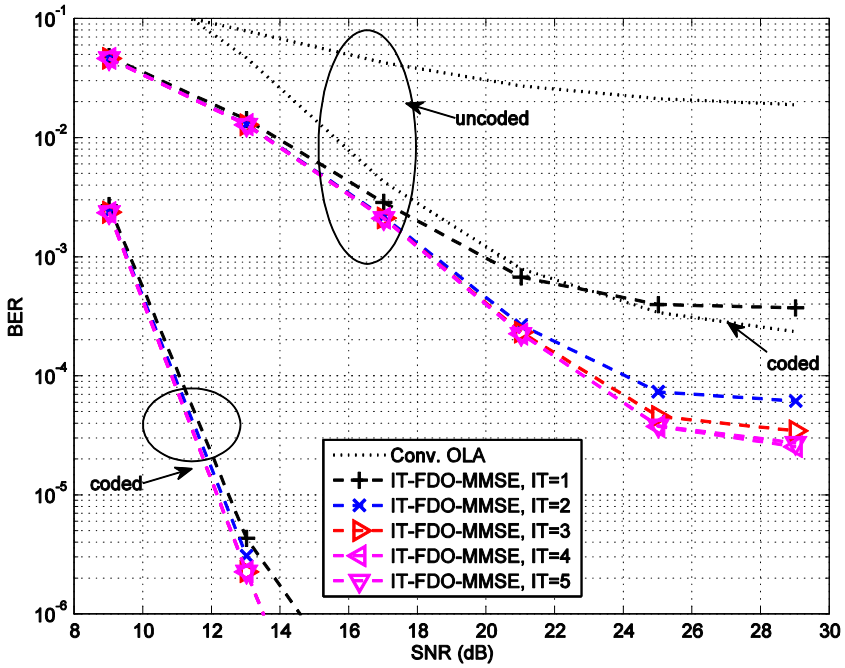

Fig. 3-12. Comparisons of IT-FDO-MMSE for ZP MC-CDMA with insufficient GI and ε=5%

The BER performance comparison of the IT-FDO-MMSE receiver with different iterations in the uncoded and coded ZP MC-CDMA over a long multipath delay channel with normalized carrier frequency offset ε=5% (i.e., 5% subcarrier spacing) is shown in Fig. 3-12. We can find that the curves of the fourth and fifth iterations almost overlap, and are only slightly lower than that of the third iteration in the uncoded ZP MC-CDMA system. It means that 4 iterations are acceptable for the IT-FDO-MMSE receiver. With channel coding, the IT-FDO-MMSE with different iterations can have similar BER performance. It means that only one iteration is acceptable for the IT-FDO-MMSE receiver. Hence, in the following simulations, we choose 4 iterations for the IT-FDO-MMSE in the uncoded system and 1 iteration in the coded system.

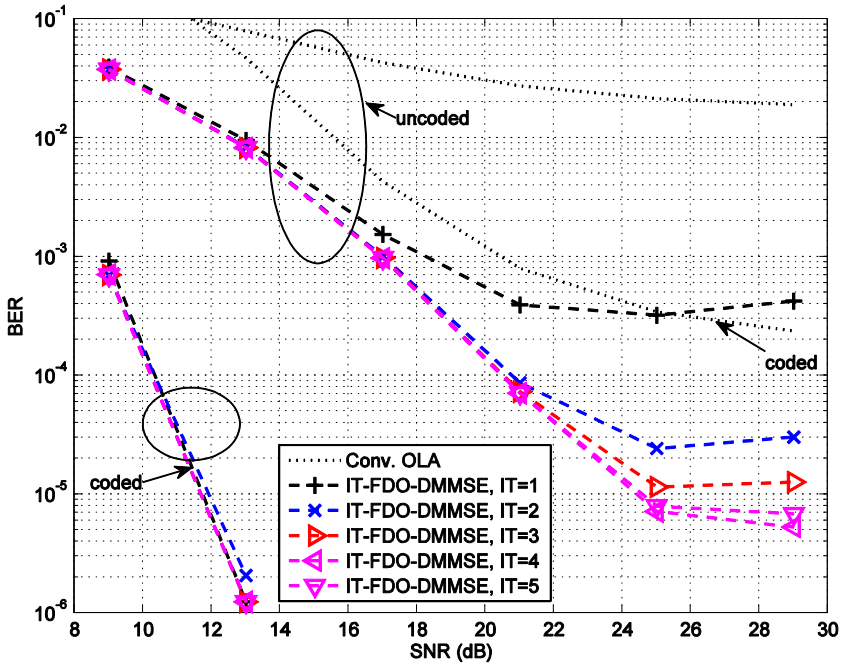

Fig. 3-13. Comparisons of IT-FDO-DMMSE for ZP MC-CDMA with insufficient GI

The BER performance comparison of the IT-FDO-DMMSE receiver with different iterations in the uncoded and coded ZP MC-CDMA over a long multipath delay channel is shown in Fig. 3-13. Same as the IT-FDO-MMSE, the IT-FDO-DMMSE equalizer has similar BER performance after 4 iterations in the uncoded system and almost the same BER performance after the first iteration in the coded system. It means that 4 iterations are acceptable for IT-FDO-DMMSE in the uncoded system and only 1 iteration is also acceptable in the coded system. Hence, in the following simulations, we choose 4 iterations for IT-FDO-DMMSE in the uncoded system and 1 iteration in the coded system.

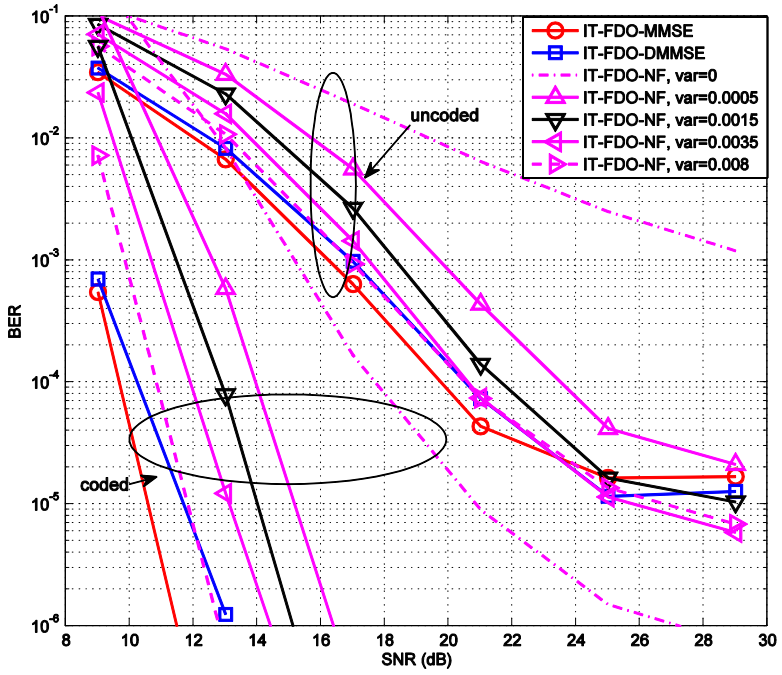

Fig. 3-14. Comparisons of IT-FDO-NF for ZP MC-CDMA with insufficient GI

The BER performance comparison of the IT-FDO-NF receiver with different fixed noise variances in the uncoded and coded ZP MC-CDMA over a long multipath delay channel is shown in Fig. 3-14. For different noise variance, the IT-FDO-NF receiver has the best BER performance when the selected variance matches the SNR range. For example, in the uncoded system, the IT-FDO-NF receiver with variance 0.0035 (about 24.5 dB) has the best BER performance around 25 dB compared to it with other variances. In the coded system, because the expected SNR level (e.g., less than 18 dB) is smaller than that of the uncoded system, the choice of large variance (i.e., 0.008) for the IT-FDO-NF can offer similar BER performance to the IT-FDO-DMMSE.

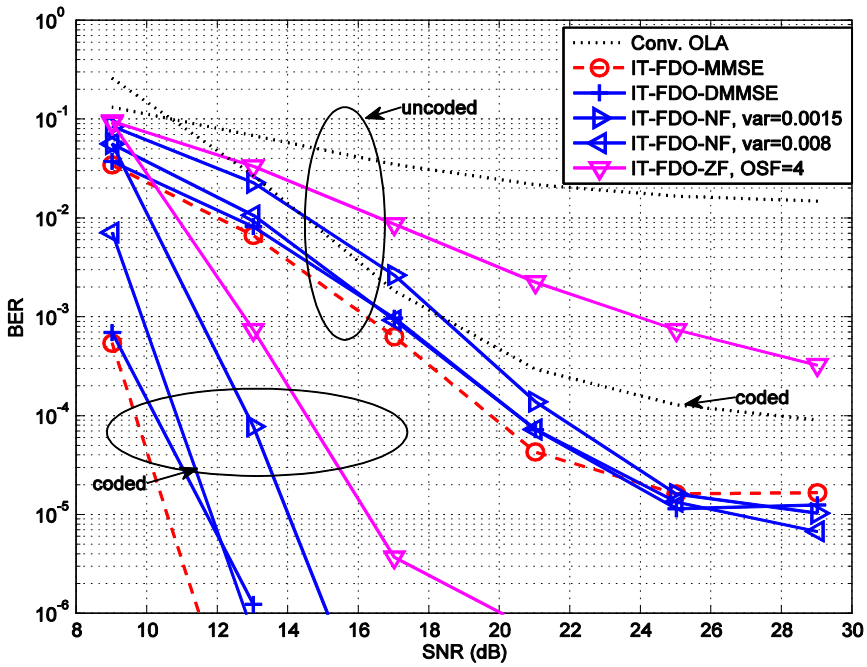

Fig. 3-15. Comparison of FDO equalizers for ZP MC-CDMA with insufficient GI

The BER performance comparison of the proposed equalizers in the uncoded and coded ZP MC-CDMA system over a long multipath delay channel is shown in Fig. 3-15. The conventional OLA equalizer presents a high BER floor due to ISI from the adjacent symbols. The proposed iterative FDO based receivers can significantly improve the BER performance and greatly reduce the BER floor from around 1×10^{-2} to around 1×10^{-5} level in the uncoded system. The IT-FDO-MMSE and IT-FDO-DMMSE receiver can have much better BER performance than IT-FDO-ZF receiver with OSF=4. In high SNR area (e.g., SNR > 23dB), the IT-FDO-DMMSE and IT-FDO-NF receivers with variance 0.0035 and 0.008 can even offer better BER performance than the IF-FDO-MMSE receiver after 4 iterations. In the coded system, the IT-FDO-MMSE can still achieve the best BER performance. The IT-FDO-DMMSE receiver can offer the moderate BER performance with moderate complexity compared with the IT-FDO-MMSE and the IT-FDO-ZF. The less complex IT-FDO-NF receiver can have similar BER curve to the IT-DO-DMMSE if an appropriate variance is chosen (e.g., 0.008) in the expected SNR range. Although the IT-FDO-ZF is not as good as other FDO based equalizers in terms of BER performance, it still can offer better BER performance than the conventional OLA equalizer and it is easier to implement compared

with other equalizers.

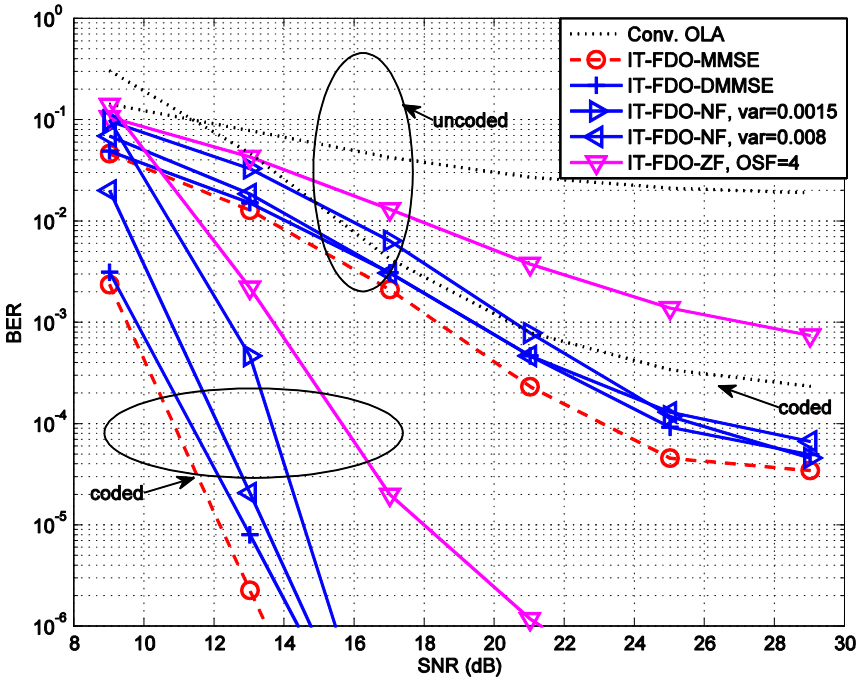

Fig. 3-16. Comparisons of FDO equalizers for ZP MC-CDMA with insufficient GI and ε=5%

The BER performance comparison of proposed equalizers in the uncoded ZP MC-CDMA over a long multipath delay channel with normalized carrier frequency offset ε=5% (i.e., 5% of subcarrier spacing) is shown in Fig. 3-16. We can find that the frequency offset ε=5% can only slightly reduce the BER performance of the proposed iterative FDO receivers in the uncoded system. In the coded system, the effect of frequency offset ε=0.05 is insignificant. Although the conventional OLA equalizer has a large BER floor at around 10^{-4} level, the FDO-MMSE, FDO-DMMSE, FDO-NF (with var=0.008) and FDO-ZF (with OSF=4) equalizers can easily achieve a BER of 1×10^{-6} at the SNR around 13.5 dB, 14.3 dB, 14.8 dB, and 21 dB, respectively. In the uncoded system, the FDO-MMSE, FDO-DMMSE, FDO-NF (with var=0.0015) and FDO-ZF (with OSF=4) equalizers can reduce the BER floor from 2×10^{-2} to 3.5×10^{-5}, 5×10^{-5}, 5×10^{-5} and 7.5×10^{-4}, respectively. In the both uncoded and coded systems, the proposed iterative FDO receivers outperform the OLA equalizer on the BER performance. It means the proposed iterative FDO receivers can tolerate large carrier frequency offset.

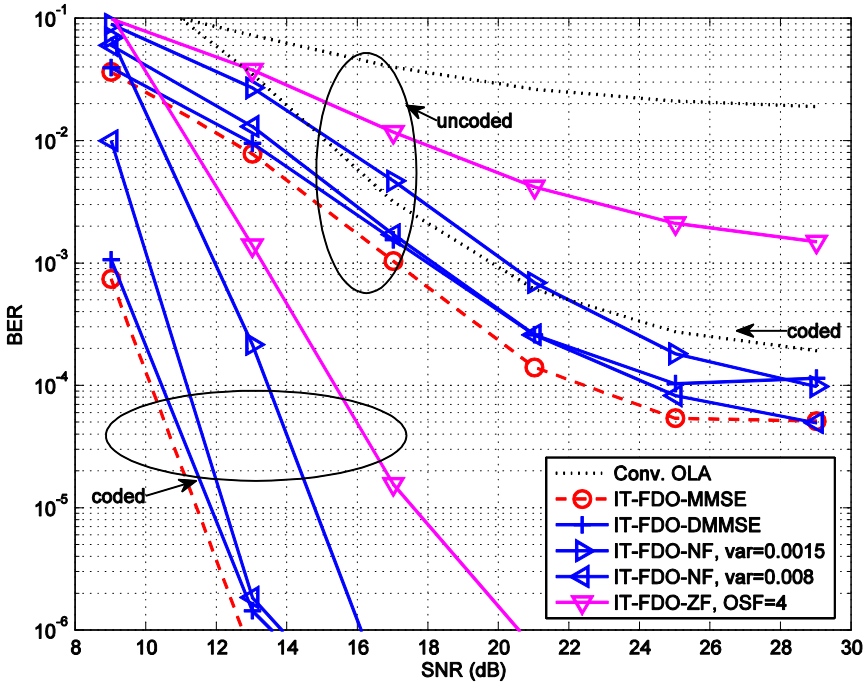

Fig. 3-17. Comparison of FDO equalizers for ZP MC-CDMA with insufficient GI and f_d=2%

The BER performance comparison of proposed equalizers in the uncoded ZP MC-CDMA system over a long multipath delay with normalized Doppler frequency shift f_d=0.02 (i.e., 2%/T) is shown in Fig. 3-17. Compared with the curves in Fig. 3-15, the effect of Doppler frequency shift for the proposed FDO based receivers is quite small in the coded system. In the uncoded system, the Doppler frequency shift slightly degrades the BER performance of the proposed iterative FDO receivers in high SNR level. Compared to the conventional OLA equalizer, the IT-FDO-MMSE receiver can achieve the much better BER performance in all SNR level and can significantly reduce the BER floor from 2×10^{-2} to 5×10^{-5}, it is stable than IT-FDO-DMMSE and IT-FDO-NF receivers. In the coded system, although the IT-FDO-MMSE has the best BER performance among the 4 proposed FDO equalizers, it only can achieve about 1 dB SNR gain at a BER of 1×10^{-6} compared with the IT-FDO-DMMSE and the IT-FDO-NF. Because the IT-FDO-NF does not require to calculate the matrix inverse and to estimate the noise power, it is quite easy to implement. It means IT-FDO-NF is a good choice for a practical application.

3.7.3 Comparison between ZP OFDM and ZP MC-CDMA Systems

Finally we compare the proposed FDO based equalizers between ZP OFDM and ZP MC-CDMA systems. We assume that the same multipath channel (used in Section 3.7.1 and 3.7.2) is used in the both ZP OFDM and ZP MC-CDMA systems. For short multipath delay channel, we assume i=1 and Q=8. For long multipath delay channel we assume that i=2 and Q=15, and the iterative FDO based receivers are adopted.

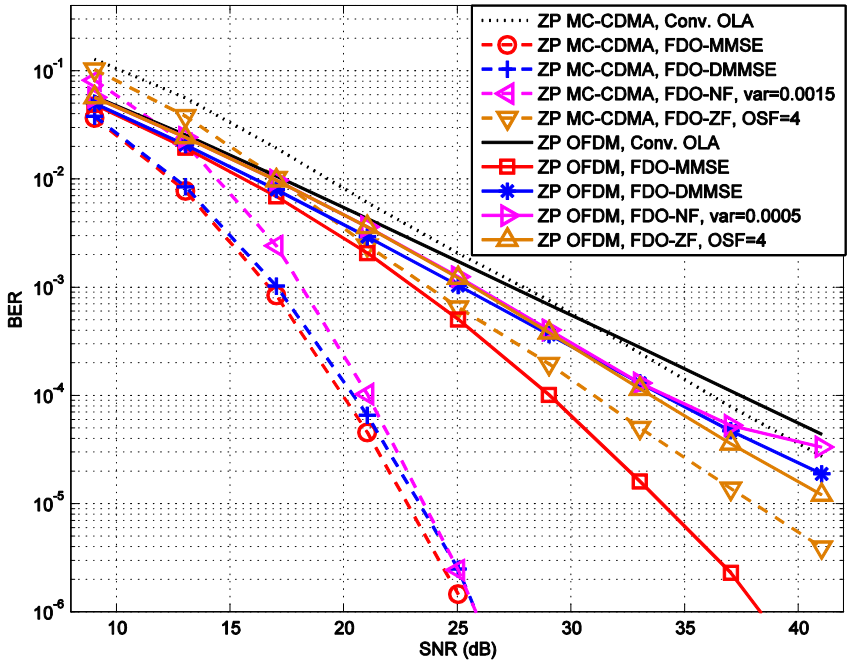

Fig. 3-18. Comparison between uncoded ZP MCM systems with sufficient GI

The BER performance comparison of the FDO-based equalizers between the uncoded ZP OFDM and ZP MC-CDMA system over a short multipath delay channel is shown in Fig. 3-18. The FDO-ZF equalizer in the uncoded ZP MC-CDMA system is just better than it in the uncoded ZP OFDM system when SNR is more than about 16 dB. However, The FDO-MMSE, FDO-DMMSE and FDO-NF have much better BER performance in the uncoded ZP MC-CDMA system than they in the uncoded ZP OFDM system. Compared with the FDO-MMSE in the uncoded ZP OFDM system, the FDO-MMSE in the uncoded ZP MC-CDMA system can offer about 12 dB SNR gain at a BER of 1×10^{-6}. The FDO-DMMSE and FDO-NF can even achieve

more than 20 dB SNR gain at a BER of 1×10^{-5} level in the uncoded ZP MC-CDMA system compared with them in the uncoded ZP OFDM system. It means that in the uncoded ZP MC-CDMA system, the FDO based equalizers can benefit from the large frequency diversity gain due to the spreading codes.

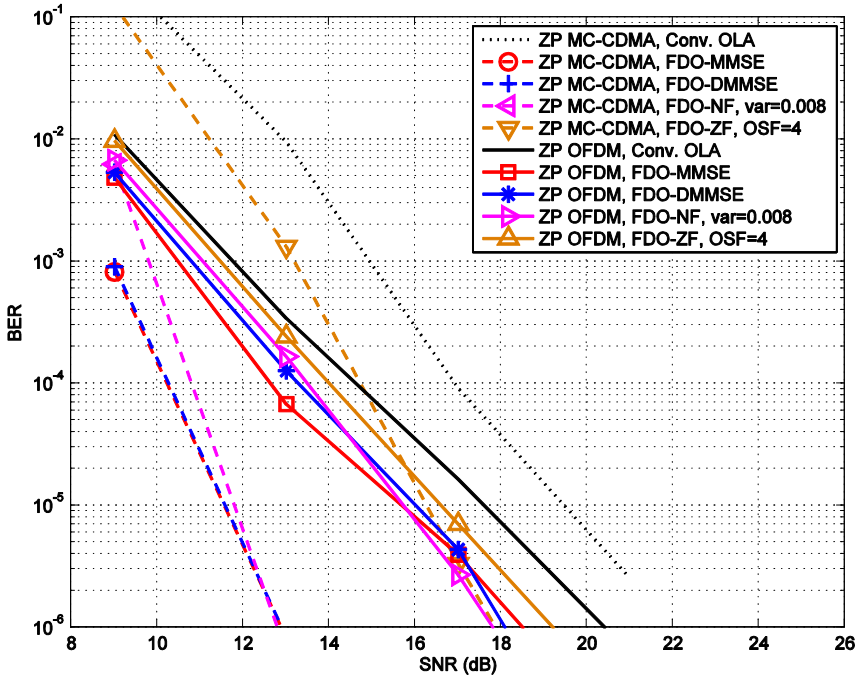

Fig. 3-19. Comparison between coded ZP MCM systems with sufficient GI

The BER performance comparison of the FDO-based equalizers between the coded ZP OFDM and ZP MC-CDMA systems over a short multipath delay channel is shown in Fig. 3-19. Although the conventional OLA equalizer cannot offer better BER performance in the coded ZP MC-CDMA system compared with it in the coded ZP OFDM system, the proposed FDO-MMSE, FDO-DMMSE and FDO-NF can have about 6 dB SNR gain at a BER of 1×10^{-6} level in the coded ZP MC-CDMA system compared with them in the coded ZP OFDM system. However, the FDO-ZF equalizer shows better performance in the coded ZP MC-CDMA system than it in the coded ZP OFDM only when SNR is more than about 16 dB. It means that in the coded ZP MC-CDMA system, the proposed FDO-MMSE, FDO-DMMSE and FDO-NF can benefit from the frequency diversity gain caused by the spreading codes. The FDO-ZF can benefit from the frequency

diversity gain when SNR becomes large, e.g , more than 16 dB.

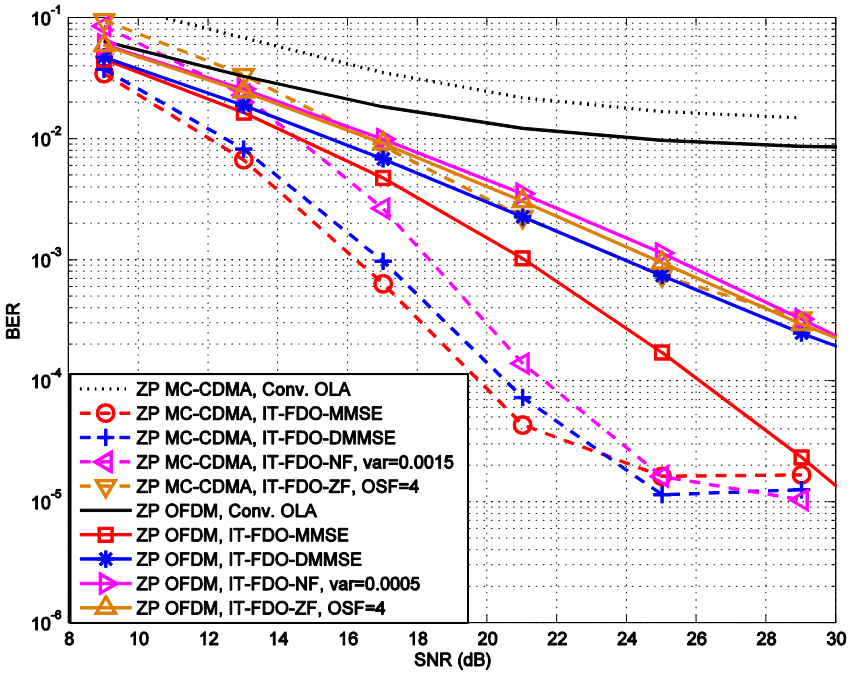

Fig. 3-20. Comparison between uncoded ZP MCM systems with insufficient GI

The BER performance comparison of the FDO-based equalizers between the uncoded ZP OFDM and ZP MC-CDMA system over a long multipath delay channel is shown in Fig. 3-20. Although the proposed FDO-MMSE, FDO-DMMSE and FDO-NF present a BER floor at 1×10^{-5} level in the uncoded ZP MC-CDMA system, their BER curves can more quickly fall to 1×10^{-5} level compared with them in the uncoded ZP OFDM. Because the proposed iterative receivers cannot fully remove the ISI from the adjacent OFDM symbols, which will introduce additional IUI between each users and finally degrade the BER performance. However, the proposed FDO equalizers in the uncoded ZP OFDM system do not show the BER floor in the high SNR level. Hence, if the SNR is not large enough, the proposed FDO equalizers in the uncoded ZP MC-CDMA can have better BER performance than they in the uncoded ZP OFDM. For example, when SNR is small than 29 dB, the FDO-MMSE equalizer can have better BER performance in the uncoded ZP MC-CDMA than it in the uncoded ZP OFDM.

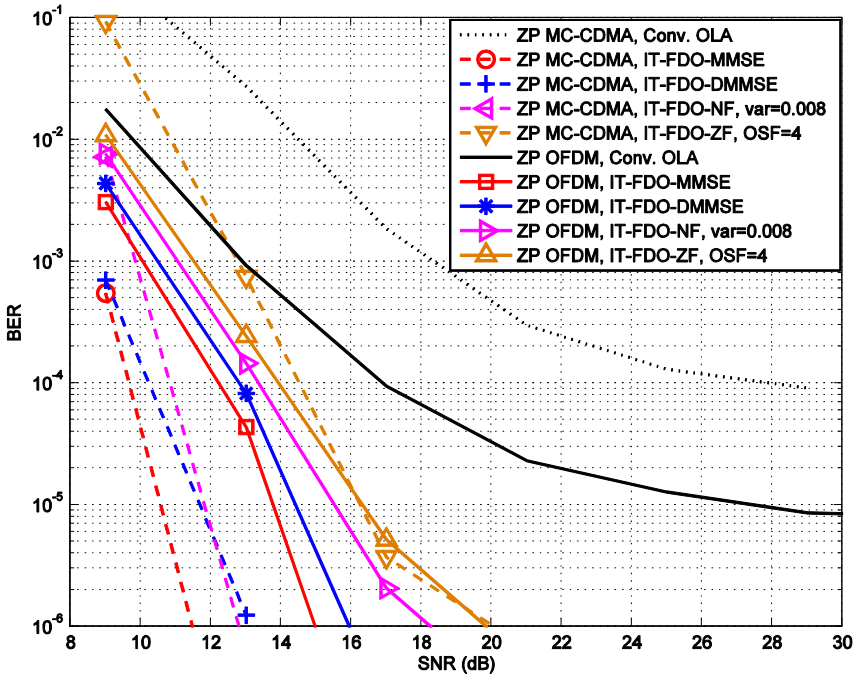

Fig. 3-21. Comparison between coded ZP MCM systems with insufficient GI

The BER performance comparison of the FDO-based equalizers between the coded ZP OFDM and ZP MC-CDMA system over a long multipath delay channel is shown in Fig. 3-21. With channel coding, the proposed FDO-MMSE, FDO-DMMSE and FDO-NF equalizers can achieve a SNR gain of 4 dB, 4 dB and 5.8 dB in the ZP MC-CDMA system compared with them in the ZP OFDM system at a BER of 1×10^{-6}, respectively. The FDO-ZF equalizer has similar BER performance in the coded ZP MC-CDMA and the coded ZP OFDM system. The proposed FDO-MMSE, FDO-DMMSE and FDO-NF can still benefit from the frequency diversity gain caused by the spreading codes in the coded system even when the guard interval is insufficient to avoid ISI. However, compared with the results in Fig. 3-19, the SNR gain achieved at a BER of 1×10^{-6} is slightly reduced due to the residual ISI.

In summary, the proposed FDO-ZF equalizer in ZP MC-CDMA system can show better BER performance than it in ZP OFDM system over the short multipath delay channel, and may not show better performance in ZP MC-CDMA over the long multipath delay channel due to the IUI introduced by the SR method. Similarly, the proposed FDO-MMSE, FDO-DMMSE and FDO-NF

in ZP MC-CDMA system can achieve much better BER performance than they in ZP OFDM system due to the frequency diversity gain caused by the spreading code. However, for the long multipath delay channel, the SR method will introduce additional IUI in ZP MC-CDMA system, which will cause the BER floor in the high SNR range for the proposed FDO equalizers.

3.8 Conclusions

In this chapter, we investigate the FDO based equalizers for ZP MCM system that includes ZP OFDM and ZP MC-CDMA systems. Four FDO based equalizers, i.e., FDO-MMSE, FDO-DMMSE, FDO-NF and FDO-ZF equalizers are designed in this chapter. The expressions of the AI-BER for FDO based equalizers are developed and verified. All the four FDO based equalizers can offer better BER performance than the conventional ZF equalizer under different channel environment including multipath, frequency offset and Doppler frequency shift. The FDO-MMSE equalizer can offer the best BER performance, but the implementation of it is quite complex because it requires the calculation of matrix inverse. The FDO-ZF equalizer is easy to be implemented, but the BER performance of it is not as good as that of the FDO-MMSE, FDO-DMMSE and FDO-NF equalizers. One good feature of the FDO ZF equalizer is that the BER performance of it can be improved by increasing the oversampling factor. The FDO-DMMSE equalizer can offer moderate BER performance with moderate complexity compared with the FDO-MMSE and the FDO-ZF. To further reduce the complexity of implementation of the FDO-DMMSE equalizer, we propose the FDO-NF equalizer with fixed noise variance, which can offer good BER performance similar to the FDO-DMMSE in the expected SNR range. It is a trade-off to select a suitable FDO based equalizer for a practical application.

In the case that the channel delay is longer than the guard interval in ZP OFDM and ZP MC-CDMA system, the iterative FDO based equalizers that combine the SR method and FDO technique are designed to achieve much better BER performance than the conventional equalizer. In order to reduce the ISI from the adjacent symbols, the SR method is proposed to be used before FDO based equalizers. The simulations are performed to verify the performance of the proposed equalizers. In addition, combining with channel coding such as convolutional encoder, the

proposed FDO based equalizers can offer much better BER performance than the conventional equalizer.

Finally we compare the proposed FDO based equalizers in ZP OFDM and ZP MC-CDMA systems. The proposed FDO-ZF equalizer in ZP MC-CDMA system can show better BER performance than it in ZP OFDM system over the short multipath delay channel, and may not show better performance in ZP MC-CDMA over the long multipath delay channel due to the IUI introduced by the SR method. Similarly, the proposed FDO-MMSE, FDO-DMMSE and FDO-NF in ZP MC-CDMA system can benefit from the frequency diversity gain caused by the spreading codes and can achieve much better BER performance in ZP MC-CDMA system than they in ZP OFDM system. However, for the long multipath delay channel, the SR method will introduce additional IUI in ZP MC-CDMA system, which will cause the BER floor in the high SNR range for the proposed FDO equalizers.

4 Frequency Domain Oversampling for CP Based MCM Systems

4.1 Introduction

In Chapter 3, we have demonstrated that the FDO based equalizers can offer better BER performance and tolerate larger interference caused by frequency offset, Doppler frequency shift and multipath fading channel in ZP OFDM system and ZP MC-CDMA system compared with the conventional MMSE equalizer. However, there is also a high demand to have the high performance equalizers for CP based MCM systems because CP OFDM has been widely used in various communication systems such as DAB, DVB, IEEE802.11a/g/n, IEEE802.16d/e/m and LTE due to its simple implementation. Hence, in this chapter, we extend our proposed FDO based equalizers for CP based MCM systems such as CP OFDM and CP MC-CDMA. In OFDM system, two adjacent OFDM symbols always overlap due to the multipath fading channel, which will cause inevitable ISI if the guard interval is not removed. The conventional MMSE receiver always discards the CP part to avoid ISI. However, since the CP part also includes the useful signal, it is possible to improve the BER performance by fully take advantage of the useful information of the CP part. In this chapter we propose the MMSE equalizer combining with the frequency domain oversampling method to fully exploit the signal energy of the CP part.

The proposed receivers consist of two stages. At the first stage, the channel information is estimated by using traditional methods, and the received OFDM symbols are equalized by the conventional receiver. At the second stage, the CP and tail parts of the current OFDM symbol are reconstructed by eliminating the ISI from the previous and the subsequent symbols. The re-constructed OFDM symbol including CP and tail parts is oversampled in the frequency domain and equalized by using the proposed MMSE or ZF equalizer. Simulations show that the proposed FDO approach with MMSE and ZF equalizer can achieve much better performance than the traditional CP OFDM receiver and even better than the FSFD-MMSE for ZP OFDM in [28] on a

multipath channel. The proposed receivers are quite different from FSFD-MMSE that is suitable for ZP OFDM only. It is the first time combining the OFDM symbol reconstruction and FDO method for CP OFDM, which enables the MMSE equalizer to more efficiently exploit the received signal and the channel state information in the high dimensional space and greatly suppress the interference, hence to improve the system BER performance for frequency selective channel.

4.2 System Model for CP based MCM System

4.2.1 CP Based MCM System

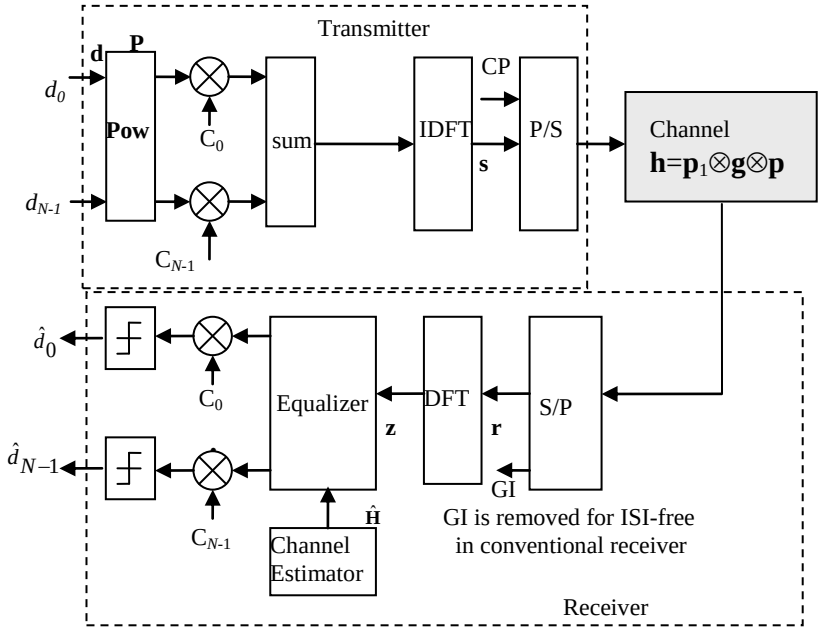

Fig. 4-1. Basic structure of conventional CP OFDM and CP MC-CDMA systems.

The structure of the conventional CP based MCM systems (i.e., CP OFDM and CP MC-CDMA) is shown in Fig. 4-1. We assume that the OFDM symbol duration is *T* and sampling interval in the system is *T/N*, we further assume that the number of user is also *N* for simplicity. We describe all the signals in discrete sequence. The input information **d** is scaled with power matrix **P** and spread over all subcarriers with spreading code **C**. For OFDM system, **P** and **C** shall be set to **I**, i.e., each user transmits the data on one subcarrier with the same power. The result is modulated by the *N*-

point IDFT matrix $\mathbf{F}_N^{-1}$ to generate time domain signal **s**. The signal **s** will be passed through a transmitter filter $\mathbf{p}_1$, frequency-selective channel **g** and receiver filter **p** in sequence. It is reasonable to define the equivalent channel **h** as $\mathbf{h}=\mathbf{p}_1\otimes\mathbf{g}\otimes\mathbf{p}$, where $\otimes$ denotes the convolution operation. The received signal **r**, excluding the CP part, is converted to frequency domain signal **z** by *N*-point DFT matrix $\mathbf{F}_N$ for channel estimation and equalization. For better understanding, we define the related signals for one OFDM symbol period as follows:

Assume that $\mathbf{F}_N$ is the *N*-point DFT matrix. The elements $F_{n,m}$ of the matrix $\mathbf{F}_N$ are defined by:

$$F_{n,m}=\frac{1}{\sqrt{N}}e^{-j2\pi\frac{nm}{N}} \qquad (n,m=0,1,...,N-1). \tag{4.1}$$

We can define the matrix $\mathbf{F}_{\text{cp}}^{-1}$ for the modulation of the CP part with length *G*, where $\mathbf{F}_{\text{cp}}^{-1}$ is the last *G* rows of $\mathbf{F}_N^{-1}$ (i.e., the IDFT matrix, which is the inverse of $\mathbf{F}_N$). The transmitted signal is defined as

$$\mathbf{s}=[s_0\ s_1\ \ldots\ s_{L-1}]^{\text{T}}=\begin{bmatrix}\mathbf{F}_{\text{cp}}^{-1}\\ \mathbf{F}_N^{-1}\end{bmatrix}\mathbf{CPd}, \tag{4.2}$$

where *L* is the length of transmitted signal and $L=N+G$, $\mathbf{C}=[\mathbf{c}_0,\mathbf{c}_1,\ldots,\mathbf{c}_{N-1}]$ $\frac{1}{\sqrt{N}}$ is the normalized spreading code satisfying $\mathbf{C}^{\text{H}}\mathbf{C}=\mathbf{I}$, **I** is the $N\times N$ identity matrix, $\mathbf{d}=[d_0,\ d_1,\ \ldots,\ d_{N-1}]^{\text{T}}$ and $\mathbf{P}=\text{diag}\left\{\sqrt{P_0},\sqrt{P_1},...,\sqrt{P_{N-1}}\right\}$ represent modulated data symbols and transmission power adjustment for *N* users respectively. $\mathbf{P}=\mathbf{I}$ means that the power for each user is not adjusted.

If we consider that $\mathbf{C}=\mathbf{I}$ and $\mathbf{P}=\mathbf{I}$, we can have a CP OFDM system. Hence, we can say that MC-CDMA system is a kind of OFDM system. The channel estimation and channel equalization for CP OFDM can also be able to be used for MC-CDMA system.

We consider the time varying multipath fading channel described by the WSSUS model, and assume the number of paths is *Q*. The equivalent channel impulse response can be modeled as

$$h(t,\tau)=\sum_{q=0}^{Q-1}h_q(t)\delta(\tau-\tau_q) \tag{4.3}$$

where the channel path $h_q(t)$ of delay τ_q is a complex random process representing the multipath components with different Doppler frequency shifts and $\delta(\tau-\tau_q)$ is Kronecker delta function. The channel can be characterized by a correlation function

$$\mathrm{E}[h_q(t)h_{q+\Delta q}(t+\Delta t)^*]=\sigma_q^2\delta(\Delta q)\mathrm{J}_0(2\pi f_d\Delta t) \tag{4.4}$$

where $\mathrm{J}_0(\ )$ is the zeroth-order Bessel function of the first kind, f_d is the maximum Doppler frequency, σ_p^2 is the variance of $h_q(t)$. Please note that the channel $h(t,\tau)$ changes with time within an OFDM symbol due to the Doppler frequency shifts. It's difficult to completely compensate the effect of the Doppler frequency shifts. Since the residual Doppler frequency shifts are unknown to the receiver, we can simply assume that the channel is quasi-static frequency-selective fading channel modeled as (4.5) for analysis. The Doppler effect is introduced in simulations for BER performance comparison.

$$h(\tau)=\sum_{q=0}^{Q-1}h_q\delta(\tau-\tau_q),\ \text{and}\ \sum_{q=0}^{Q-1}\mathrm{E}[|h_q|^2]=1 \tag{4.5}$$

and the frequency response of the channel $h(\tau)$ is given by

$$H(f)=\int_0^{\infty}h(\tau)e^{-j2\pi f\tau}d\tau=\sum_{q=0}^{Q-1}h_q e^{-j2\pi f\tau_q}\ . \tag{4.6}$$

In discrete time domain, we can assume the delays $\tau_q = q$ is an integer from 0 to Q-1, which represents a multiple of the sample period in (4.5). Hence, the discrete channel is $\mathbf{h}_Q=[h_0\ \ldots\ h_{Q-1}]^{\mathrm{T}}$. For ISI free system, the length Q of equivalent channel shall be less than G. The received one OFDM symbol $\mathbf{y}_M=[y_0\ y_1\ \ldots\ y_{M-1}]^{\mathrm{T}}$ (where $M=L+Q$) after channel can be represented by the convolution of equivalent channel impulse response and the transmitted signals **s**. i.e.,

$$\mathbf{y}_M = \Lambda_M(\varepsilon)\Xi_{ML}^{\mathrm{t}}\begin{bmatrix}\mathbf{F}_{\mathrm{cp}}^{-1}\\ \mathbf{F}_N^{-1}\end{bmatrix}\mathbf{CPd}+\mathbf{v} = \Lambda_M(\varepsilon)\Xi_M^{\mathrm{c}}\begin{bmatrix}\mathbf{F}_{\mathrm{cp}}^{-1}\\ \mathbf{F}_N^{-1}\\ \mathbf{0}_Q\end{bmatrix}\mathbf{CPd}+\mathbf{v} \tag{4.7}$$

where Ξ_{ML}^{t} is an $M \times L$ lower triangular Toeplitz matrix with the first column $\mathbf{h}=[h_0 \ldots h_{Q-1}\ 0 \ldots 0]^{\mathrm{T}}$ and Ξ_M^{c} is an $M \times M$ circular matrix with the same first column $\mathbf{h}$; $\mathbf{0}_Q$ is $Q \times N$ zero matrix; $\mathbf{v}=[v_0\ v_1 \ldots v_{M-1}]^{\mathrm{T}}$ denotes zero mean Gaussian noise with variance σ^2; ε is the residual carrier frequency offset (CFO) between the transmitter and receiver after frequency offset compensation, and the diagonal matrix $\Lambda_M(\varepsilon)$ is expressed as $\Lambda_M(\varepsilon)$ = diag{1, $e^{j2\pi\varepsilon/N}$, $e^{j2\pi\varepsilon 2/N}$ …, $e^{j2\pi\varepsilon(M-1)/N}$}, which represents the effect of CFO.

For conventional CP based MCM receiver, The CP part is removed to eliminate ISI. After N-point DFT, in frequency domain, the $N \times 1$ data $\mathbf{z}_N = [z_0\ z_1 \ldots z_{N-1}]^{\mathbf{T}}$ can be expressed by

$$\mathbf{z}_N = \mathbf{F}_N\Lambda_N(\varepsilon)\Xi_N^{\mathrm{c}}\mathbf{F}_N^{-1}\mathbf{CPd}+\mathbf{F}_N\mathbf{v}_N = \tilde{\mathbf{H}}(\varepsilon)\mathbf{F}_N\Lambda_N(\varepsilon)\mathbf{F}_N^{-1}\mathbf{CPd}+\mathbf{w}_N \tag{4.8}$$

where $\tilde{\mathbf{H}}(\varepsilon)$ is a diagonal matrix with $\mathbf{H}=\mathbf{F}_N\mathbf{\Lambda}_N(\varepsilon)\ [h_0 \ldots h_{Q-1}\ 0 \ldots 0]^{\mathrm{T}} = [H_0(\varepsilon), \ldots, H_{N-1}(\varepsilon)]^{\mathrm{T}}$ on the main diagonal, and $\mathbf{w}_N=\mathbf{F}_N\mathbf{v}_N = [w_0\ w_1 \ldots w_{N-1}]^{\mathrm{H}}$ denotes zero mean Gaussian noise with variance σ^2 in frequency domain where $\mathbf{v}_N=[v_0\ v_1 \ldots v_{N-1}]^{\mathrm{T}}$. $H_n(\varepsilon)$ is actually the sample of (4.6) at frequency $f=n+\varepsilon$. Since the residual CFO ε is unknown to the receiver, we can assume ε=0 for the following analyses, which leads to expression $\Lambda_N(\varepsilon)=\mathbf{I}$. The residual CFO is introduced in the simulation for BER performance comparison.

4.2.2 Conventional CP OFDM Equalization

For the CP OFDM system, we have **C**=**I** and **P**=**I**. Usually the transmitted data **d** can be regarded as a random variable and assume that $\mathrm{E}\{\mathbf{dd}^{\mathrm{H}}\}=\mathbf{I}$. The optimal MMSE receiver for CP OFDM can be derived according to the orthogonality principle, i.e., the estimation error $\mathbf{d}\text{-}\hat{\mathbf{d}}_{\mathrm{MMSE}}$ shall be orthogonal to the known random variable $\mathbf{z}_N$. i.e., $\mathrm{E}\{(\mathbf{d}-\hat{\mathbf{d}}_{\mathrm{MMSE}})\mathbf{z}_N^{\mathrm{H}}\}=\mathbf{0}$, Based on

(4.8), the MMSE receiver for CP OFDM can be derived as follows

$$\hat{\mathbf{d}}_{\mathrm{MMSE}} = \tilde{\mathbf{H}}^{\mathrm{H}}(\tilde{\mathbf{H}}\tilde{\mathbf{H}}^{\mathrm{H}} + \mathbf{I}\sigma^2)^{-1}\mathbf{z}_N \tag{4.9}$$

where $\tilde{\mathbf{H}} = \tilde{\mathbf{H}}(0)$ with ε=0. The ZF receiver can be easily obtained as (4.10) by ignoring the noise part.

$$\hat{\mathbf{d}}_{\mathrm{ZF}} = \tilde{\mathbf{H}}^{-1}\mathbf{z}_N . \tag{4.10}$$

Since $\tilde{\mathbf{H}}$ is a diagonal matrix, the received data on subcarrier k can be represented as $z_k = H_k d_k + V_k$. Therefore, the optimal MMSE and ZF estimators of CP OFDM can be reduced to the N scalar MMSE estimator $\hat{d}_{k,\,\mathrm{MMSE}} = H_k^{\mathrm{H}}(H_k H_k^{\mathrm{H}} + \sigma^2)^{-1} z_k$ and the ZF estimator $\hat{d}_{k,\mathrm{ZF}} = H_k^{-1} z_k$, respectively. The MMSE estimate is actually scaled version of ZF estimate, which means that the MMSE receiver will not improve the error rate performance compared to ZF receiver ([18], [19]). Hence, for the conventional CP OFDM receiver, we only adopt the practical ZF receiver in (4.10) for reference.

Similarly, for CP MC-CDMA system, based on (4.8), the conventional ZF receiver can be obtained as (4.11)

$$\hat{\mathbf{d}}_{\mathrm{ZF,MC\text{-}CDMA}} = \mathbf{P}^{-1}\mathbf{C}^{\mathrm{H}}\tilde{\mathbf{H}}^{-1}\mathbf{z}_N . \tag{4.11}$$

4.2.3 Channel Estimation for CP OFDM

It is necessary to evaluate the performance of our proposed receivers with estimated channel state information since the actual channel is unknown to the receiver. The estimation of channel **H** has been studied in numerous papers ([50]-[57]). Here we only review the basic least-squares (LS) channel estimation for CP OFDM with comb-type pilot that is used in simulations for performance comparison.

For comb-type pilot symbols (i.e., parts of subcarriers are pilot carrier) [57], we assume that the number of pilot subcarriers is N_{p}. the channel information of the pilot carriers

$\boldsymbol{\lambda} = [\lambda_0 \quad \lambda_1 \quad \cdots \quad \lambda_{N_P-1}]^{\mathrm{T}}$ in the frequency domain can be estimated by the LS method first.

$$\hat{\lambda}_k = R_k / d_k \tag{4.12}$$

where k denotes the index of the pilot carriers. For simplicity, here we assume that the N_p pilot subcarriers are evenly distributed and the channel length Q is less than or equal to N_p. Hence, the simple channel estimation can be achieved in (4.13) as follows: Firstly according to (4.12) we obtain the estimated sub-channels $\boldsymbol{\lambda}$ of the pilot subcarriers in frequency domain and we next calculate time domain channel information $\mathbf{h}=[h_0\ h_1\ \ldots\ h_{Np-1}]^{\mathrm{T}}$ by converting $\boldsymbol{\lambda}$ to time domain with N_p-point IDFT and forcing h_k (where $k>Q-1$) to 0 for noise reduction [51]. Then we extend N_p-point time domain channel to N points by padding zeros, and convert the N points channel to frequency domain. Finally we obtain channel information $\hat{\mathbf{H}}$ for all subcarriers.

$$\begin{aligned} \hat{\mathbf{h}} &= \mathbf{F}_{N_p}^{-1}\hat{\boldsymbol{\lambda}} \\ \hat{\mathbf{H}} &= \mathbf{F}_N \begin{bmatrix} \hat{\mathbf{h}} \\ \mathbf{0} \end{bmatrix} \end{aligned} \tag{4.13}$$

where $\hat{\mathbf{h}}$ is the estimated channel impulse response in time domain and $\mathbf{0}$ is $(N\text{-}Np)\times 1$ zero matrix, $\mathbf{F}_{N_p}$ is the N_p-points DFT matrix and can be derived from $\mathbf{F}_N$ based on equation (4.1). i.e., the columns and rows of $\mathbf{F}_N$ are chosen evenly to form $\mathbf{F}_{N_p}$ according to the pilot position.

Since MC-CDMA is an OFDM based system, the above channel estimation can also suitable for MC-CDMA.

4.3 Proposed iterative FDO Receivers for CP Based MCM System

In this section, we propose a new frequency oversampling method to improve the BER performance of the traditional CP OFDM and CP MC-CDMA receiver based on the above system model.

4.3.1 Symbol Reconstruction

The received adjacent OFDM symbols interfere with each other due to multipath channel. In order to remove the ISI of the x-th symbol, we need estimate the adjacent symbols by using the

estimated channel and transmitted data.

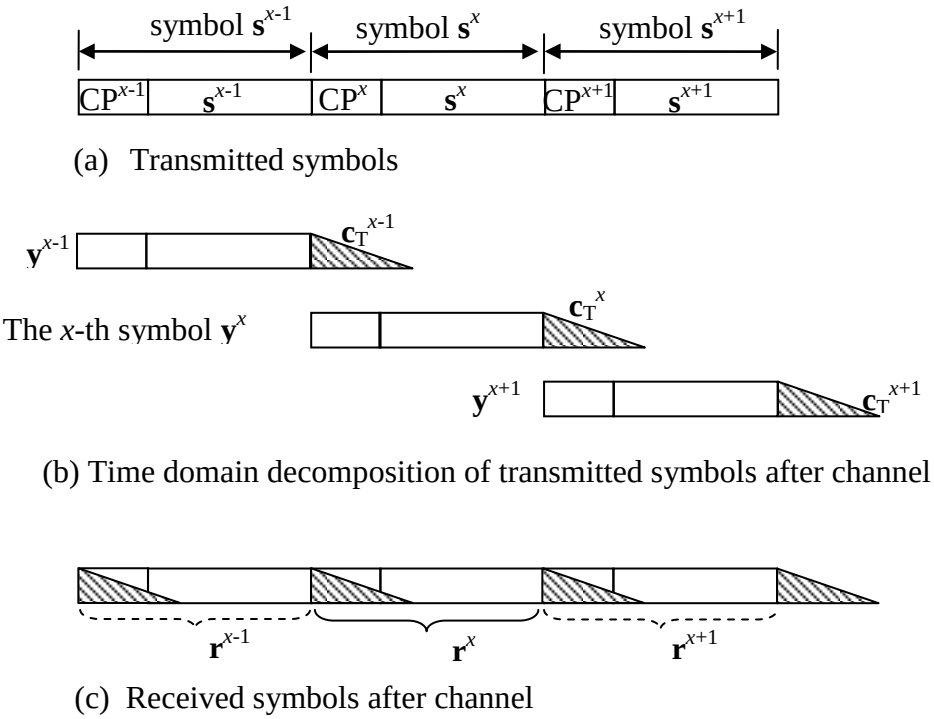

Fig. 4-2. Decomposition for transmitted and received CP MCM signal

The decomposition of the transmitted and received CP OFDM signals is shown in Fig. 4-2. The cyclic prefix of the x-th symbol $\mathbf{s}^x$ is added before $\mathbf{s}^x$ to avoid the ISI from the previous symbol. The superscript ^{x} represents the x-th symbol. The multipath channel $\mathbf{h}$ can be modeled as a finite impulse response (FIR) filter, which filters the transmitted OFDM symbol and output to the receiver. Hence, the filtered OFDM symbol $\mathbf{y}^x = [y_0^x \quad y_1^x \quad ... \quad y_{M-1}^x]^T$ is extended to M and consists of 3 parts: The CP part $\mathbf{c}^x = [y_0^x \quad y_1^x \quad ... \quad y_{G-1}^x]^T$, OFDM symbol body $[y_G^x \quad y_{G+1}^x \quad ... \quad y_{L-1}^x]^T$, and an additional tail part $\mathbf{c}_T^x = [y_L^x \quad y_{L+1}^x \quad ... \quad y_{M-1}^x]^T$ caused by multipath channel. In time domain, the adjacent two filtered OFDM symbols will overlap in the guard interval. In the receiver side, the first Q data of the received symbol $\mathbf{r}^x$ includes the tail part $\mathbf{c}_T^{x-1}$ of the filtered symbol $\mathbf{y}^{x-1}$ and the CP part $\mathbf{c}^x$ of the filtered symbol $\mathbf{y}^x$. Thus, the m-th element of the received x-th OFDM symbol $\mathbf{r}^x = [r_0^x \quad r_1^x \quad ... \quad r_{M-1}^x]^T$ can be expressed as

$$r_m^x = \begin{cases} y_{m+N+G}^{x-1} + y_m^x & m = 0,1,...Q-1 \\ y_m^x & m = Q,...,L-1 \\ y_m^x + y_{m-N-G+1}^{x+1} & m = L,...,M-1 \end{cases}. \quad (4.14)$$

Eq. (4.14) shows that the x-th filtered OFDM symbol $\mathbf{y}^x$ with ISI free can be reconstructed once $\mathbf{y}^{x-1}$, $\mathbf{y}^{x+1}$ and $\mathbf{r}^x$ are obtained.

Based on eq. (4.7), if the noise part is ignored, the estimations of the x-th symbol $\mathbf{y}^x$ can be calculated by

$$\hat{\mathbf{y}}^x = \mathbf{\Xi}^{t,x} \begin{bmatrix} \mathbf{F}_{cp}^{-1} \\ \mathbf{F}_N^{-1} \end{bmatrix} \mathbf{d}^x \quad (4.15)$$

where $\hat{\mathbf{y}}^x$ denotes the estimation of the x-th symbol; $\mathbf{d}^x$ represents the mapped data of the x-th symbol, which can be replaced with the equalized data $\hat{\mathbf{d}}$; Channel $\mathbf{\Xi}^{t,x}$ is $M \times L$ lower triangular Toeplitz matrix with the first column $[h_0 \ldots h_{Q-1}\ 0 \ldots 0]^T$ for the x-th symbol. Both $\mathbf{\Xi}^{t,x}$ and $\hat{\mathbf{d}}$ are estimated in the first step. Hence, the estimation of the x-1-th and x+1-th filtered OFDM symbols $\hat{\mathbf{y}}^{x-1}$ and $\hat{\mathbf{y}}^{x+1}$ can be obtained from (4.15).

Substituting $\mathbf{y}^{x-1}$ and $\mathbf{y}^{x+1}$ in (4.14) with the estimated $\hat{\mathbf{y}}^{x-1}$ and $\hat{\mathbf{y}}^{x+1}$ from (4.15), the x-th filtered symbol $\mathbf{y}^x$ after removing ISI from the adjacent symbols can be reconstructed by

$$\overline{y}_m^x = \begin{cases} r_m^x - \hat{y}_{m+N+G}^{x-1} & m = 0,1,...Q-1 \\ r_m^x & m = Q,...,L-1 \\ r_m^x - \hat{y}_{m-N-G}^{x+1} & m = L,...,M-1 \end{cases} \quad (4.16)$$

where $\overline{y}_m^x$ denotes the m-th element of the x-th reconstructed symbol $\overline{\mathbf{y}}^x$.

Normally the equalized data $\hat{\mathbf{d}}^{x-1}$ and $\hat{\mathbf{d}}^{x+1}$ in (4.15) suffer from noise and may not be accurate, which leads to noise-amplified for the calculation of $\overline{\mathbf{y}}^x$ in (4.16). Hence, we propose a data-aided (DA) SR method to improve the accuracy of $\overline{\mathbf{y}}^x$ as follows: The equalized data $\hat{\mathbf{d}}$ are de-mapped first to get the estimated binary data and then the binary data are reversely mapped again to get $\overline{\mathbf{d}}$ to reduce the effect of noise. The result $\overline{\mathbf{d}}$ is used to replace $\mathbf{d}^x$ in (4.15). Although errors will be

introduced in $\bar{\mathbf{d}}$ by de-mapping and re-mapping if the equalized data $\hat{\mathbf{d}}$ are far from the expected points. It will happen at low SNR level. With SNR increasing, the equalized data are closer to the expected points and the errors in $\bar{\mathbf{d}}$ will be smaller.

4.3.2 Proposed 2-stage FDO Based Receiver

In traditional CP OFDM receiver, the CP is removed for ISI elimination and the energy of CP is wasted. If the received symbol with CP is oversampled in the frequency domain, the total useful signal energy is increased and spread over all fractional spaced subcarriers, which is beneficial to the data recovery from multipath channel. However, the CP part cannot be directly used due to ISI from the preceding symbol. It's necessary to reconstruct the CP part for ISI elimination. Hence, for the proposed FDO-based receivers, we shall firstly reconstruct the receiver symbol, including CP, to remove ISI by using the result of the conventional CP OFDM channel estimation and equalization. This is followed by oversampling the reconstructed symbol in frequency domain. Finally the MMSE or ZF equalizer is used to estimate the transmitted data.

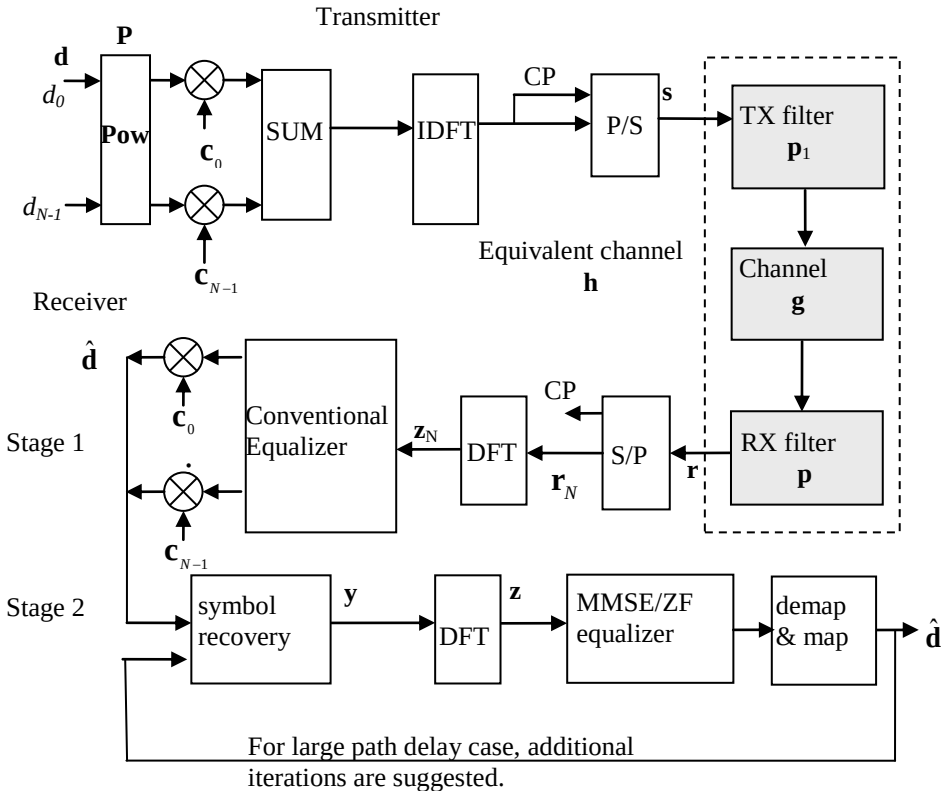

Fig. 4-3. Basic structure of proposed FDO-based receiver for CP MCM systems

The basic structure of our proposed receivers is shown in Fig. 4-3. For CP OFDM, **C** is set to **I**. The detailed procedures are shown as follows:

1) Perform conventional channel estimation and equalization to obtain the estimate of the transmitted data $\hat{\mathbf{d}}$. We can use methods in Section 4.2.2 and 4.2.3 to estimate the channel $\mathbf{h}=[h_0\ h_1 \ldots\ h_{Q-1}]^{\mathrm{T}}$ in time domain and $\hat{\mathbf{H}}$ in frequency domain, and calculate the transmitted data $\hat{\mathbf{d}}$ by using (4.10). It is the first stage of our proposed receivers. We set the iteration index I to one at this step.

2) Reconstruct the x-th OFDM symbol $\mathbf{y}^x$ to reduce the ISI. Firstly estimate the two adjacent OFDM symbols $\mathbf{y}^{x-1}$ and $\mathbf{y}^{x+1}$ by using $\hat{\mathbf{d}}$ and the equation (4.15) in Section 4.3.1 to obtain $\hat{\mathbf{y}}^{x-1}$ and $\hat{\mathbf{y}}^{x+1}$. Thus, the CP part $\mathbf{c}^{x+1}$ of the x+1-th symbol and the tail part $\mathbf{c}_{\mathrm{T}}^{x-1}$ of the x-1-th symbol are obtained. The reconstructed x-th symbol $\overline{\mathbf{y}}^x$ with CP and tail parts can be calculated by subtracting $\mathbf{c}_{\mathrm{T}}^{x-1}$ and $\mathbf{c}^{x+1}$ from the received x-th symbol to reduce the ISI based on (4.16).

3) Oversample the reconstructed x-th symbol $\overline{\mathbf{y}}^x$ in the frequency domain and then retrieve the transmitted data $\hat{\mathbf{d}}^x$ of the x-th symbol by using the FDO-based MMSE or ZF equalizer proposed in Section 4.3.3 as the second stage equalizer. The retrieved transmitted data $\hat{\mathbf{d}}^x$ shall be more accurate than the result in step 1).

4) If I is equal to the pre-defined maximum iteration number IT, the FDO receiving is finished. Otherwise, we can increase the iteration index I by 1, and go back to step 2) for another iteration. The retrieved data $\hat{\mathbf{d}}^x$ at the step 3) will be used for symbol reconstruction (SR) at step 2). In most cases, the BER curves converge at the first iteration. There is no need to go back to step 2). However, if the multipath delay is longer than the CP, the ISI cannot be eliminated at step 1). The estimated $\hat{\mathbf{d}}$ at step 1) suffers from high error floor, which leads to small error floor of $\hat{\mathbf{d}}^x$ at step 3). In this case, an additional iteration can further decrease the error floor of $\hat{\mathbf{d}}^x$.

For the proposed receiver, the first stage is to estimate the channel information and equalized data. No matter what methods are adopted at this step, the next stage FDO-based MMSE or ZF

equalizer can improve the performance of stage 1 by fully oversampling the OFDM symbol with CP and tail parts.

4.3.3 FDO Based MMSE Equalizers

The FDO based equalizer is adopted for each OFDM symbol. It is not necessary to distinguish each symbols, hence the superscript ^{x} for the x-th symbol is not used again in the following discussions.

If we oversample the reconstructed symbol in the frequency domain by using M-point DFT on the both sides of (4.7) (we assume ε=0, since ε is unknown), according to circular convolution theorem, the symbol in frequency domain can be represented as

$$\begin{aligned}\mathbf{z} = \mathbf{F}_M \mathbf{y}_M &= \mathbf{F}_M \boldsymbol{\Xi}_M^{\mathrm{C}} \begin{bmatrix} \mathbf{F}_{\mathrm{cp}}^{-1} \\ \mathbf{F}_N^{-1} \\ \mathbf{0}_Q \end{bmatrix} \mathbf{CPd} + \mathbf{F}_M \mathbf{v} + \mathbf{F}_M \zeta \\ &= \tilde{\mathbf{H}}_M \mathbf{F}_{ML} \begin{bmatrix} \mathbf{F}_{\mathrm{cp}}^{-1} \\ \mathbf{F}_N^{-1} \end{bmatrix} \mathbf{CPd} + \mathbf{F}_M \mathbf{v} + \mathbf{F}_M \zeta \\ &= \tilde{\mathbf{H}}_M \mathbf{ACPd} + \mathbf{F}_M \mathbf{v} + \mathbf{F}_M \zeta \end{aligned} \tag{4.17}$$

where $\mathbf{F}_M$ denotes an $M \times M$ DFT matrix and $\mathbf{F}_{ML}$ is a matrix with the first L columns of $\mathbf{F}_M$, $\mathbf{v}$ denotes zero mean Gaussian noise with variance σ^2, $\mathbf{A} = \mathbf{F}_{ML} \begin{bmatrix} \mathbf{F}_{\mathrm{cp}}^{-1} \\ \mathbf{F}_N^{-1} \end{bmatrix}$ is a pre-defined matrix, $\tilde{\mathbf{H}}_M$ is a diagonal matrix with channel $\mathbf{H}=\mathbf{F}_M\mathbf{h}$ on the main diagonal, and $\boldsymbol{\Xi}_M^{\mathrm{C}}$ is a circular matrix with $\mathbf{h}$ on the first column, $\zeta = \begin{bmatrix} \mathbf{y}_Q^{x-1} - \hat{\mathbf{y}}_Q^{x-1} \\ \mathbf{0} \\ \mathbf{y}_Q^{x+1} - \hat{\mathbf{y}}_Q^{x+1} \end{bmatrix}$ denotes the ISI from the adjacent symbol, where $\mathbf{y}_Q^{x-1}$ denotes the last Q points of the x-1-th symbol and, $\mathbf{y}_Q^{x+1}$ denotes the first Q points of the x+1-th symbol, $\hat{\mathbf{y}}_Q^{x-1}$ and $\hat{\mathbf{y}}_Q^{x+1}$ are the estimation of $\mathbf{y}_Q^{x-1}$ and $\mathbf{y}_Q^{x+1}$, respectively. Since the number of nonzero elements of ζ is only $2Q$ and the iterative equalizers can minimize the ISI, for simplicity of the FDO-based equalizers, it can be assumed that the ISI is zero, i.e., $\zeta = \mathbf{0}$.

For linear equalizer, the transmitted data **d** of the *x*-th symbol can be estimated from the frequency-domain oversampled **z** by multiplying an optimal weight matrix $\mathbf{W}^{H}$. i.e.

$$\hat{\mathbf{d}} = \mathbf{W}^{H}\mathbf{z} \tag{4.18}$$

where **z** is given by (4.17) mathematically. The optimal linear MMSE equalizer can be derived from orthogonality principle, i.e., the estimation error $\mathbf{d}-\hat{\mathbf{d}}$ shall be orthogonal to the known random variable **z**. i.e. $E\{(\mathbf{d}-\hat{\mathbf{d}})\mathbf{z}^{H}\}=\mathbf{0}$, where $E\{\bullet\}$ denotes expectation and $(.)^{H}$ denotes the conjugate transpose operation. Combining it with (4.17) and defining $\mathbf{\Phi} = \tilde{\mathbf{H}}_{M}\mathbf{ACP}$, the FDO-MMSE equalizer $\mathbf{W}^{\mathbf{H}}$ can be expressed as

$$\mathbf{W}^{H} = \mathbf{\Phi}^{H}(\mathbf{\Phi}\mathbf{\Phi}^{H} + \mathbf{I}\sigma^{2})^{-1}. \tag{4.19}$$

When σ^{2} is quite small, the matrix $\mathbf{\Phi}\mathbf{\Phi}^{H} + \mathbf{I}\sigma^{2}$ is close to singular due to $M>N$, the result of matrix inverse may be inaccurate. Hence, it is better to replace the matrix inverse with the Moore-Penrose pseudo-inverse. $\tilde{\mathbf{H}}_{M}$ in $\mathbf{\Phi}$ can be replaced with the estimated channel in the step 1). For the simplicity of analysis, we assume that the transmission power is not changed, i.e., **P** equals to **I**.

Since the matrix inverse is involved in the FDO-MMSE equalizer, the implementation complexity of the FDO-MMSE equalizer (i.e., on the order of $O(M^{3})$) is highly depended on the matrix dimension *M*. In order to reduce the computation of the matrix inverse, equation (4.19) can be written as the equivalent form in (4.20).

$$\mathbf{W}^{H} = (\mathbf{\Phi}^{H}\mathbf{\Phi} + \mathbf{I}\sigma^{2})^{-1}\mathbf{\Phi}^{H} \tag{4.20}$$

which can be verified by using the singular value decomposition of $\mathbf{\Phi}$ in (4.19) and (4.20). Thus, the dimension of matrix to be inversed is reduced from $M\times M$ to $N\times N$.

For conventional receiver without oversampling, *N* subcarriers are orthogonal. The weight matrix $\mathbf{W}^{H}$ is a diagonal matrix. Hence, the optimal estimator of CP OFDM is reduced to *N* scalar MMSE receivers, and the scalar MMSE receiver will not improve the error rate performance in comparison with the ZF receiver ([18], [19]). However, if FDO method is adopted, $\mathbf{W}^{H}$ is not a

square matrix again, thus the MMSE receiver cannot be reduced to scalar MMSE receivers. The data on N subcarriers can be recovered from M ($M>N$) sampled subcarriers while the noise is suppressed when it spreads over M subcarriers.

4.3.4 FDO Diagonal MMSE Equalizer

The FDO-MMSE equalizer is computationally intensive since there is an inverse operation of matrix in (4.19). It will then be highly desirable to have an equalizer with much lower complexity while the performance degradation is marginal or negligible.

For the simplicity of analysis, we assume that the transmission power is not changed, i.e., $\mathbf{P}$ equals to $\mathbf{I}$. We have

$$\begin{aligned}
\mathbf{\Phi\Phi}^{\mathrm{H}} &= \tilde{\mathbf{H}}_M \mathbf{A}\mathbf{A}^{\mathrm{H}} \tilde{\mathbf{H}}_M^{\mathrm{H}} = \tilde{\mathbf{H}}_M \mathbf{F}_{ML} \begin{bmatrix} \mathbf{F}_{\mathrm{cp}}^{-1} \\ \mathbf{F}_N^{-1} \end{bmatrix} \begin{bmatrix} \mathbf{F}_{\mathrm{cp}}^{-1} \\ \mathbf{F}_N^{-1} \end{bmatrix}^{\mathrm{H}} \mathbf{F}_{ML}^{\mathrm{H}} \tilde{\mathbf{H}}_M^{\mathrm{H}} \\
&= \tilde{\mathbf{H}}_M \mathbf{F}_{ML} \begin{bmatrix} \mathbf{I}_G & \mathbf{0} & \mathbf{I}_G \\ \mathbf{0} & \mathbf{I}_{N-G} & \mathbf{0} \\ \mathbf{I}_G & \mathbf{0} & \mathbf{I}_G \end{bmatrix} \mathbf{F}_{ML}^{\mathrm{H}} \tilde{\mathbf{H}}_M^{\mathrm{H}} \\
&\approx \tilde{\mathbf{H}}_M \mathbf{F}_{ML} \mathbf{I}_{N+G} \mathbf{F}_{ML}^{\mathrm{H}} \tilde{\mathbf{H}}_M^{\mathrm{H}} = \tilde{\mathbf{H}}_M \mathbf{F}_{ML} \mathbf{F}_{ML}^{\mathrm{H}} \tilde{\mathbf{H}}_M^{\mathrm{H}} \\
&\approx \tilde{\mathbf{H}}_M \mathbf{I}_M \tilde{\mathbf{H}}_M^{\mathrm{H}} = \tilde{\mathbf{H}}_M \tilde{\mathbf{H}}_M^{\mathrm{H}}
\end{aligned} , \tag{4.21}$$

where $\mathbf{I}_G$ represents the identity matrix of size G. Since G is much smaller than $G+N$, we have the above approximation. Hence, we have $\mathbf{\Psi} = \mathbf{\Phi\Phi}^{\mathrm{H}} + \mathbf{I}\sigma^2 \approx \tilde{\mathbf{H}}_M \tilde{\mathbf{H}}_M^{\mathrm{H}} + \mathbf{I}\sigma^2$, which will cause the diagonalization of the matrix $\mathbf{\Psi}$. Now the inverse of diagonal matrix $\mathbf{\Psi}$ is much simpler than that of the original matrix. We refer to the obtained equalizer as the FDO Diagonal MMSE equalizer (FDO-DMMSE), the optimal weight matrix $\mathbf{W}_{\mathrm{FD}}^{\mathrm{H}}$ of which can be rewritten as

$$\mathbf{W}_{\mathrm{FD}}^{\mathrm{H}} = (\mathbf{AC})^{\mathrm{H}} \tilde{\mathbf{H}}_M^{\mathrm{H}} (\tilde{\mathbf{H}}_M \tilde{\mathbf{H}}_M^{\mathrm{H}} + \mathbf{I}\sigma^2)^{-1} . \tag{4.22}$$

From (4.21) we can find that there are two approximation operations during the diagonalization of the matrix $\mathbf{\Psi}$, which cause more noise introduced by the FDO-DMMSE in CP MCM systems than it in ZP MCM systems. Hence, the performance of the FDO-DMMSE in CP MCM systems is not as good as that in ZP MCM systems.

The complexity of the simplified FDO diagonal MMSE equalizer decreases significantly since that the inverse of diagonal matrix is much simpler than the inverse of non-diagonal matrix. The FDO diagonal equalizer is easily to understand based on the eqn. (4.22). It firstly equalizes the received data on *M*-subcarriers domain by $\tilde{\mathbf{H}}_M^{\mathrm{H}}(\tilde{\mathbf{H}}_M\tilde{\mathbf{H}}_M^{\mathrm{H}}+\mathbf{I}\sigma^2)^{-1}$, then converts the equalized data to *N*-subcarriers domain by $(\mathbf{AC})^{\mathrm{H}}$.

The FDO-DMMSE equalizer needs to estimate the noise power for a better performance, which will cause additional computations. If the noise is forced to a fixed value (i.e., let $\sigma^2 = \sigma_0^2$), the FDO-DMMSE equalizer can be further simplified to the FDO-DMMSE equalization with noise fixed (i.e., FDO-NF). The FDO-NF equalizer requires only the additional *M*-point IDFT and *N*-point DFT compared to a conventional receiver. Therefore, it is suitable for the practical applications. σ_0^2 can be set according to the rough estimation of the noise in the practical scenario. Round this point, the FDO-NF equalizer can offer a similar BER performance to the FDO-DMMSE equalizer. If the σ_0^2 is set to zero, the FDO-NF equalizer becomes the FDO-ZF equalizer.

4.3.5 FDO ZF Equalizer

The FDO-MMSE equalizer is difficult to implement due to the calculation of the matrix inverse in (4.19). If we ignore the noise part in (4.19), the less complex FDO-ZF equalizer can be easily derived as

$$\mathbf{W}^{\mathrm{H}} = \mathbf{C}^{\mathrm{H}}\mathbf{A}^{\mathrm{H}}(\mathbf{A}\mathbf{A}^{\mathrm{H}})^{-1}\tilde{\mathbf{H}}_M^{-1} = \mathbf{C}^{\mathrm{H}}\mathbf{A}^{+}\tilde{\mathbf{H}}_M^{-1}. \tag{4.23}$$

Although the FDO-ZF equalizer in (4.23) cannot offer better BER performance than the MMSE equalizer in (4.19), it is easily implemented because $\mathbf{A}^{+}$ can be pre-calculated and the inverse of diagonal matrix $\tilde{\mathbf{H}}_M$ can be easily calculated. Compared with the conventional ZF/MMSE equalizer for CP OFDM, the FDO-ZF equalizer needs one more matrix multiplication by $\mathbf{A}^{+}$, which represents the map from *M*-subcarrier domain to *N*-subcarrier domain. In addition, the DFT size shall be increased from *N* points to *M* points. The matrix $\mathbf{A}^{+}$ can be calculated by

$$\mathbf{A}^{+}=(\mathbf{F}_{ML}\begin{bmatrix}\mathbf{F}_{\mathrm{cp}}^{-1}\\ \mathbf{F}_{N}^{-1}\end{bmatrix})^{+}=(\begin{bmatrix}\mathbf{F}_{\mathrm{cp}}^{-1}\\ \mathbf{F}_{N}^{-1}\end{bmatrix})^{+}\mathbf{F}_{ML}^{+}=\begin{bmatrix}\frac{1}{2}\mathbf{F}_{\mathrm{cp}} & \mathbf{F}_{NG} & \frac{1}{2}\mathbf{F}_{\mathrm{cp}}\end{bmatrix}\mathbf{F}_{ML}^{\mathrm{H}} \tag{4.24}$$

where $\mathbf{F}_{\mathrm{cp}}$ and $\mathbf{F}_{NG}$ are the last G and first N-G columns of $\mathbf{F}_N$, respectively.

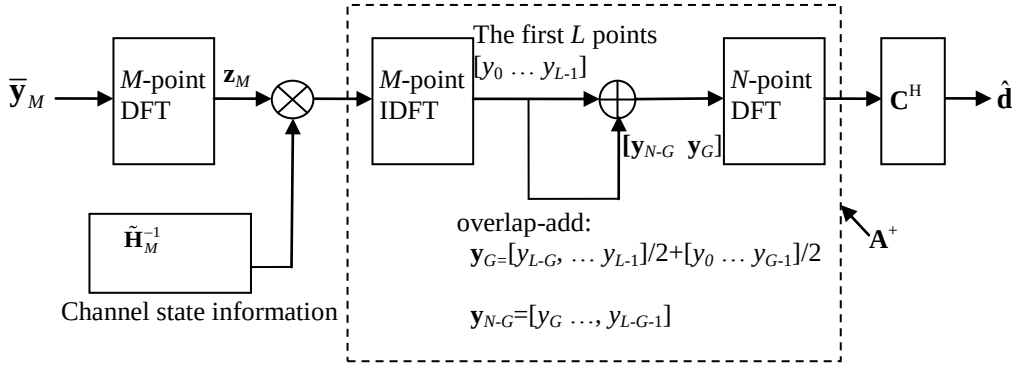

Fig. 4-4. The implementation of FDO-ZF equalizer for CP MCM systems

Based on the equations (4.23) and (4.24), the FDO-ZF equalizer for CP MCM systems can be implemented as shown in Fig. 4-4. We assume that the result of the M-point IDFT is $\mathbf{y}=[y_0 \quad y_1 \quad \ldots \quad y_{M-1}]$. We have $\begin{bmatrix}\frac{1}{2}\mathbf{F}_{\mathrm{cp}} & \mathbf{F}_{NG} & \frac{1}{2}\mathbf{F}_{\mathrm{cp}}\end{bmatrix}\mathbf{y}^{\mathrm{T}}=\mathbf{F}[\mathbf{y}_{N-G} \quad \mathbf{y}_G]^{\mathrm{T}}$, where $\mathbf{y}_{N-G}=[y_G \quad y_{G+1} \quad \ldots \quad y_{L-G-1}]$ and $\mathbf{y}_G=\frac{[y_{L-G} \quad y_{L-G+1} \quad \ldots \quad y_{L-1}]+[y_0 \quad y_1 \quad \ldots \quad y_{G-1}]}{2}$. $\mathbf{y}_G$ implies the overlap-add operation. Hence, $\mathbf{A}^{+}$ actually can be implemented by the M-point IDFT followed by overlap-add operation and the N-point DFT as shown in Fig. 4-4.

To improve the performance of the FDO-ZF equalizer, we can increase the oversampling rate M/N for the FDO-ZF (i.e., increase the DFT size M). For FDO-based equalizer, the size of estimated symbol $\bar{\mathbf{y}}^{x}$ in (4.16) is N+G+Q, i.e., the OFDM symbol including the CP portion and tail part. If we increase the DFT size M, i.e., M> N+G+Q, $\bar{\mathbf{y}}^{x}$ shall be padded with zeros to increase its size to M, and then be converted to M-subcarrier frequency domain by M-point DFT. Substituting (4.17) and (4.23) into (4.18) and considering $\mathbf{A}^{+}\mathbf{A}=\mathbf{I}$ (since columns of $\mathbf{A}$ are linearly independent), we have

$$\hat{\mathbf{d}} = \mathbf{C}^{\mathrm{H}}\mathbf{A}^{+}\mathbf{A}\mathbf{C}\mathbf{d} + \mathbf{A}^{+}\tilde{\mathbf{H}}_M^{-1}\mathbf{F}_M\bar{\mathbf{v}} = \mathbf{d} + \begin{bmatrix} \mathbf{F}_{\mathrm{cp}}^{-1} \\ \mathbf{F}_N^{-1} \\ \mathbf{0}_{(M-G-N)\times N} \end{bmatrix}^{+} \mathbf{F}_M^{-1}\tilde{\mathbf{H}}_M^{-1}\mathbf{F}_M\bar{\mathbf{v}} \qquad (4.25)$$

where $\bar{\mathbf{v}}$ is the noise vector $\mathbf{v}$ padded with [M-(N+G+Q)] zeros, $\mathbf{0}_{(M-G-N)\times N}$ is a zero matrix with M-G-N rows and N columns. The second part represents the equivalent noise in frequency domain. Please note that $\mathbf{F}_M^{-1}$ and $\mathbf{F}_M$ will not change the power of noise $\mathbf{v}$. When oversampling rate increases, the size of matrix $\mathbf{0}_{(M-G-N)\times N}$ increases, which will decrease the noise power because more rows of $\mathbf{F}_M^{-1}\tilde{\mathbf{H}}_M^{-1}\mathbf{F}_M\mathbf{v}$ are truncated by the zero matrix and hence increase the average SNR. However, with oversampling rate increasing, $\tilde{\mathbf{H}}_M^{-1}$ in $\mathbf{F}_M^{-1}\tilde{\mathbf{H}}_M^{-1}\mathbf{F}_M\mathbf{v}$ will increase the noise power given the assumption of quasi-static multipath channel $\sum_{q=0}^{Q-1}\mathrm{E}[|h_q|^2]=1$ (i.e., $\sum_{k=0}^{M-1}\mathrm{E}[|H_k|^2]=1$ in frequency domain). Thus, the reduction of noise power (i.e., the increasing of the average SNR) is limited by the channel $\tilde{\mathbf{H}}_M^{-1}$. In general, the BER performance of the ZF equalizer can be improved by increasing the oversampling rate M/N (i.e., increasing DFT size M), but the improvement will be limited by the channel attenuation.

For our proposed FDO-MMSE equalizer for CP OFDM, the whole OFDM symbol including CP and tail parts is sampled by DFT. The total noise power remains unchanged after DFT. However, because the CP part is highly correlated with other samples of the OFDM symbol, the signal power after DFT is eventually enhanced. Thus, the CP part is beneficial to the BER performance and increasing the CP length will improve the BER performance.

Comparing with the conventional CP OFDM, the above two proposed FDO-based equalizers can guarantee the symbol recovery regardless of zero subchannels. The FDO-based equalizers convert the channel from N-subcarrier domain to M-subcarrier domain and process the data in M-subcarrier domain. Thus, the zero or deep faded subchannels in N-subcarrier domain estimated by

the conventional receiver will be recovered in *M*-subcarrier domain by the FDO-based equalizers.

4.4 BER Performance Analysis

Although the close-form BER performance of the proposed receiver is difficult to calculate, it can be estimated by using the AI-BER of a large amount of OFDM symbols.

Combining (4.17) and (4.18), the estimated transmitted data $\hat{\mathbf{d}}$ can be represented by

$$\hat{\mathbf{d}} = \mathbf{W}^{\mathrm{H}}\mathbf{Y} = \mathbf{W}^{\mathrm{H}}\tilde{\mathbf{H}}_M\mathbf{F}_{ML}\begin{bmatrix}\mathbf{F}_{\mathrm{cp}}^{-1}\\ \mathbf{F}_N^{-1}\end{bmatrix}\mathbf{d} + \mathbf{W}^{\mathrm{H}}\mathbf{F}_M\mathbf{v} = \mathbf{B}\mathbf{d} + \mathbf{J}\mathbf{v} \tag{4.26}$$

where $\mathbf{B} = \mathbf{W}^{\mathrm{H}}\tilde{\mathbf{H}}_M\mathbf{F}_{ML}\begin{bmatrix}\mathbf{F}_{\mathrm{cp}}^{-1}\\ \mathbf{F}_N^{-1}\end{bmatrix}$ with element $B_{m,n}$ on the *m*-th row and *n*-th column, and $\mathbf{J} = \mathbf{W}^{\mathrm{H}}\mathbf{F}_M$ with the element $J_{m,n}$ on the *m*-th row and *n*-th column. Thus, the data on each subcarrier can be expressed as

$$\hat{d}_k = \sum_{n=0}^{N-1} B_{k,n}d_n + \sum_{m=0}^{M-1} J_{k,m}v_m \tag{4.27}$$

where $M=N+G+Q$, d_n is the mapped data and is a sequence of independent and identically distributed random variables, v_m denotes zero mean Gaussian noise with variance σ^2 ($m=Q, \ldots, N+G-1$). When *m* is less than *Q* or larger than $N+G$, the variance of v_m will be more than σ^2 due to SR. Normally *Q* is quite small compared with *N*, the first and last *Q* elements of v_m will not significantly affect the BER performance. For simplicity, we just assume the noise caused by SR is still Gaussian noise with zero mean and the variance σ^2. Hence, the variance of the first *Q* and last *Q* elements of v_m is $2\sigma^2$.

According to the central limit theorem, when *N* is large, both $\sum_{n=0}^{N-1} B_{k,n}d_n$ and $\sum_{m=0}^{M-1} J_m v_m$ approximate to normal distribution, hence $\hat{d}_k$ approximates to a normal distribution. For QPSK modulation, we can assume the mean and variance of the real and imaginary part of d_n are 0 and 1/2, respectively. Therefore, the instantaneous BER on subcarrier *k* of the *x*-th OFDM

symbol can be calculated from

$$\beta_k^x = Q\left(\frac{\Re(B_{k,k})}{\sqrt{\sum_{n\neq k}\Re(B_{k,n})^2+\sum_{n\neq k}\Im(B_{k,n})^2+\sum_{m=0}^{M-1}\left(\Re(J_m)^2+\Im(J_m)^2\right)2\sigma^2}}\right) \tag{4.28}$$

where $Q(t)=\frac{1}{\sqrt{2\pi}}\int_t^\infty e^{-y^2/2}dy$, $\Re(y)$ and $\Im(y)$ represent the real and imaginary part of y, respectively. $\sum_{n\neq k}\Re(B_{k,n})^2+\sum_{n\neq k}\Im(B_{k,n})^2$ denotes the ICI that caused by the oversampling, and $\sum_{m=0}^{M-1}\left(\Re(J_m)^2+\Im(J_m)^2\right)\sigma^2$ denotes the suppressed noise by equalizers. The AI-BER of X OFDM symbols is given by

$$\beta=\frac{1}{X}\sum_{x=0}^{X-1}\frac{1}{N}\sum_{k=0}^{N-1}\beta_k^x\,. \tag{4.29}$$

4.5 Simulation Results

Firstly, the BER performance of the proposed iterative FDO based equalizers is evaluated in CP OFDM system, i.e., **C**=**I** and **P**=**I**. Then, the BER performance of the proposed FDO based equalizers in CP MC-CDMA system is evaluated. In CP MC-CDMA, the proposed FDO based equalizers show more merits than they in CP OFDM due to the spreading coding. Finally, the proposed FDO based equalizers are compared between CP OFDM and CP MC-CDMA, and between the CP based system and the ZP based system.

4.5.1 Simulation Results for CP OFDM

We assume that 256 subcarriers (i.e., N=256) and QPSK modulation are employed. The CP length is set to one-eighth of the OFDM symbol length (i.e., G=32). The transmitted signal is passed through a quasi-static multipath channel **h** and is corrupted by additive white Gaussian noise. The normalized quasi-static channel has N_q=15 linearly decaying multipath components

with delays of {0, iT/N, …, $i(N_q\text{-}1)T/N$} and total power of 1, where T is the OFDM symbol duration and i denotes the normalized multipath interval. The maximal path delay $Q= i(N_q\text{-}1)+1$. In addition, hard decision is assumed for demodulation and the transmitted data are not coded. We further assume that $N/8$ pilot subcarriers are evenly distributed across subcarriers to simplify channel estimation. The conventional OFDM receiver is actually the first stage of the proposed receivers, and described in Section 4.2.2 and 4.2.3, i.e., the estimation methods in (4.10), (4.12) and (4.13), respectively. The FSFD-MMSE receiver for ZP OFDM is described in [28]. The maximal iteration number is set to 1 if the channel path delay is less than the CP length. We assume that both CP OFDM and ZP OFDM use the same amount of energy for the main part (without the guard interval) transmission for fair comparison. In this case, the conventional receivers for the two OFDM systems have the similar BER performance, but the ZP OFDM scheme will consume lower transmission energy in total.

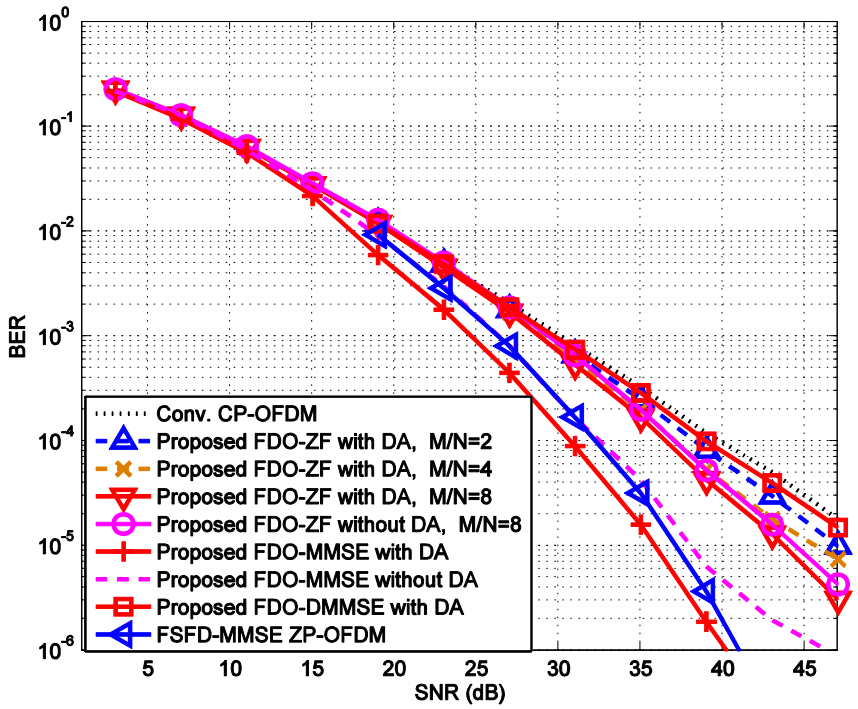

Fig. 4-5. BER versus SNR for the proposed FDO-based CP OFDM receivers

The BER performance of the proposed 2-stage FDO-MMSE, FDO-DMMSE and FDO-ZF receivers described in Section 4.3.3, 4.3.4 and 4.3.5 for CP OFDM is shown in Fig. 4-5. The

normalized multipath interval i=2 (i.e., the maximal path delay Q=29) and the channel is estimated by the conventional estimation method in (4.13). To simplify the design, we use hard decision demapping for DA SR described in Section 4.3.1. Compared with the receivers without DA, the FDO-MMSE receiver with DA improves the BER performance significantly, and the FDO-ZF receiver with DA also improves the BER performance. It can be found the proposed receivers with DA and without DA have almost same BER performance at low SNR level (3 to 15 dB). The proposed DA method will not amplify the total errors at low SNR level. It means that the DA method is robust to the observed SNR region. Since the implementation cost for hard decision demapping is quite small, we always adopt DA SR for the remaining simulations, even we do not mention it explicitly. From Fig. 4-5 we find that the performance of the proposed FDO-MMSE receiver with DA for CP OFDM is much better than that of the conventional receiver and slightly better than that of FSFD-MMSE receiver for ZP OFDM. The BER of the conventional receiver decreases more slowly when SNR increases compared with the proposed FDO-based receivers. It can only reach 1×10^{-4} at the SNR of 40 dB. However, the BER of the proposed FDO-MMSE receiver can quickly reduce to 1×10^{-6} at the same SNR. Although the performance of the FDO-ZF receiver is not as good as that of the FDO-MMSE receiver, it is still better than that of the conventional receiver, and can be improved by increasing the oversampling factor M/N. The advantage of FDO-ZF receiver is low complexity of implementation compared with the FDO-MMSE receiver. In the following simulations, we set M/N to 8 for comparison (i.e., M=8*N). In this case, the estimated $\mathbf{y}^x$ (the length of it is $G+N+Q$) shall be padded with zeros to increase the size of it to M. It also can be found that the FDO-DMMSE equalizer only offer the similar BER performance to the conventional ZF equalizer. It is because that the approximation of matrix diagonalization in (4.22) degrades the BER performance of it. Hence, the FDO-DMMSE equalizer is not suitable for CP OFDM. However, it still can work well in CP MC-CDMA system and can benefit from the frequency diversity gain caused by the spreading codes.

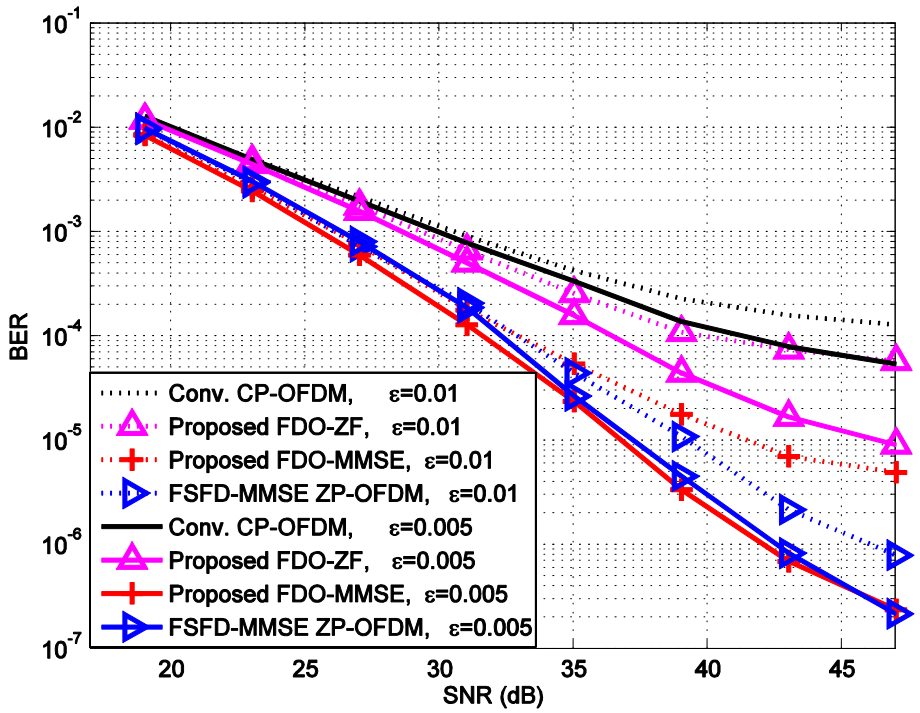

Fig. 4-6. BER versus SNR for the FDO-based CP OFDM receivers with frequency offset.

The conventional CP OFDM receiver is susceptible to the CFO. The results in Fig. 4-6 show that it has a BER floor of 6×10^{-5} even when the residual CFO ε is very small (i.e., ε=0.005 of the subcarrier spacing) under the assumed multipath channel with N_q=15 and i=2. The proposed FDO-MMSE CP OFDM receiver can greatly reduce the error floor to 2×10^{-7}, and it can offer equivalent BER of FSFD-MMSE for ZP OFDM. However, when ε is large (i.e., ε=0.01), although the FDO-MMSE for CP OFDM can offer better performance than the conventional CP OFDM, it is not as good as the FSFD-MMSE for ZP OFDM. This is because the estimated channel $\hat{\mathbf{H}}$ by the conventional CP OFDM is distorted by the residual frequency offset. The residual error caused by estimated channel exists in the reconstructed symbol, which lead to performance degradation of FDO-MMSE for CP OFDM. The proposed FDO-ZF receiver in CP OFDM is slightly better than the conventional receiver and the BER floor can be reduced to 6×10^{-5} and 9×10^{-6} for ε=0.01 and ε=0.005, respectively. From the observed results, it can be concluded that the proposed FDO-MMSE and FDO-ZF receivers can tolerate a larger frequency offset than the conventional receiver.

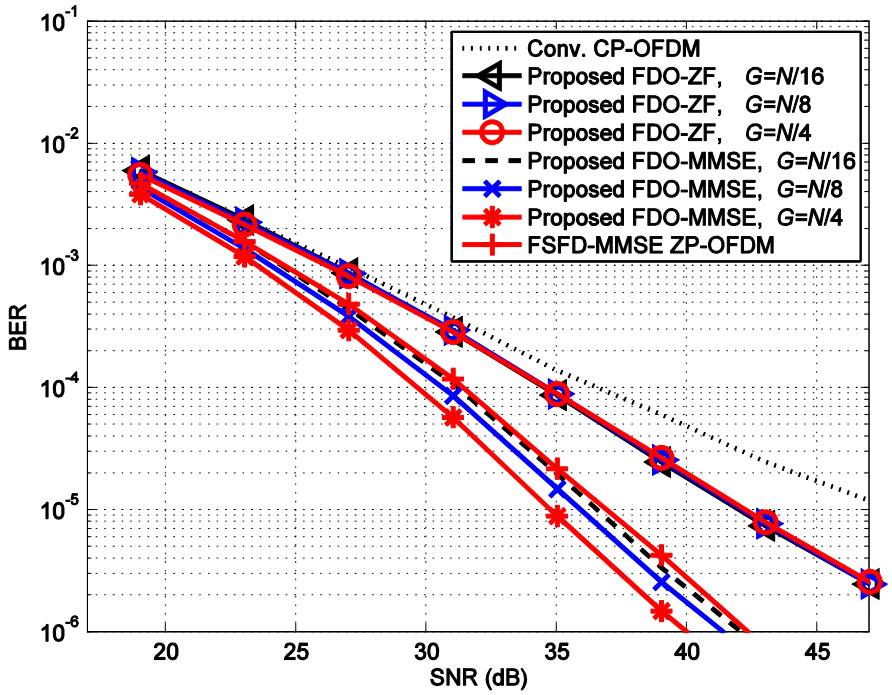

Fig. 4-7. The BER performance for different CP length.

The effect of CP length is evaluated in the simulation. We compare three CP OFDM systems with different CP length: $G=N/16$, $G=N/8$, $G=N/4$. Accordingly, for FSFD-MMSE ZP OFDM, the ZP length is equal to CP length for comparison. We assume that the channel is perfectly estimated and normalized multipath interval $i = 1$ (i.e., $Q=15$, and less than the CP and ZP length). Under such assumption, the ZP length does not affect the BER performance of FSFD-MMSE for ZP OFDM. This is because increasing the ZP length does not increase the useful signal power for ZP OFDM when the ZP length is larger than the multipath delay. Hence, only one curve for ZP OFDM is shown in Fig. 4-7 for comparison. We find that the proposed FDO-MMSE can improve the BER performance by increasing CP length. Compared with the conventional receiver, the FDO-MMSE receiver with CP length $N/16$ and CP length $N/4$ can achieve about 10 dB and 12 dB SNR gain at the BER of 1×10^{-5}, respectively. Furthermore, the FDO-MMSE for CP OFDM can offer better BER performance than FSFD-MMSE for ZP OFDM for all three cases, and about 2.5 dB SNR gain can be achieved at the BER of 1×10^{-6} for $G=N/4$. In addition, although the FDO-ZP for CP OFDM does not improve the BER performance distinctly by increasing CP length, it still

can offer better BER performance than conventional receiver for all three cases.

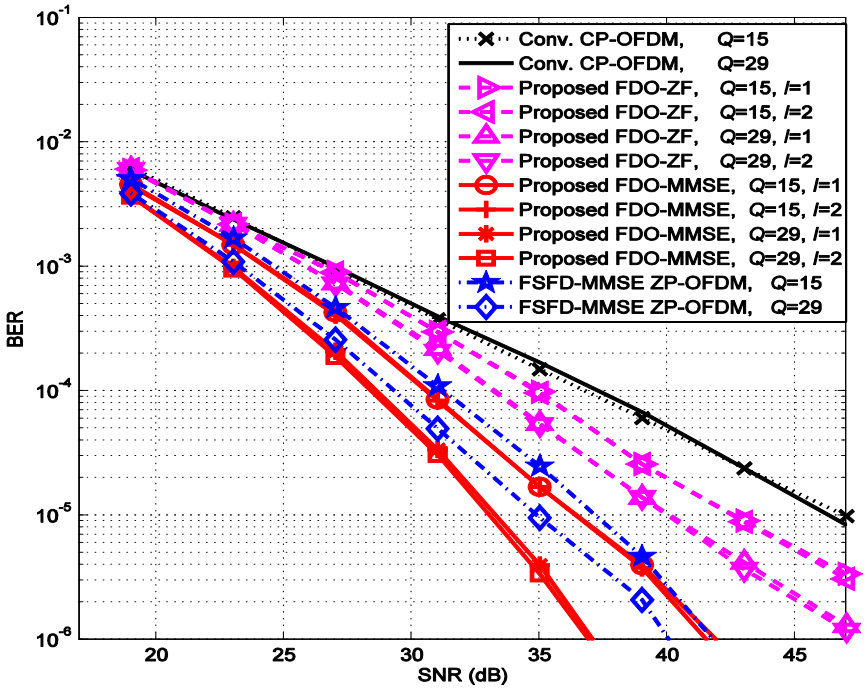

Fig. 4-8. The BER performance for different maximal path delays (*Q*=15 and 29)

The proposed FDO-MMSE and FDO-ZF receivers for CP OFDM exhibit good properties for multipath channel. In this simulation, we fix the CP length (or ZP length for ZP OFDM) $G=N/8$ and the number of multipath N_q=15. The normalized multipath interval i is set to 1, 2, and 4, which lead to different path delay Q=15, Q=29 and Q=57, respectively. The largest delay Q=57 exceeds the length of CP, which means the ISI cannot be removed by the conventional CP OFDM and ZP OFDM receivers. We assume that the channel state information is perfectly estimated for Fig. 4-8 and Fig. 4-9 (i.e., the full channel state information is available). The results in Fig. 4-8 show that for i=1 and i=2, the proposed the FDO-MMSE for CP OFDM with 1 iteration (i.e., I=1) can offer much better BER performance than the conventional CP OFDM, and better BER performance than the FSFD-MMSE ZP OFDM. It can be found that the additional iteration can only slightly improve the BER performance of the proposed receivers. In this case, one iteration is enough for the proposed receivers. Although the BER performance of the FDO-ZF is not as good as that of FSFD-MMSE, it can achieve about 5 dB SNR gain at the BER of 1×10^{-5} compared with

the conventional CP OFDM.

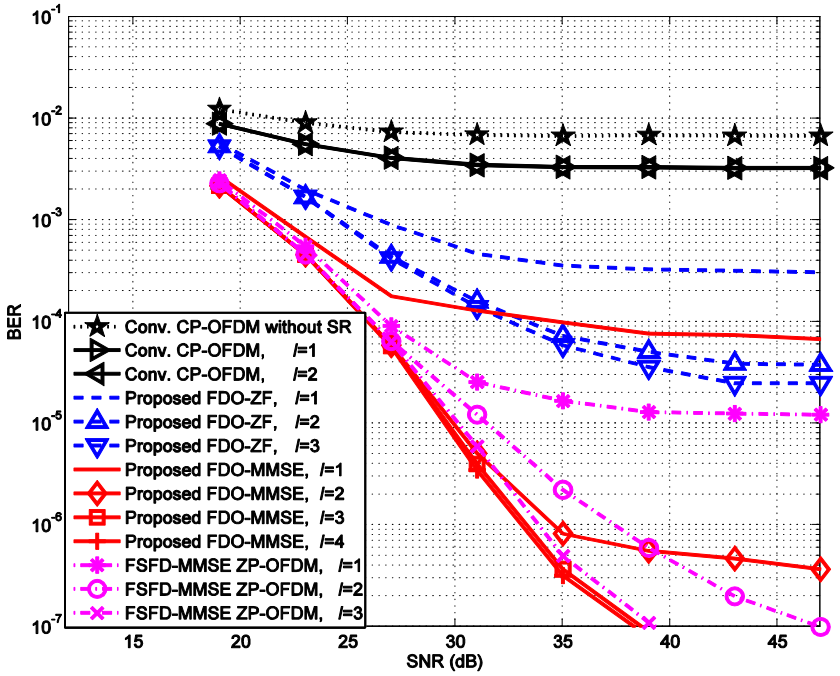

Fig. 4-9. The BER performance for large maximal path delay (Q=57).

The conventional CP OFDM receiver without SR shown in Fig. 4-9 suffers from high error floor due to the ISI for the largest delay (Q=57) case (i=4) due to the ISI. However, the proposed FDO-MMSE for CP OFDM can significantly reduce the error floor to a BER of 3×10^{-5}. If an additional iteration (I=2,3,4) is performed, the error floor can be further reduced to a BER that is less than 1×10^{-7}. Furthermore, the proposed FDO-ZF for CP OFDM can also reduce the error floor to 3×10^{-4}, 4×10^{-4} and 2.5×10^{-5} for I=1, I=2, and I=3, respectively. However, more iterations will lead to more complexity of implementation. It is a trade off to select the number of iterations. For the conventional CP OFDM receiver, the SR method with two iterations can only slightly reduce the BER floor. However, for FSFD-MMSE receiver in ZP OFDM, the SR method with three iterations can significantly improve the BER performance. With three iterations, the proposed FDO-MMSE for CP OFDM is even slightly better than the FSFD-MMSE with SR for ZP OFDM in terms of BER performance. The main reason is that proposed FDO-MMSE receiver can fully take advantage of the CP portion.

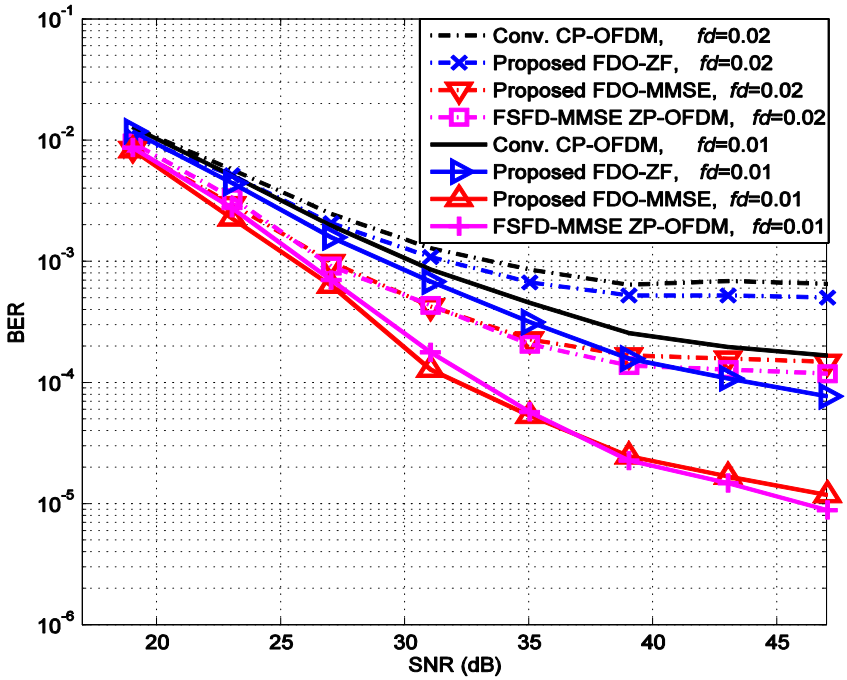

Fig. 4-10. The BER performance for different normalized residual Doppler frequency shift f_d.

Although our proposed FDO-based receivers are designed based on the quasi-static frequency-selective fading channel, they can also work well under a dispersive time-varying fading channel, where the ICI is introduced by Doppler frequency shift. In this case, the channel is varying inside the OFDM symbol, which destroys the orthogonality among the subcarriers. We still assume a multipath fading channel with N_q =15 and i=2. The normalized Doppler frequency shift f_d is introduced in the channel. The channel is estimated by the first stage equalizer (i.e., the conventional CP OFDM). The results in Fig. 4-10 show that the proposed FDO-based receivers are robust with respect to time-varying fading. Compared with the conventional CP OFDM, the FDO-MMSE in CP OFDM can reduce the BER error floor from 1.7×10^{-4} to 1.2×10^{-5} when the normalized Doppler frequency shift f_d is 0.01 (1% of the symbol rate $1/T$), and the less complex FDO-ZF can also slightly lower the BER error floor in CP OFDM. The proposed FDO-MMSE in CP OFDM and the FSFD-MMSE in ZP OFDM can offer similar BER performance for the both Doppler frequency shifts f_d = 0.01 and f_d = 0.02.

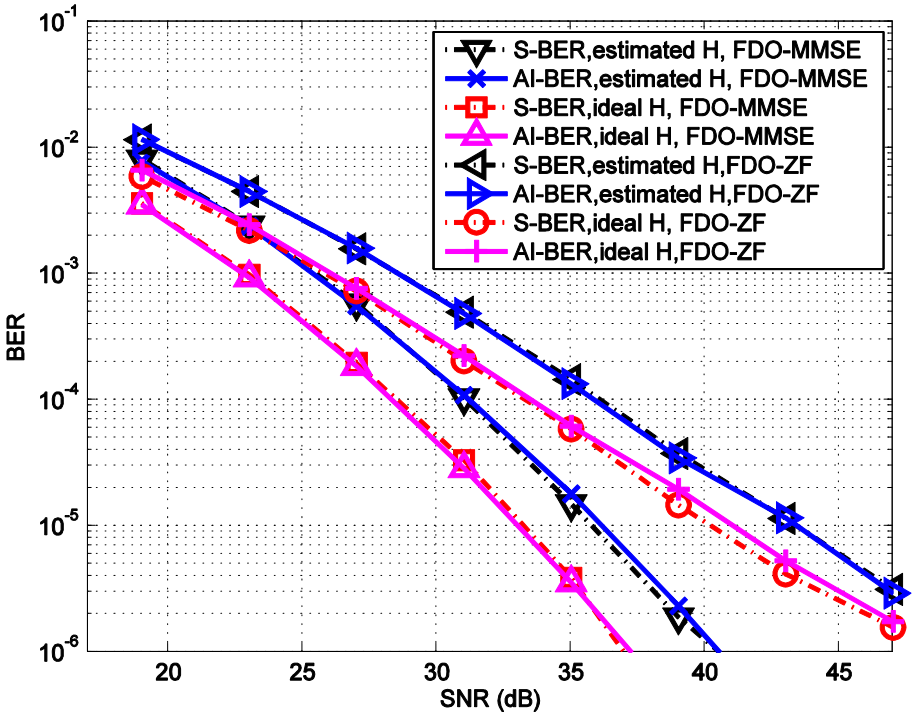

Fig. 4-11. The BER performance comparison between S-BER and AI-BER

The simulated BER (i.e., S-BER) and the AI-BER results for FDO-MMSE and FDO-ZF receivers are presented in Fig. 4-11. The S-BER is obtained based on the statistics of the number of error bits received in the simulations. The AI-BER is calculated based on (4.28) and (4.29). We assume a multipath fading channel with N_q =15 and i=2, and there is no CFO or Doppler frequency shifts. It is shown that the AI-BER curves match very well with the S-BER curves regardless of whether the channel information in (4.19) is perfectly known (i.e., ideal H) or unknown (i.e., estimated H). The results in Fig. 4-11 indicate that the AI-BER expression is relatively accurate for evaluating the BER performance of the proposed receivers.

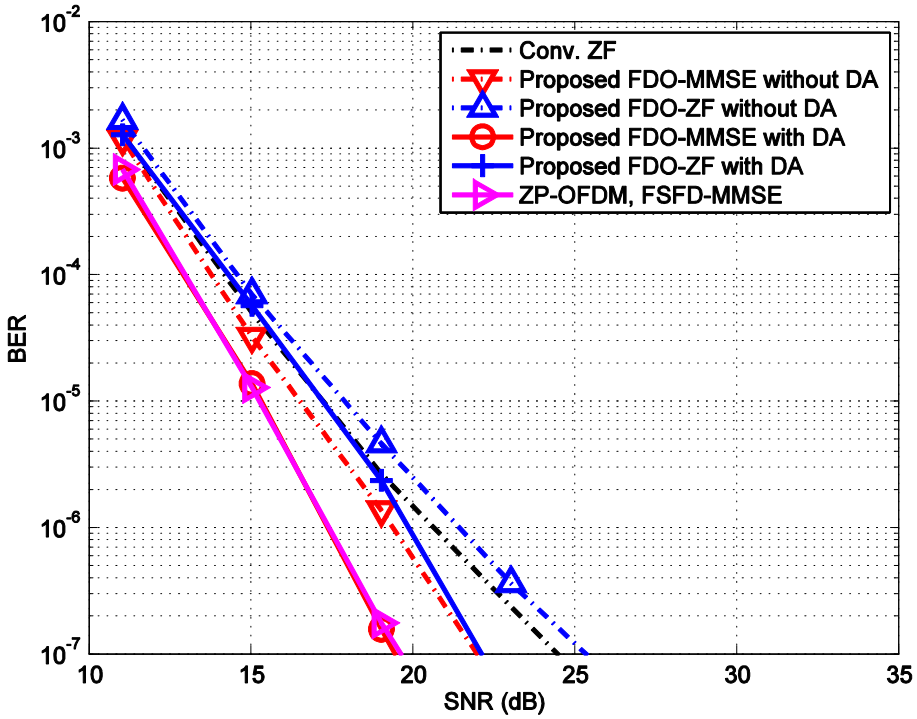

Fig. 4-12. The BER performance comparison with channel coding

Usually channel coding is applied in the practical communication systems. The results in Fig. 4-12 show the BER performance of the proposed FDO equalizers in the CP OFDM system with channel coding. A rate ½ convolutional encoder with constraint-length 7 and generator polynomial [171 133] is adopted in the transmitter and a hard-decision Viterbi decoder with a traceback length 32 is used in the receiver. With DA method, the FDO-MMSE and FDO-ZF receiver can significantly improve the BER performance compared with them without DA. The FDO-MMSE with DA in CP OFDM and the FSFD-MMSE in ZP OFDM can have similar BER performance, which is much better than that of the conventional ZF receiver in the observed SNR range. The FDO-ZF with DA can also offer better BER performance than the conventional ZF receiver when SNR becomes high.

4.5.2 Simulation Results for CP MC-CDMA

In the simulations, we compare the BER performance of the conventional ZF, the proposed iterative FDO based receivers (i.e., IT-FDO-MMSE, IT-FDO-DMMSE, IT-FDO-NF and IT-FDO-ZF equalizers) for CP MC-CDMA system. We consider a downlink with N=64 subcarriers,

K = 64 users, P = 8, QPSK modulated signals, and Walsh-Hadamard spreading codes. The SNR is defined as P_d/σ^2, where P_d is fixed to 1. We assume that the normalized quasi-static channel has N_q=8 linearly decaying multipath components with delays {0, iT/N, 2iT/N, 3iT/N, 4iT/N, 5iT/N, 6iT/N, 7iT/N} and the total power is normalized to 1 (i.e., the power of each component is {8/36, 7/36, 6/36, 5/36, 4/36, 3/36, 2/36, 1/36}), where i represents the interval between two path components. Each component follows a complex normal distribution. We assume that the channel coefficients without frequency offset information can be perfectly estimated. The proposed FDO based equalizers in the both uncoded and coded OFDM systems are simulated. For the coded OFDM system, we consider a rate ½ convolutional encoder with constraint-length 7 and generator polynomial [171 133] in transmitter. The receiver adopts a hard-decision Viterbi decoder with a traceback length 32. We assume that i=1 and the maximum multipath delay Q=8. In this case the guard interval is sufficient to avoid ISI for conventional ZF equalizer.

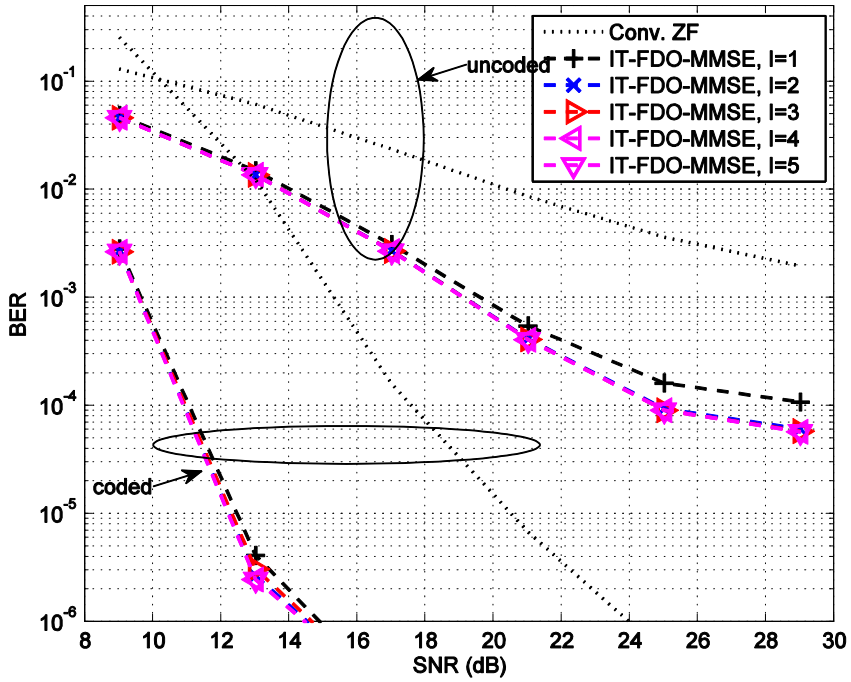

Fig. 4-13. Comparisons of IT-FDO-MMSE for CP MC-CDMA

For the IT-FDO-MMSE receiver, we evaluate the number of iterations required in Fig. 4-13. From the second iteration (I=2), all the BER curves almost overlap in the uncoded CP MC-CDMA system. It means that two iterations are acceptable for the IT-FDO-MMSE receivers. In

the coded system, only one iteration (I=1) is acceptable because the curves of all iterations are quite close. Thus, in the following simulations, we choose 2 iterations and 1 iteration for IT-FDO-MMSE receiver in the uncoded and coded system, respectively. Compared with 4 iterations required in CP OFDM system, the IT-FDO-MMSE receiver converges more quickly in the uncoded CP MC-CDMA system.

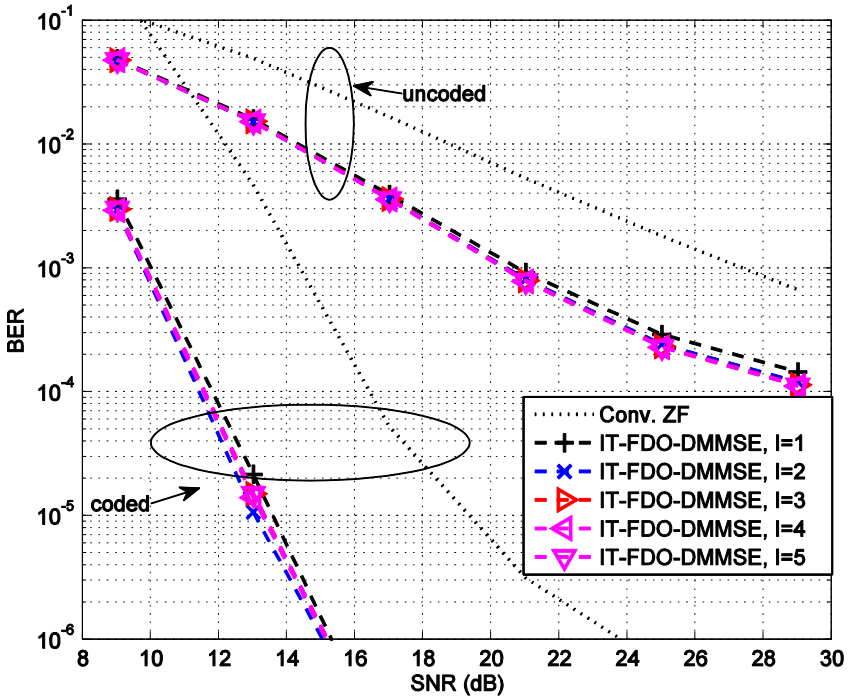

Fig. 4-14. Comparisons of IT-FDO-DMMSE for uncoded and coded CP MC-CDMA

The BER performance comparison of the IT-FDO-DMMSE receiver with different iterations in the uncoded and coded CP MC-CDMA is shown in Fig. 4-14. It can be found that one iteration is acceptable for the IT-FDO-DMMSE receivers in the both uncoded and coded systems, because the BER performance improvement is quite limited with more iterations. Hence, in the following simulations, we set the iteration number I of the IT-FDO-DMMSE receiver to 1 in the both coded and uncoded systems. In addition, the IT-FDO-DMMSE receiver cannot offer better BER performance than the conventional ZF equalizer in CP OFDM. However, it can offer much better BER performance in CP MC-CDMA system because it can benefit from the frequency diversity gain due to the spreading codes.

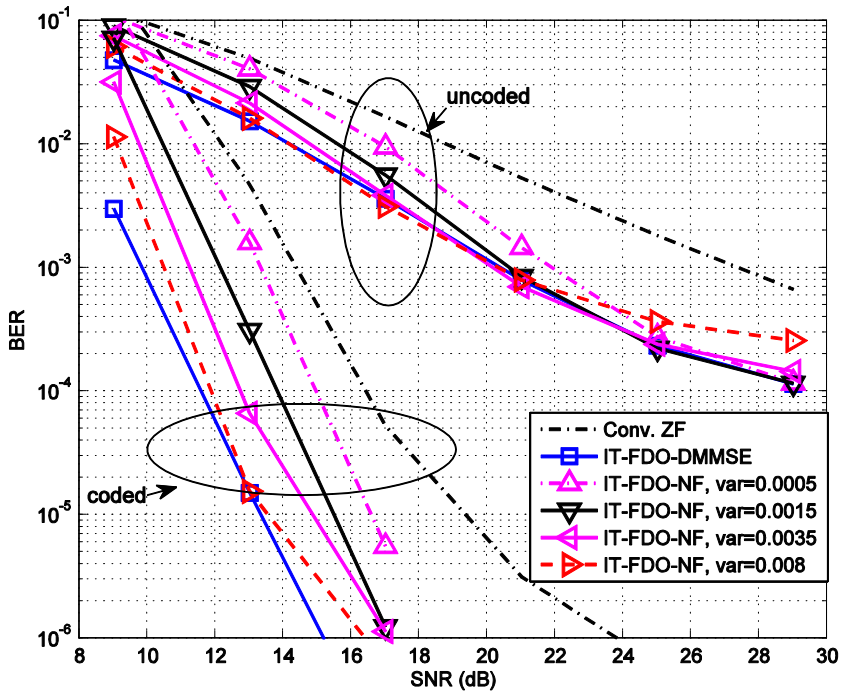

Fig. 4-15. Comparison of IT-FDO-NF for uncoded and coded CP MC-CDMA

The BER performance comparison of the IT-FDO-NF receiver with different fixed noise variances in the uncoded and coded CP MC-CDMA systems is shown in Fig. 4-15. With different fixed noise variances, the IT-FDO-NF receiver will have similar BER performance to the IT-FDO-DMMSE in different SNR range. For example, in the uncoded system, if we know that the SNR range in the system is from 18 dB to 29 dB, the variance can be set to 0.0035 (i.e., around 24 dB) for better performance in this SNR range. Simulation shows that the BER performance of the IT-FDO-NF with var=0.0035 is similar to that of the IT-FDO-DMMSE from 18 dB to 29 dB. In the coded system, if the expected SNR is small than 18 dB, the variance can be set to 0.008 or more. The BER curve of the IT-FDO-NF with variance 0.008 is more close to that of the IT-FDO-DMMSE than that with other variances.

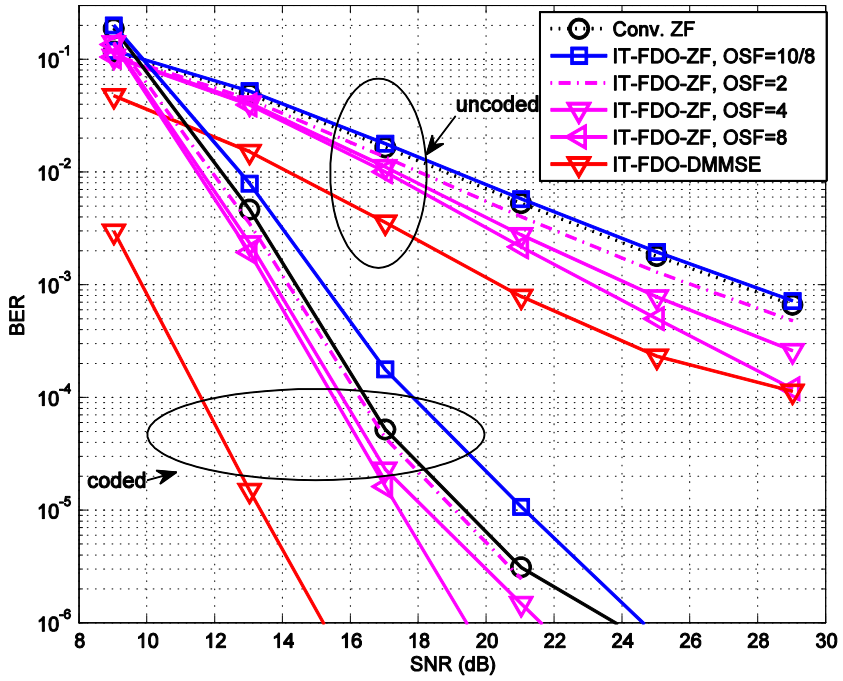

Fig. 4-16. Comparison of IT-FDO-ZF for uncoded and coded CP MC-CDMA

The BER performance comparison of the IT-FDO-ZF receiver with different OSF in the uncoded and coded CP MC-CDMA systems is shown in Fig. 4-16. If the OSF is only 10/8 (i.e., the DFT symbol includes the OFDM symbol, the CP part and the tail part caused by multipath), the IT-FDO-ZF actually cannot provide better BER performance than the conventional ZF equalizer. It means that the ZF equalizer cannot fully take advantage of the CP part and the tail part, and the noise on each subcarrier is not suppressed. However, it can be found that the BER performance of the IT-FDO-ZF is improved in the both uncoded and coded systems if the OSF is increased, which matches our analysis. For other OSFs (e.g., 2, 4 and 8), the IT-FDO-ZF can offer better BER performance than the conventional ZF equalizer. The SNR gain of about 5 dB can be achieved for the OSF of 8 at a BER level of 1×10^{-6} in the coded system.

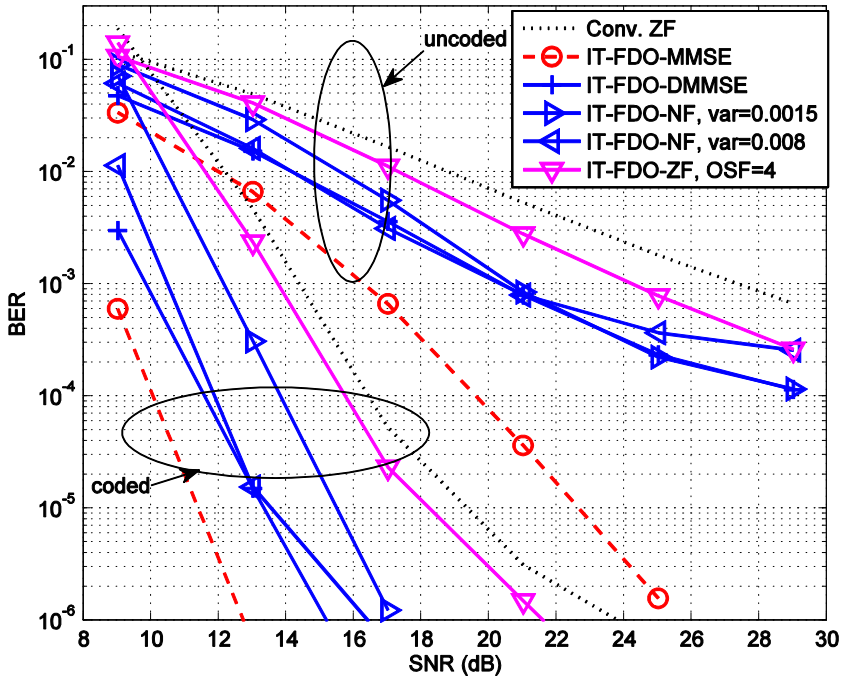

Fig. 4-17. Comparisons of the proposed equalizers for CP MC-CDMA system

The BER performance comparison of the proposed equalizers in the uncoded and coded CP MC-CDMA systems over the channel without frequency offset and Doppler frequency shift is shown in Fig. 4-17. Among all receivers, the IT-FDO-MMSE can achieve the best BER performance in the both uncoded and coded systems, and it is much better than the conventional ZF equalizer. In the coded system, the SNR gain achieved by the IT-FDO-MMSE can be up to 13 dB at a BER level of 1×10^{-6}. Compared with the conventional ZF equalizer, The IT-FDO-DMMSE can offer significant performance improvement (about 9 dB SNR gain at a BER of 1×10^{-6}), and the IT-FDO-ZF can also offer small performance improvement (about 2 dB SNR gain for OSF=4 at a BER of 1×10^{-6}). To reduce the implement complexity, we can use the IT-FDO-NF to replace the IT-FDO-DMMSE. The BER performance of the IT-FDO-NF can be similar to that of the IT-FDO-DMMSE if the variance is chosen properly. The variance choice can be based on the expected SNR range as we explain for Fig. 4-15. In the uncoded system, all the proposed iterative receivers can also offer better BER performance than the conventional ZF equalizer. Same as the analyses in the coded system, the IT-FDO-MMSE can obtain the best BER

performance among all 4 receivers. The IT-FDO-DMMSE and IT-FDO-NF receivers can offer the moderate BER performance with the moderate complexity compared with the IT-FDO-MMSE and IT-FDO-ZF receivers. The IT-FDO-ZF receiver can only offer slightly better BER performance. It can also be concluded that the IT-FDO-MMSE, IT-FDO-DMMSE and IT-FDO-NF can benefit from the frequency diversity gain due to the spreading codes, but the IT-FDO-ZF can benefit from the large OSF.

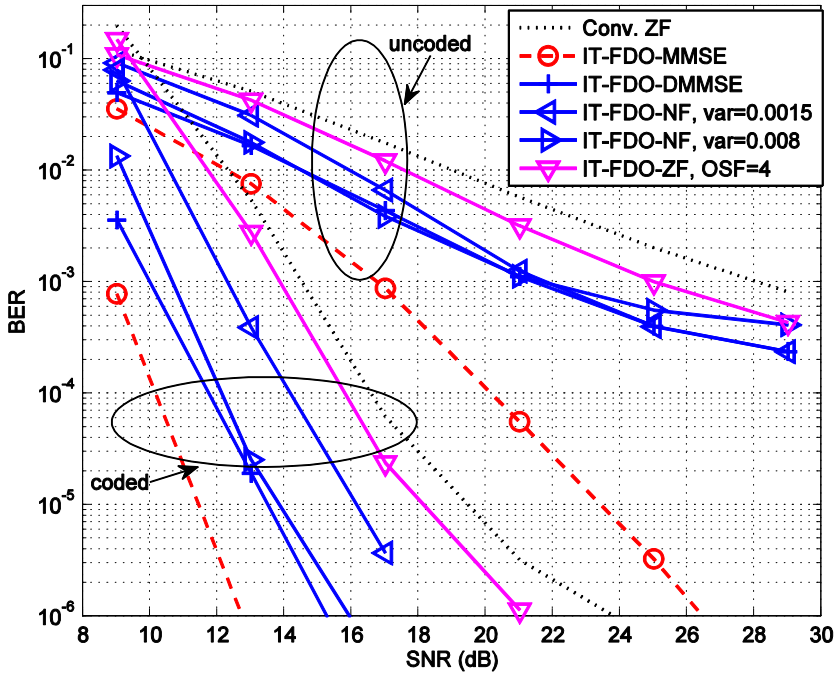

Fig. 4-18. Comparison of proposed equalizers for CP MC-CDMA with ε=0.02

The BER performance comparison of the proposed equalizers in the uncoded and coded CP MC-CDMA systems on the multipath channel with normalized carrier frequency offset ε=0.02 is shown in Fig. 4-18. Compared with the BER curves shown in Fig. 4-17, the BER curves of the proposed FDO based receivers do not show much difference in the both uncoded and coded systems. The IT-FDO-MMSE can obtain the best BER performance among all 4 receivers at the cost of the highest complexity, and with the moderate complexity, the IT-FDO-DMMSE and IT-FDO-NF receivers can offer clearly better BER performance than the conventional ZF receiver. The IT-FDO-ZF receiver can offer slightly better BER performance than the conventional ZF

receiver. It means that the proposed FDO based receivers have quite stable performance in the multipath environment with such frequency offset.

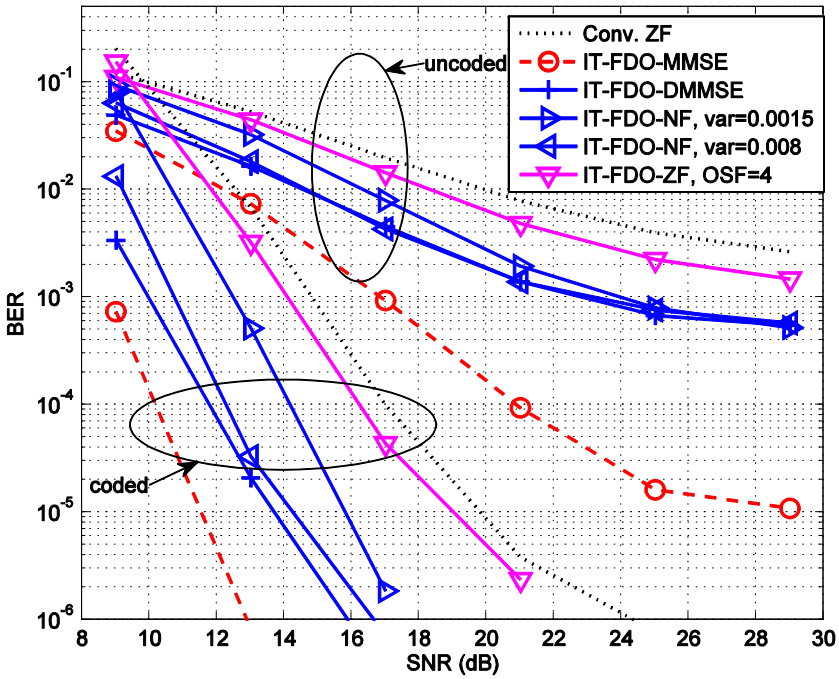

Fig. 4-19. Comparison of proposed equalizers for CP MC-CDMA system with f_d=0.02

The BER performance comparison of the proposed equalizers in the uncoded and coded CP MC-CDMA systems on the multipath delay channel with normalized Doppler frequency shift f_d=0.02 (2% of the symbol rate 1/T) is shown in Fig. 4-19. The normalized Doppler frequency shift is introduced in the Rayleigh fading channel by using the Matlab function "rayleighchan". Since the channel is not fixed during one OFDM symbol period, the instantaneous path gain of one sample is adopted for channel equalization, which is obtained from the property "PathGains" of the Rayleigh channel object. Comparing Fig. 4-17 and Fig. 4-19, it can be found that the BER performance of the proposed iterative FDO based receivers is just slightly reduced by Doppler frequency shift in the both uncoded and coded MC-CDMA systems, and it is much better than that of the conventional ZF receiver. It still can be observed that the IT-FDO-MMSE can obtain the best BER performance among all 4 receivers, and the IT-FDO-DMMSE and IT-FDO-NF receivers with the moderate complexity can offer the clearly better BER performance than the

conventional receiver. The IT-FDO-ZF receiver can only offer slightly better BER performance. In other words, the proposed the iterative FDO based receivers can also tolerate larger Doppler frequency shift than the conventional ZF receiver.

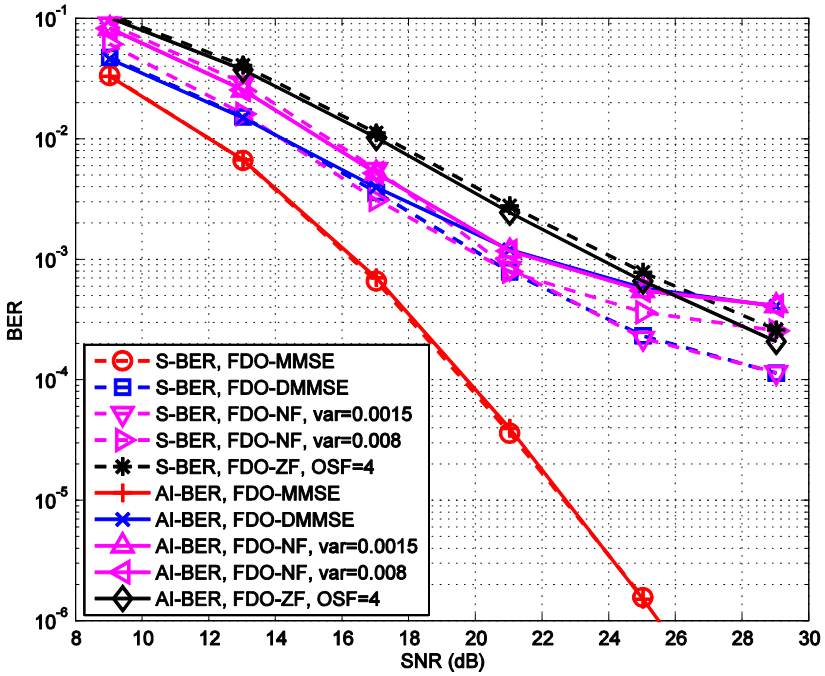

Fig. 4-20. Comparison between AI-BER and S-BER for uncoded CP MC-CDMA system

The BER performance comparison of proposed equalizers between average instantaneous BER solution (i.e., AI-BER) and simulation (i.e., S-BER) in the uncoded CP MC-CDMA system is shown in Fig. 4-20. S-BER is calculated by counting the number of error bits in the simulations. We can find that for IT-FDO-MMSE and IT-FDO-ZF receivers, their AI-BER curves are quite close to their S-BER curves. However, the IT-FDO-DMMSE and IT-FDO-NF receivers present slightly large BER difference between AI-BER and S-BER in high SNR level. This is mainly because that the received signal for S-BER is not same as that for AI-BER due to the SR method.

4.6 The Performance Comparisons between OFDM and MC-CDMA Systems

In this section, we compare the proposed FDO based equalizers between the ZP and CP based

MCM systems. It is assumed that 64 subcarriers (i.e., N=64) and QPSK are employed. The ZP and CP length are set to one-eighth of the OFDM symbol length (i.e., G=8). The transmitted signal is passed through a quasi-static multipath channel **h** and is corrupted by additive white Gaussian noise. The normalized quasi-static channel has N_q =8 linearly decaying multipath components with delays of {0, iT/N, …, $i(N_q\text{-}1)T/N$} and total power of 1 (i.e., the power of each component is {8/36, 7/36, 6/36, 5/36, 4/36, 3/36, 2/36, 1/36}), where T is the OFDM symbol duration and i denotes the normalized multipath interval. The maximal path delay Q= i(N_q-1)+1. The proposed FDO based equalizers in the both uncoded and coded OFDM systems are simulated. For coded OFDM systems, we consider a rate ½ convolutional encoder with constraint-length 7 and generator polynomial [171 133] in transmitter. The receiver adopts a hard-decision Viterbi decoder with a traceback length 32. We compare the four proposed equalizers (FDO-MMSE, FDO-DMMSE, FDO-NF and FDO-ZF) between ZP OFDM and CP OFDM system, between CP OFDM and CP MC-CDMA systems, and between ZP MC-CDMA and CP MC-CDMA systems. For CP based systems, the iterative FDO based equalizers shall be adopted.

For short multipath delay channel (i.e., sufficient GI), we assume i=1 and Q=8. Hence, the guard interval is enough to avoid ISI. For long multipath delay channel (i.e., insufficient GI) we assume that i=2 and Q=15, i.e., the guard interval is not enough to avoid ISI. In this case, the iterative FDO based equalizers shall be adopted.

For a fair comparison between ZP and CP MCM systems, we assume that both CP and ZP MCM use the same amount of energy for the main part (without the guard interval) transmission. In this case, the conventional receivers for the two types of MCM systems have the similar BER performance, but the ZP MCM scheme will consume lower transmission energy in total.

4.6.1 The Performance Comparison between ZP OFDM and CP OFDM Systems

In the simulations, we compare the proposed FDO based equalizers between ZP OFDM and CP OFDM systems. For ZP OFDM with the insufficient guard interval and CP OFDM, the iterative FDO based equalizers are adopted.

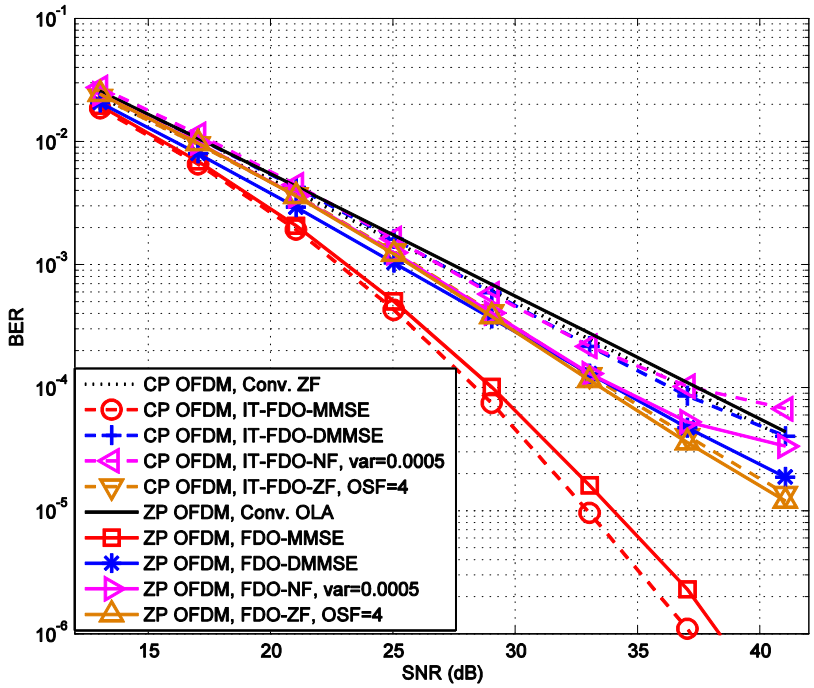

Fig. 4-21. Comparison between uncoded ZP and CP OFDM with sufficient GI

The BER performance comparison of the proposed FDO-based equalizers in the uncoded ZP OFDM and CP OFDM system over a short multipath delay channel is shown in Fig. 4-21. The conventional ZF in CP OFDM and the conventional ZF with OLA in the uncoded ZP OFDM can provide almost same BER performance, which match the analysis in [5]. The proposed FDO-MMSE in the uncoded CP OFDM can have slightly better BER performance than it in the uncoded ZP OFDM, and about 1 dB SNR gain can achieve at a BER of 1×10^{-6} in the uncoded CP OFDM. This is because that the IT-FDO-MMSE in CP OFDM can take advantage of the CP part. The FDO-ZF equalizer in the uncoded ZP OFDM can offer slightly better BER performance than it in the uncoded CP OFDM system. In the uncoded CP OFDM, the FDO-DMMSE equalizer cannot offer better BER performance than the conventional ZF equalizer due to the noise amplification caused by the matrix diagonalization and symbol reconstruction. However, in the uncoded ZP OFDM, the FDO-DMMSE equalizer can improve the BER performance compared with the conventional ZF equalizer. The reason is that the diagonalization of matrix and symbol reconstruction in CP OFDM introduces more interference than that in ZP OFDM.

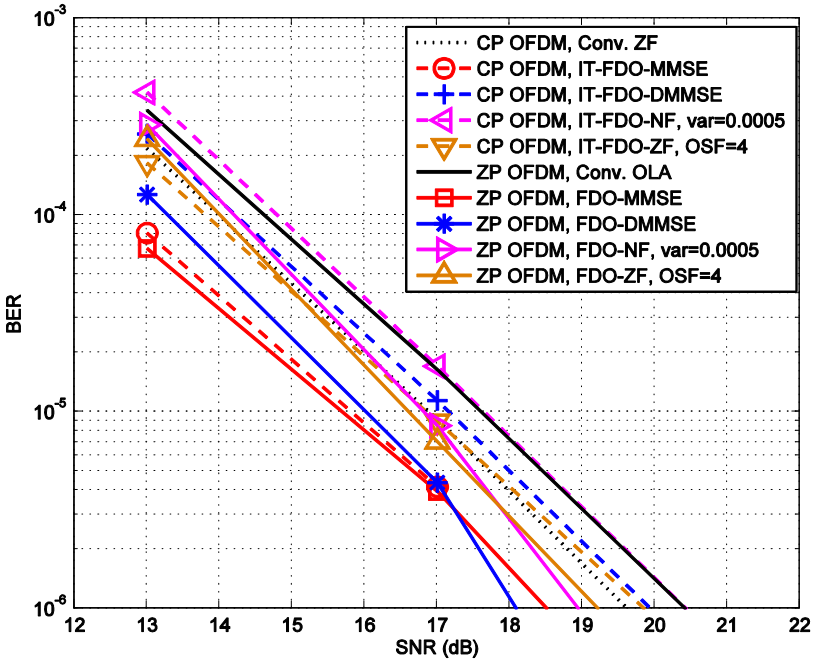

Fig. 4-22. Comparison between coded ZP and CP OFDM with sufficient GI

The BER performance comparison of the proposed FDO-based equalizers in the coded ZP OFDM and CP OFDM systems over a short multipath delay channel is shown in Fig. 4-22. Similarly, the FDO-DMMSE and FDO-NF equalizers cannot offer better BER performance in the coded CP OFDM than they in the coded ZP OFDM due to the noise amplification caused by the matrix diagonalization. Although the FDO-MMSE can take advantage of the CP part to improve the BER performance, it is also degraded by the noise amplification caused by symbol reconstruction. In the low SNR range (e.g., <20dB), the noise amplification becomes large, therefore the FDO-MMSE equalizer in the both ZP and CP OFDM systems demonstrates similar BER performance. Because the iterative FDO-ZF, FDO-DMMSE and FDO-NF in CP OFDM encounter the noise amplification caused by the symbol reconstruction, they cannot offer BER performance as good as that in the ZP OFDM. The FDO-DMMSE and FDO-NF equalizers can have better BER performance than the conventional ZF equalizer in the coded ZP OFDM system. However, they cannot provide better BER performance in the coded CP OFDM system.

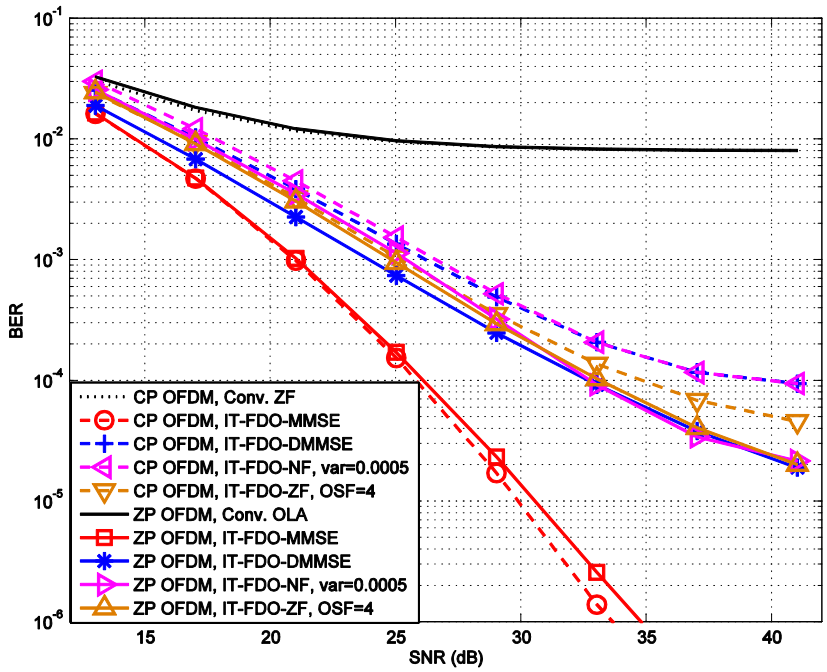

Fig. 4-23. Comparison between uncoded ZP and CP OFDM with insufficient GI

The BER performance comparison of the iterative FDO-based equalizers between the uncoded ZP OFDM and CP OFDM systems over a long multipath delay channel is shown in Fig. 4-23. We can have the same results as that in Fig. 4-21. The FDO-MMSE receiver in the uncoded CP OFDM system can have slightly better BER performance than it in the uncoded ZP OFDM system, and about 1 dB SNR gain can be achieved at a BER of 1×10^{-6} in the uncoded CP OFDM system. It is because that the FDO-MMSE equalizer in CP OFDM can take advantage of the CP part to improve the BER performance, even it also encounters the noise amplification caused by the SR. In addition, the FDO-DMMSE and FDO-NF equalizers can have better BER performance in the uncoded ZP OFDM system than they in the uncoded CP OFDM system. This is because the matrix diagonalization and SR in CP OFDM system introduces more interference than it in ZP OFDM system due to the repeated CP part. The FDO-ZF equalizer can offer slightly better BER performance in the uncoded ZP OFDM system than it in the uncoded CP OFDM system due to the noise amplification by SR.

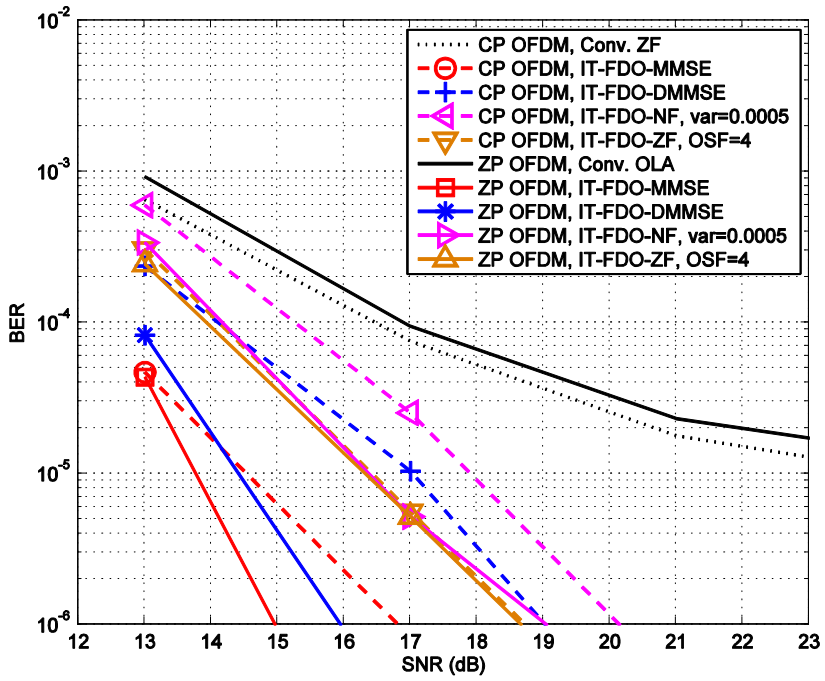

Fig. 4-24. Comparison between coded ZP and CP OFDM with insufficient GI

The BER performance comparison of the iterative FDO based equalizers between the coded ZP OFDM and CP OFDM systems over a long multipath delay channel is shown in Fig. 4-24. Although CP OFDM can take advantage of the CP part to improve the BER performance by using MMSE equalizer, it encounters more ISI from the adjacent symbols for FDO based equalizer at low SNR level because the CP part is not removed and SR method cannot fully remove ISI, which actually can degrade the BER performance. The results in Fig. 4-24 show that the FDO-MMSE demonstrates better BER performance in the coded ZP OFDM than it in the coded CP OFDM. The main reason is that in low SNR level (e.g., less than 20 dB), ISI introduced by SR in CP OFDM is larger than that in ZP OFDM. In high SNR level (e.g., large than 20 dB), the signal power becomes high, the signal power in CP part can help to improve the BER performance for the FDO-MMSE in the coded CP OFDM, which is verified in the uncoded systems shown in Fig. 4-21 and Fig. 4-23.

In summary, the conventional ZF equalizer shows the same BER performance in ZP and CP OFDM system. The iterative FDO based equalizers introduce more noise by the SR method in CP

system, and the matrix diagonalization of the FDO-DMMSE and FDO-NF in CP system also introduce more noise than they in ZP system, Hence, the FDO-DMMSE and FDO-NF can offer much better performance in ZP OFDM system than they in CP OFDM system, and the FDO-ZF can offer slightly better performance in ZP OFDM system than it in CP OFDM system. However, the FDO-MMSE can take advantage of the CP part to improve the BER performance. In high SNR range, the effect of CP part can exceed the side-effect of the SR method, but in low SNR range, it can only counteract the side-effect of the SR method. Hence, the FDO-MMSE equalizer has slightly better BER performance in the uncoded CP OFDM system than it in the uncoded ZP OFDM system. However, when SNR becomes low, the noise caused by SR is increased, the performance of the FDO-MMSE is degraded in the coded CP OFDM system, and is worse than it in the coded ZP OFDM system.

4.6.2 The Performance Comparison between CP OFDM and CP MC-CDMA Systems

In this section, the BER performance of the proposed FDO based equalizers is compared between CP OFDM and CP MC-CDMA systems. It is assumed that the same system model and multipath channel (used in Section 4.5.2) is used in the both CP OFDM and CP MC-CDMA systems. The only difference is that the CP OFDM system does not apply the spreading code in frequency domain. For short multipath delay channel (i.e., sufficient GI), we assume i=1 and Q=8. For long multipath delay channel (i.e., insufficient GI) we assume that i=2 and Q=15. It is also assumed that there is no frequency offset and Doppler frequency shift for comparison.

The BER performance comparison between the uncoded CP OFDM and CP MC-CDMA systems over a short multipath delay channel is shown in Fig. 4-25. Clearly, the IT-FDO-MMSE in the uncoded CP MC-CDMA system can have much better BER performance than it in the uncoded CP OFDM system, and about 11 dB SNR gain can be achieved at a BER of 1×10^{-6}. Although the approximation of matrix diagonalization introduces large interference in both CP OFDM and CP MC-CDMA, The IT-FDO-DMMSE and IT-FDO-NF in the uncoded CP MC-CDMA can still provide much better BER performance than they in the uncoded CP OFDM

system. However, the IT-FDO-ZF in CP MC-CDMA is just slightly better than it in CP OFDM system in terms of the BER performance. It can be concluded that the spreading coding used for the proposed FDO based equalizers in the uncoded CP MC-CDMA system can quickly reduce the BER results with SNR increasing.

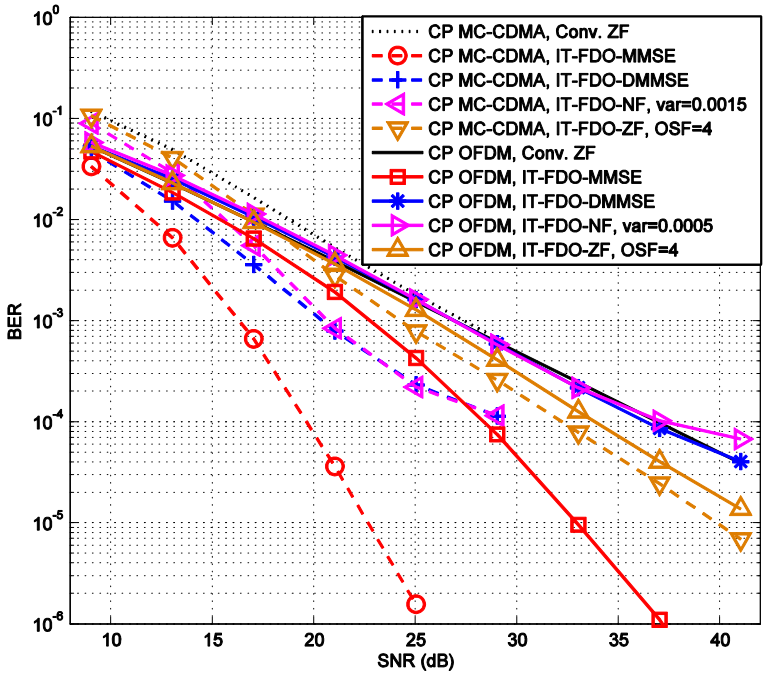

Fig. 4-25. Comparison between uncoded CP MCM systems with sufficient GI

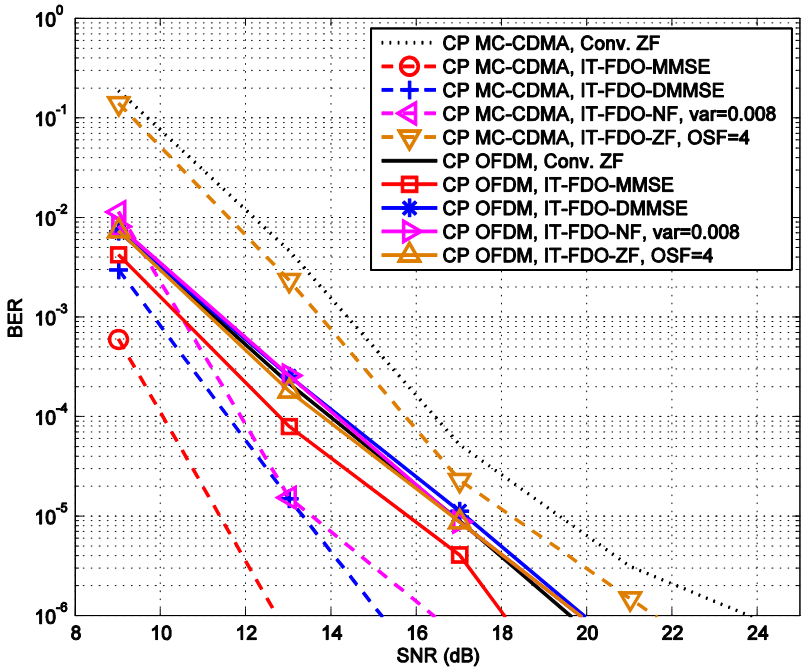

Fig. 4-26. Comparison between coded CP MCM systems with sufficient GI

The BER performance comparison between the coded CP OFDM and CP MC-CDMA systems over a short multipath delay channel is shown in Fig. 4-26. With channel coding, the BER performances of the IT-FDO-MMSE, IT-FDO-DMMSE and IT-FDO-NF equalizers in the coded CP MC-CDMA system can be rapidly reduced to a BER level of 1×10^{-6} when SNR increases. When SNR is more than 10 dB, , the IT-FDO-MMSE, IT-FDO-DMMSE and IT-FDO-NF in the coded CP MC-CDMA system can offer better BER performance than they in the coded CP OFDM system. About 5 dB, 5 dB and 4 dB SNR gain can be achieved in the coded CP MC-CDMA system at a BER level of 1×10^{-6}, respectively. It means that in coded CP MC-CDMA system, the proposed IT-FDO-MMSE, IT-FDO-DMMSE and IT-FDO-NF can benefit from the frequency diversity gain. However, the IT-FDO-ZF and conventional ZF cannot provide better BER performance in the coded CP MC-CDMA system in the simulated SNR range due to the IUI that caused by the low SNR.

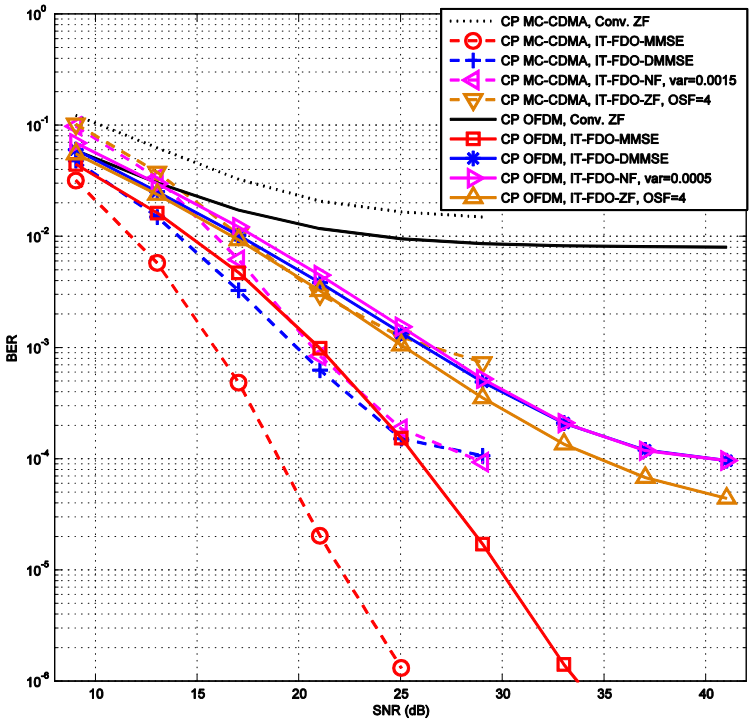

Fig. 4-27. Comparison between uncoded CP MCM systems with insufficient GI

For the long multipath delay channel, the BER results of the proposed FDO based equalizers in the uncoded CP MCM systems are shown in Fig. 4-27. The IT-FDO-MMSE, IT-FDO-DMMSE and IT-FDO-NF can offer better BER performance in the uncoded CP MC-CDMA system than they in the uncoded CP OFDM system because they can benefit from the frequency diversity gain caused by the spreading codes. The IT-FDO-MMSE can have about 8 dB SNR gain at a BER of 1×10^{-6} in the uncoded CP MC-CDMA system than it in uncoded CP OFDM system. The IT-FDO-DMMSE and IT-FDO-NF can have about 10 dB SNR gain at a BER of 1×10^{-4} because the two equalizers actually cannot offer good performance in CP OFDM system due to the large noise introduced by the approximation of the matrix diagonalization. The proposed IT-FDO-MMSE, IT-FDO-DMMSE and IT-FDO-NF equalizers are able to combat large ISI caused by the long multipath delay channel in the uncoded CP MC-CDMA system.

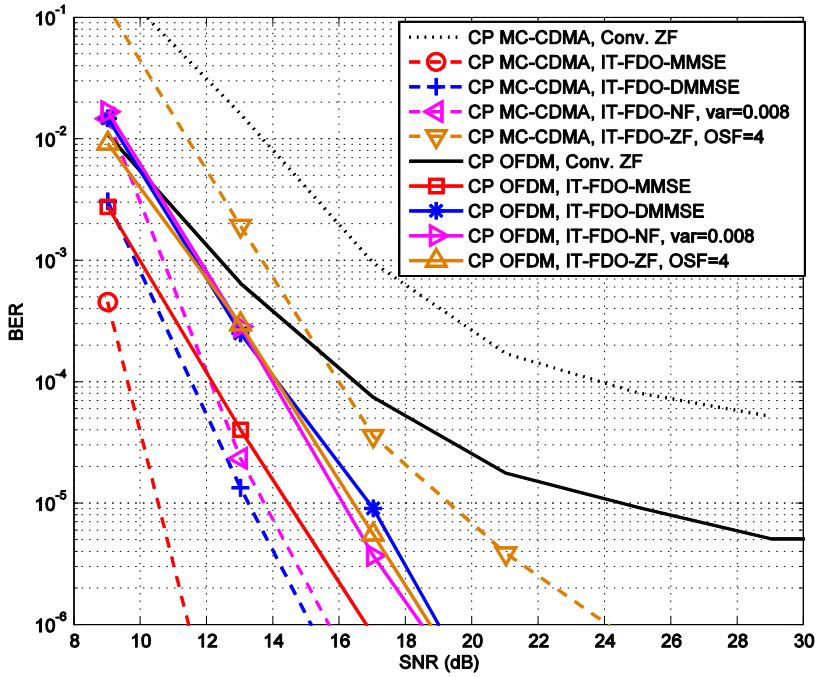

Fig. 4-28. Comparison between coded CP MCM systems with insufficient GI

The BER performance comparison between the coded CP OFDM and CP MC-CDMA system over a long multipath delay channel is shown in Fig. 4-28. In the coded CP MC-CDMA system, the IT-FDO-MMSE, IT-FDO-DMMSE and IT-FDO-NF can achieve 5 dB, 4 dB and 3 dB SNR gain at a BER of 1×10^{-6}, respectively, compared with them in coded CP OFDM system. However, the IT-FDO-ZF and conventional ZF in the coded CP OFDM can offer slightly better BER performance than they in the coded CP MC-CDMA system when SNR is small. It means that in the coded CP MC-CDMA system, the proposed IT-FDO-MMSE, IT-FDO-DMMSE and IT-FDO-NF can still benefit from the frequency diversity gain.

In summary, the IT-FDO-MMSE, IT-FDO-DMMSE and IT-FDO-NF receivers in CP MC-CDMA system can achieve better BER performance than they in CP OFDM system due to the spreading code that actually leads to the frequency diversity gain in CP MC-CDMA. The BER curves of the three receivers in CP MC-CDMA system decline more quickly than they in CP OFDM with SNR increasing. However, if the IT-FDO-ZF and conventional ZF are adopted, the CP OFDM can offer slightly better BER performance than the CP MC-CDMA system.

4.6.3 The Performance Comparison between ZP and CP MC-CDMA Systems

In this subsection, we compare the proposed FDO based equalizers between ZP and CP MC-CDMA systems. We assume that the same system model and multipath channel (used in Section 4.5.2) is used in the both ZP and CP MC-CDMA systems. For short multipath delay channel (i.e., sufficient GI), we assume i=1 and Q=8. For long multipath delay channel (i.e., insufficient GI) we assume that i=2 and Q=15. For CP MC-CDMA system, the iterative FDO based receivers are adopted. We further assume that there is no frequency offset and Doppler frequency shift.

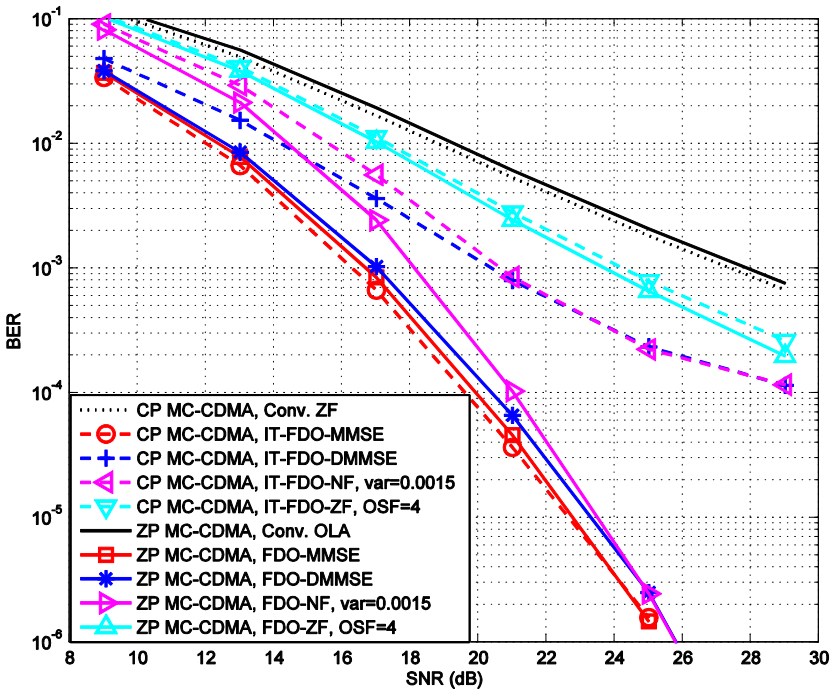

Fig. 4-29. Comparison between uncoded ZP and CP MC-CDMA system with sufficient GI

The BER performance comparison between the uncoded ZP MC-CDMA and CP MC-CDMA system in short multipath delay channel is shown in Fig. 4-29. The conventional ZF equalizer does not present much difference of BER performance in the uncoded ZP and CP MC-CDMA systems. The FDO-MMSE can offer slightly better BER performance in the uncoded CP MC-CDMA than it in the uncoded ZP MC-CDMA, because it can take advantage of the CP part. The FDO-DMMSE and FDO-NF in the uncoded ZP MC-CDMA can also offer better BER performance than they in the uncoded CP MC-CDMA system. It is mainly because the diagonalization of

matrix and the SR in CP MC-CDMA system introduces more noise than that in ZP MC-CDMA system. However, the FDO-ZF cannot take advantage of the CP part and the SR in CP system introduces more noise, it has slightly better BER performance in the uncoded ZP MC-CDMA than it in the uncoded CP MC-CDMA.

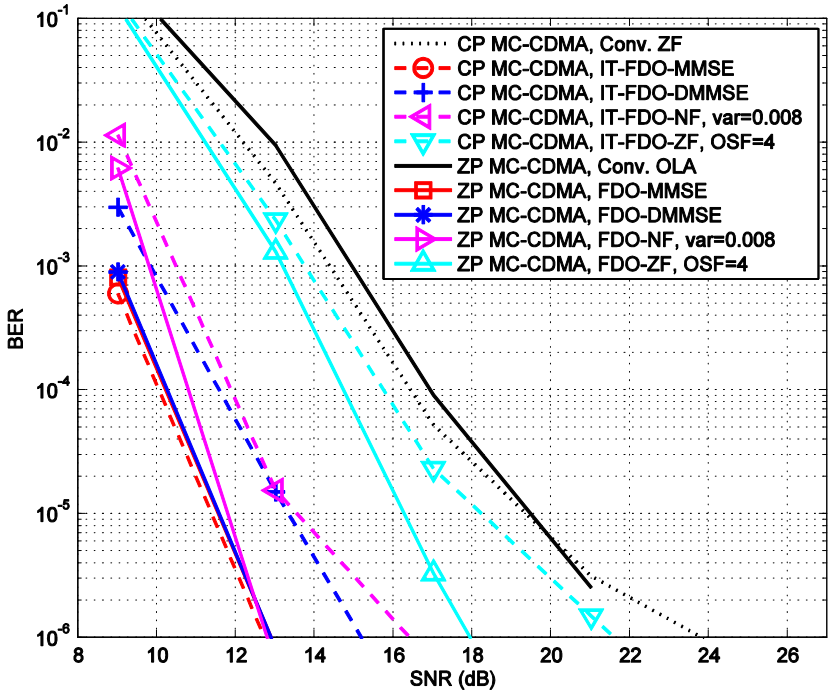

Fig. 4-30. Comparison between coded ZP and CP MC-CDMA system with sufficient GI

The BER performance comparison between the coded ZP MC-CDMA and CP MC-CDMA system over a short multipath delay channel is shown in Fig. 4-30. With channel coding, the similar results can be found. The FDO-DMMSE, FDO-NF and FDO-ZF equalizers in the coded ZP MC-CDMA system can provide better BER performance than they in the coded CP MC-CDMA system. The above three equalizers can achieve about 3 dB, 4 dB and 4 dB SNR gain in the coded ZP MC-CDMA system at a BER level of 1×10^{-6}, respectively. The main reason is that CP MC-CDMA encounters more ISI from the adjacent symbols if the FDO based equalizers are adopted. As we analyze before, in CP based system, the FDO-MMSE can take advantage of the CP part to improve the BER performance, but the SR method may introduce more noise. In the low SNR range (i.e., less than 13 dB), the effect of repeated CP part just counteracts the side-

effect of the SR method. Hence, the FDO-MMSE equalizer in the coded CP MC-CDMA has similar BER performance to it in the coded ZP MC-CDMA system in the low SNR range.

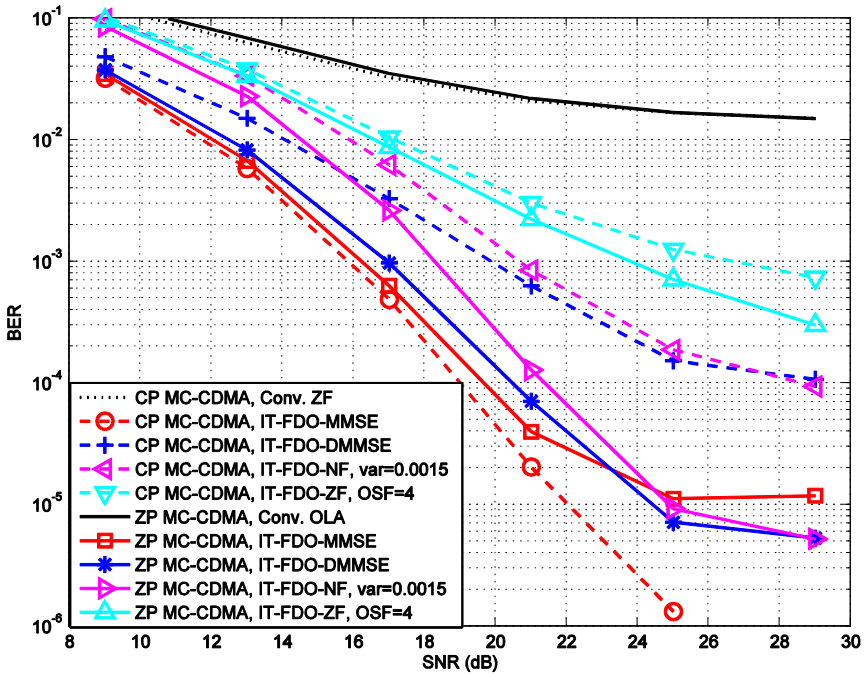

Fig. 4-31. Comparison between uncoded ZP and CP MC-CDMA system with insufficient GI

We consider the long multipath channel in Fig. 4-31 in the uncoded ZP MC-CDMA and CP MC-CDMA systems. Because the ISI exists, the iterative FDO based equalizers are adopted for the both ZP and CP MC-CDMA systems. The ISI leads the BER floor for the iterative FDO based equalizers in high SNR range. The conventional ZF does not show much difference in the uncoded ZP and CP systems. The IT-FDO-MMSE in the uncoded CP MC-CDMA system has lower BER floor than it in the uncoded ZP MC-CDMA system. The reason is that the CP part in CP MC-CDMA is used for equalization and MMSE method can fully take advantage of the power of the CP part to improve the BER performance. However, the IT-FDO-DMMSE and IT-FDO-NF equalizers in the uncoded ZP MC-CDMA system can have much better BER performance compared with them in the uncoded CP MC-CDMA system because the CP MC-CDMA system introduces more noise caused by SR and the matrix diagonalization. The IT-FDO-ZF equalizer in the uncoded ZP MC-CDMA system can also exhibit better BER performance than it in the

uncoded CP MC-CDMA system due to less noise introduced by SR in ZP MC-CDMA system.

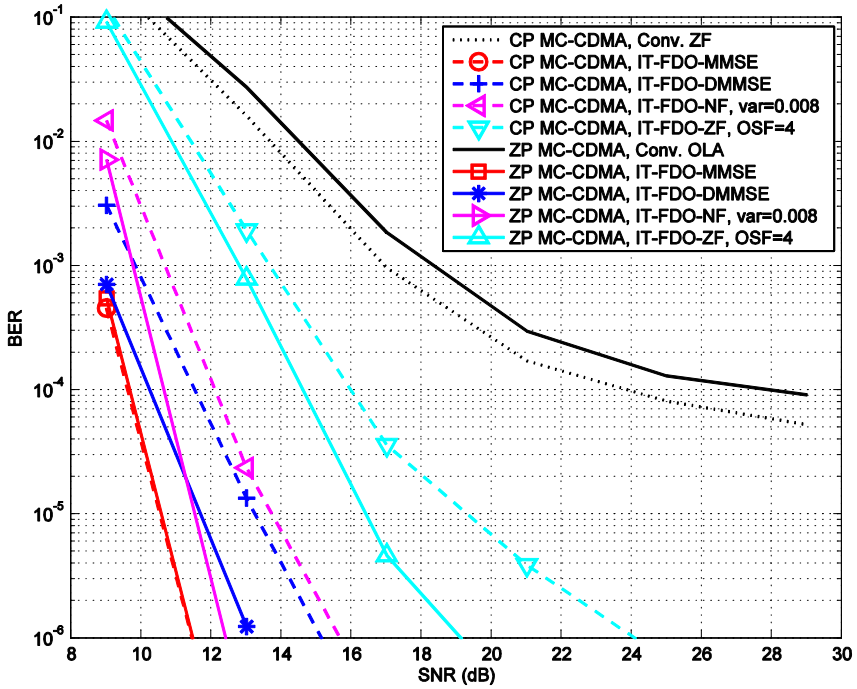

Fig. 4-32. Comparison between coded ZP and CP MC-CDMA system with sufficient GI

The BER performance comparison between the coded ZP MC-CDMA and CP MC-CDMA systems over the long multipath delay channel is shown in Fig. 4-32. With channel coding, the IT-FDO-MMSE in CP and ZP system has almost same BER performance, which is similar to the result in the case of short multipath delay channel. For other FDO based receivers, the coded ZP MC-CDMA system can have better BER performance than the coded CP MC-CDMA system because the matrix diagonalization and SR in CP system introduce more noise than that in ZP system. The IT-FDO-DMMSE, IT-FDO-NF and IT-FDO-ZF equalizers can achieve about 3 dB, 4 dB and 5 dB SNR gain in ZP MC-CDMA system at a BER level of 1×10^{-6}, respectively.

In summary, the iterative FDO based equalizers introduce more noise by the SR method in CP system, and the matrix diagonalization of the FDO-DMMSE and FDO-NF in CP system also introduces more noise than it in ZP system, which causes that the FDO-DMMSE and FDO-NF in ZP MC-CDMA system can have much better BER performance than they in CP MC-CDMA system, and FDO-ZF in ZP MC-CDMA system can have slightly better BER performance than it

in CP MC-CDMA system. However, the FDO-MMSE can take advantage of the CP part to improve the BER performance. In high SNR range, the effect of CP part can exceed the side-effect of the SR method, but in low SNR range, it can only counteract the side-effect of the SR method. Hence, the FDO-MMSE can offer similar BER performance in the coded CP and ZP MC-CDMA system. However, it can have slightly better BER performance in the uncoded CP MC-CDMA system than it in the uncoded ZP MC-CDMA system.

4.7 Conclusions

In this chapter, we proposed the novel two-stage iterative FDO-based receivers to improve the BER performance of CP OFDM and CP MC-CDMA systems by using SR method on the multipath fading channel. The expression of AI-BER is derived to accurately evaluate the BER performance of the proposed receivers. Simulations show that the BER performance of the proposed FDO-MMSE receiver in CP OFDM and CP MC-CDMA systems is much better than that of the conventional ZF equalizer and even slightly better than that of FSFD-MMSE receiver in ZP OFDM (with the same amount of transmission energy for the main part excluding the guard interval) when the residual CFO is small. Although the performance of the FDO-ZF receiver is not as good as that of the FDO-MMSE receiver, it is still better than that of the conventional CP OFDM and CP MC-CDMA receivers. Moreover, it can be improved by increasing the oversampling rate. The proposed FDO-MMSE and FDO-ZF receivers can tolerate a larger frequency offset and Doppler frequency shift than the conventional receiver for CP OFDM. It was also observed that for the proposed FDO-MMSE receiver, longer CP portion of the OFDM symbol can benefit the BER improvement. Furthermore, the proposed FDO-based receivers can tolerate large multipath delay, even when the path delay is larger than the CP length of OFDM.

For CP MC-CDMA system, The IT-FDO-DMMSE is proposed to reduce the complexity of the FDO-MMSE equalizer. It can offer the moderate BER performance with moderate complexity compared with the IT-FDO-MMSE and IT-FDO-ZF equalizers. The simplified IT-FDO-NF equalizer can obtain the similar BER performance to the IT-FDO-DMMSE in the expected SNR

range by appropriately choosing the noise variance.

In addition, the proposed FDO based receivers are compared between ZP OFDM and CP OFDM, and between ZP MC-CDMA and CP MC-CDMA. The iterative FDO based equalizers introduce more noise by the SR method in CP systems, and the matrix diagonalization of the FDO-DMMSE and FDO-NF in CP systems also introduces more noise than it in ZP systems, which cause that the FDO-DMMSE, FDO-NF and FDO-ZF in ZP MCM systems can have better BER performance than they in CP MCM systems. However, the FDO-MMSE can take advantage of the CP part to improve the BER performance. In high SNR range, the effect of CP part can exceed the side-effect of the SR method, but in low SNR range, it may or may not counteract the side-effect of the SR method because the noise is increased. Hence, the FDO-MMSE can have slightly better BER performance in the uncoded CP systems than it in the uncoded ZP systems. However, it may not offer better BER performance in the coded CP systems than it in the coded ZP systems.

The BER performance between CP OFDM and CP MC-CDMA systems are compared by simulations. If the IT-FDO-MMSE, IT-FDO-DMMSE and IT-FDO-NF receivers are adopted, CP MC-CDMA system can achieve better BER performance than CP OFDM system due to the spreading codes. The BER curves of the three receivers in CP MC-CDMA system decline more quickly than they in CP OFDM with SNR increasing. However, if the IT-FDO-ZF and conventional ZF are adopted, the CP OFDM can offer slightly better BER performance than the CP MC-CDMA system.

5 Energy Detection of Narrow-band Signal in OFDM System

5.1 Introduction

In cognitive radio (CR) networks, the basic requirement is that the cognitive user (CU) has the ability to detect the presence of the CU over the specific spectrum. Thus, the CU can adopt a feasible scheme to avoid harmful interference to the primary user (PU) by either stopping transmitting when the PU is active or transmitting in a reduced spectrum by excluding the spectrum of the PU signals after identifying or detecting the PU signals. The second spectrum management scheme (i.e., transmission in a reduced spectrum) requires that the CU is able to dynamically adjust the spectrum according to the spectrum sensing result. Since OFDM system transmits the high data rate signals on a number of subcarriers with low data rate at different frequencies simultaneously, it is a natural choice for CR networks.

To fully take the advantage of the spectrum, OFDM system may be designed to have the capability to detect which subchannels are clear for data transmission. In this case, the signal detection method in frequency domain can be adopted. Among many types of spectrum sensing method, energy detection (ED) is a popular method for the detection of unknown primary signals over fading channels owing to its low complexity. However, the probability of detection (PD) of ED is greatly reduced when SNR becomes low. On the other hand, a narrow-band PU signal is difficult to detect in OFDM system, when it straddles the boundaries of two adjacent subcarriers or the PU signals are not exactly on the subcarriers of the CU system. To overcome such problems, DFT with large size is usually suggested to detect the narrow-band signals for ED algorithms in frequency domain. The effect of DFT size on spectrum sensing is analyzed in this chapter. Our analyses show that increasing DFT size not only helps detect the narrow-band signal between two subcarriers, but also improve the probability of detection [59]. When the rough frequencies of PU signals are known, by pre-processing the received signal in time domain, a

novel method is proposed to improve the probability of detection of ED in frequency domain without increasing the DFT size. The noise smoothing method is proposed for ED to achieve high SNR gain in frequency selective fading channel. The major contributions in this chapter are the analysis of the effect of DFT size on the detection of narrow-band signal, and a proposal, named as the noise smoothed ED (NS-ED), to improve the PD performance with high SNR gain over the multipath fading channels. The close-form solution of the PD for the proposed NS-ED over the multipath fading channels is developed and verified by simulations.

5.2 System Model and Detection Performance

We assume that the CU signal is an OFDM signal with N subcarriers and the sampling period of T. i.e., the subcarrier spacing is $\frac{1}{NT}$ and the normalized bandwidth of the CU signal is N. The normalized bandwidth of the PU signal is less than $N/2$ and the symbol rate of it (i.e., the modulation rate) is much lower than the OFDM symbol rate of the CU signal. We further assume that the channel is not changed in one OFDM symbol (e.g., quasi-static multipath channel), and assume the number of paths is Q. The equivalent channel impulse response can be modeled as

$$h[\tau] = \sum_{q=0}^{Q-1} h_q \delta(\tau - \tau_q) \text{ and } \sum_{q=0}^{Q-1} \mathrm{E}[|h_q|^2] = 1 \tag{5.1}$$

and the frequency response of the channel $h(\tau)$ is given by

$$H[f] = \int_0^{\infty} h(\tau) e^{-j2\pi f\tau} d\tau = \sum_{q=0}^{Q-1} h_q e^{-j2\pi f \tau_q} \tag{5.2}$$

where the channel path h_q of delay τ_q is a complex random variable, and $\delta(\tau - \tau_q)$ is Kronecker delta function. In the discrete time domain, it can be assumed that the delay $\tau_q = q$ is an integer from 0 to Q-1 in (5.1), which represents a multiple of the sample period. Hence, the discrete channel is $\mathbf{h}=[h_0 \ \ldots \ h_{Q-1}]^{\mathrm{T}}$. The frequency response of the channel H can be obtained by taking N-point DFT on $h[\tau]$.

We assume that only PU signal is transmitted. After sampling the received PU signal at the CU system, the detection problem can be modeled as a binary hypothesis testing problem in time-domain with two hypotheses, Π_0 and Π_1, as shown in (5.3):

$$\begin{aligned} &\Pi_0 : y[n] = w[n] \\ &\Pi_1 : y[n] = h[n] \otimes x[n] + w[n], \end{aligned} \quad n = 0,1,...,N-1, \tag{5.3}$$

where $y[n]$, $x[n]$ and $w[n]$ are the received signal, the PU signal and the additive noise, respectively; the convolution operation $h[n] \otimes x[n]$ is defined as $\sum_{q=0}^{Q-1} x[n-q]h[q]$. Hypothesis Π_1 represents that the time-domain PU signal $x[n]$ appears with noise $w[n]$. Hypothesis Π_0 represents that only noise is present. We assume that signal samples and noise samples are independent, and noise samples themselves are independent. Without loss of generality, we assume that the received signal $y[n]$ at the CU is a baseband signal.

The energy detection can be performed in both time domain and frequency domain [60]. In order to find the accurate location of the narrowband signal, we consider an energy detector in frequency domain. In this case, the time domain signal $y[n]$ (n=0, 1, …, N-1) is transformed to the frequency domain signal $Y[k]$ by using an N-point DFT, where k is the subcarrier index and k=0, 1, …, N-1. The two hypotheses in (5.3) can thus be re-written as

$$\begin{aligned} &\Pi_0 : Y[k] = W[k] \\ &\Pi_1 : Y[k] = H[k]X[k] + W[k] \end{aligned} \tag{5.4}$$

where $W[k]$ is a complex Gaussian random variable with a zero mean whose real and imaginary parts are jointly normal distribution, i.e., normally distributed and independent with the variance of $\sigma^2/2$, hence, and the noise power is σ^2. $H[k]$ is the channel status information (CSI) in frequency domain and can be obtained by taking N-point DFT on $h[n]$. In the frequency domain, the signal power is calculated for all subcarriers by the conventional ED method. Firstly, the signal $y[n]$ is divided into M blocks in sequence with N samples in each block, and then each block is converted to frequency domain by one N-point DFT. The energy sensing metric can be written as

$$T[k]=\frac{1}{M}\sum_{m=1}^{M}|Y_m[k]|^2 \tag{5.5}$$

where M is the number of adjoining N-point DFTs, and $Y_m[k]$ denotes the frequency domain signal on the k-th subcarrier of the m-th DFT. $|Y_m[k]|^2$ is a sequence of i.i.d. random variables with mean and variance denoted as

$$\begin{aligned}&\mathrm{E}(|Y_m[k]|^2)=\mu_s\\&\mathrm{E}((|Y_m[k]|^2-\mu_s)^2)=\sigma_s^2\end{aligned} \tag{5.6}$$

where E(·) denotes the expectation operator.

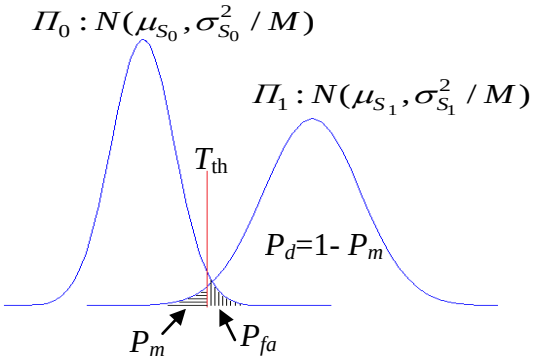

Fig. 5-1. Probability density file of metric *T*(*k*).

The OFDM system decides whether the primary signal on subcarrier k is present or not according to whether the metric $T[k]$ is greater than a predefined threshold T_{th} or not.

For this ED, we can derive its close-form solution of the PD as follows. According to the central limit theorem, when M is large, the metric $T[k]$ can be approximated as a Gaussian random variable with mean μ_s and variance σ_s^2/M as shown in Fig. 5-1 [60], where P_d is the probability of detection. P_{fa} is the false alarm probability. P_m is the miss detection probability. $N(\ )$ represents the normal distribution. For hypothesis Π_0, because only noise is present, the mean and variance of $|Y_m[k]|^2$ are $\mu_{S_0}=\sigma^2$ and $\sigma_{s0}^2=\sigma^4$, respectively. Thus, the probability of false alarm $P_{fa}=P(T[k]>T_{\text{th}}\mid \Pi_0)$ can be given in terms of Q function by

$$P_{fa}=Q\left(\sqrt{M}\frac{T_{th}-\sigma^2}{\sigma^2}\right)=Q\left(\sqrt{M}\left(\frac{T_{th}}{\sigma^2}-1\right)\right). \tag{5.7}$$

where threshold T_{th} can be calculated once P_{fa} is defined and noise variance is measured. It can be found that the threshold T_{th} is actually proportional to the noise power σ^2 for a specified P_{fa}. i.e., (5.8)

$$T_{th} = \lambda\sigma^2 \tag{5.8}$$

It is reasonable to consider that $|Y_m[k]|^2$ (m=0,1, …, M-1) are independent random variables with the same mean and variance for different m, because they are samples of the same signal. It can be assumed that the PU signal on subcarrier k is a random variable with zero mean and average power P_k and is independent of the channel $H[k]$. For OFDM system, the wideband frequency-selective fading channel is transformed to multiple narrowband flat fading channels. Thus, we can assume that the channel on subcarrier k is zero mean complex Gaussian variable whose real and imaginary has the same variance $\sigma_{h,k}^2/2$. Then, the mean and variance of $|Y_m[k]|^2$ for hypothesis Π_1 can be calculated by (5.9)

$$\begin{aligned}\mu_{s_1} &= \mathrm{E}(|Y_m[k]|^2) = \mathrm{E}(|(H(k)X(k)+W(k))^2|) = \sigma_{h,k}^2 P_k + \sigma^2 \\ \sigma_{S_1}^2 &= E(|Y_m[k]|^4) - (\mathrm{E}(|Y_m[k]|^2))^2 = \frac{3\alpha-1}{4}\sigma_{h,k}^4 P_k^2 + 4\sigma_{h,k}^2 P_k \sigma^2 + \sigma^4\end{aligned} \tag{5.9}$$

where $\alpha=\mathrm{E}(X[k]^4)/P_k^2$ is an intrinsic parameter of the signal $X[k]$. For constant-amplitude signals, e.g. BPSK, QPSK and 8-PSK, α is equal to 1 [60]. According to (5.5), the mean and variance of $T[k]$ are μ_{s_1} and $\sigma_{S_1}^2/M$, respectively, which can be calculated by using (5.9). Hence, the probability of detection $P_d = P(T[k]>T_{\mathrm{th}} \mid \Pi_1)$ for subcarrier k can be calculated by

$$P_d[k] = Q\left(\sqrt{M}\,\frac{T_{th}/\sigma^2 - \sigma_{h,k}^2 P_k/\sigma^2 - 1}{\sqrt{\frac{3\alpha-1}{4}\sigma_{h,k}^4 (P_k/\sigma^2)^2 + 4\sigma_{h,k}^2 P_k/\sigma^2 + 1}}\right) = Q\left(\sqrt{M}\,\frac{\lambda - \sigma_{h,k}^2 S_k - 1}{\sqrt{\frac{3\alpha-1}{4}\sigma_{h,k}^4 S_k^2 + 4\sigma_{h,k}^2 S_k + 1}}\right) \tag{5.10}$$

where $S_k=P_k/\sigma^2$ represents the SNR on subcarrier k in frequency domain. We can find that when SNR increases, the probability of detection $P_d[k]$ increases accordingly. For a quasi-static multipath channel, the variance of the channel $\sigma_{h,k}^2$ is fixed to 1.

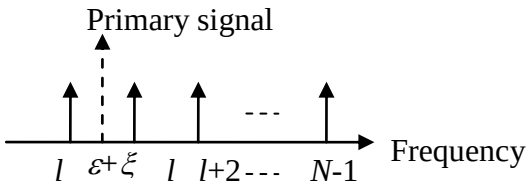

Fig. 5-2. Detection of narrow-band primary signal.

5.3 Energy Detection with Variable DFT Size

We consider a single-carrier signal as the PU signal. The results can be easily extended to a multi-carrier signal. The signal is received and sampled at CU's sampling rate N_c after normalization (i.e. the bandwidth of the PU signal is 1) by the CU and then converted to frequency domain by the N-point normalized DFT, resulting in $Y[k]=\frac{1}{\sqrt{N}}\sum_{n=0}^{N-1}y[n]e^{-j2\pi k\frac{n}{N}}$. Increasing the DFT size N means decreasing the frequency bin spacing of DFT and increasing the subcarriers, but the bandwidth of DFT is unchanged.

Since the PU signal is a narrow-band signal and it's frequency is much smaller than CU's sampling rate, we can assume that in an OFDM symbol period the PU signal is a sine wave with amplitude A, frequency $\varepsilon+\xi$ and random phase φ, where ε represents the nearest integer frequency bin after DFT (i.e., $\varepsilon=l$ or $l+1$) and ξ represents the frequency offset between the primary signal and the nearest integer bin (i.e., $|\xi|\le 0.5$) as shown in Fig. 5-2 The zero-mean white Gaussian noise $w[n]$ is added on the PU signal in the time domain to obtain SNR= A^2/σ^2 on the bandwidth of PU. Since the sampling rate is N_c and the PU's bandwidth is only 1, the noise $w[n]$ on the bandwidth of CU will have the variance $N_c\sigma^2$.

Hence, in frequency domain, the primary signal with noise can be written as

$$\begin{aligned} Y[k] &= \frac{1}{\sqrt{N}}\sum_{n=0}^{N-1}\left(Ae^{j(2\pi\frac{\varepsilon+\xi}{N}n+\varphi)}+w[n]\right)e^{-j2\pi\frac{k}{N}n} \\ &= \frac{A}{\sqrt{N}}\sum_{n=0}^{N-1}\left(e^{j(2\pi\frac{\varepsilon+\xi-k}{N}n+\varphi)}\right)+W[k]. \end{aligned} \tag{5.11}$$

where $W[k]$ is zero-mean Gaussian noise with variance $N_c\sigma^2/N$.

If the primary signal is located exactly on a frequency bin (i.e., $\xi=0$), the expression can be

simplified as

$$Y[k] = \begin{cases} \sqrt{N}Ae^{j\phi} + W[k], & k = \varepsilon \\ W[k], & k \neq \varepsilon \end{cases}. \tag{5.12}$$

If the primary signal is not exactly located on a frequency bin (i.e., $\xi \neq 0$), for $k=\varepsilon$, we have

$$\begin{aligned} Y[k] &= \frac{A}{\sqrt{N}} \sum_{n=0}^{N-1} e^{j(2\pi \frac{\xi}{N} n + \varphi)} + W[k] \\ &= \frac{A}{\sqrt{N}} \frac{\sin(\pi\xi)}{\sin\frac{\pi\xi}{N}} e^{j(\frac{N+1}{N}\pi\xi + \varphi)} + W[k] \\ &= Be^{j(\frac{N+1}{N}\pi\xi + \varphi)} + W[k] \end{aligned} \tag{5.13}$$

where $B = \frac{A}{\sqrt{N}} \frac{\sin(\pi\xi)}{\sin\frac{\pi\xi}{N}}$ is a monotonic increasing function of N for a given ξ. Thus, the SNR is given by $(N/N_c)B^2/\sigma^2$, which is proportional to the DFT size N. In the case of $\xi=0$, the SNR will be the highest and equal to $(N/N_c)A^2/\sigma^2$, which can also be directly obtained from (5.12). Obviously, increasing the DFT size can increase the SNR in frequency domain. If N is equal to N_c, the SNR after DFT will be A^2/σ^2.

On the other hand, if the DFT size N is fixed, B will decrease when ξ increases. If the primary signal is located in the middle of two frequency bins ($\xi=0.5$), the SNR on the nearest frequency bins will be the lowest and the PU signal will be more difficult to detect. Increasing the size of DFT can help to reduce the fractional frequency offset ξ, and hence improving the SNR. So far, we have shown that increasing DFT size can help increase the SNR, and hence improve the probability of detection.

5.4 Improved Energy Detection with Fixed DFT Size

In this section, we propose an improved ED method for narrow-band PU signal. Without loss of generality, we first assume there is a PU signal with normalized frequency f, where $0 < f \leq N-1$ in the N-subcarrier domain of the OFDM system. The proposed detector (abbreviated to NS-ED) is shown in Fig. 5-3, where the noise smoothing is performed before DFT for ED.

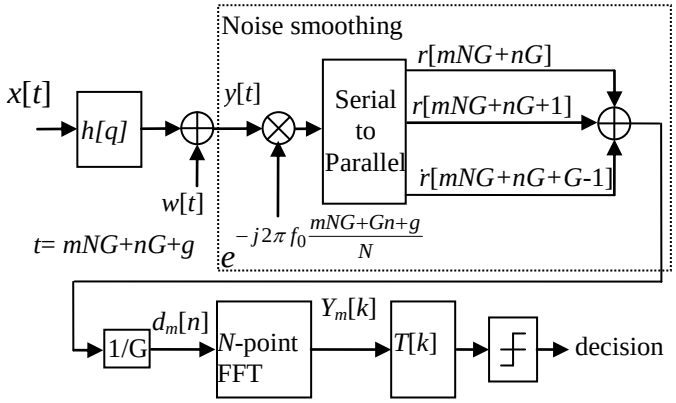

Fig. 5-3. Proposed energy detection with time domain noise smoothing

In order to achieve largest SNR gain, the PU signal will be down-converted to zero frequency position (i.e., subcarrier 0 of N-point DFT). If the frequency of the PU signal is unknown, we can use the estimated frequency f_0 for digital down-converting. Thus, the residual frequency after down-converting is f-f_0. Then, the PU signal is divided to G branches. The data of G branches are averaged for noise smoothing and fed into N-point DFT for energy detection. The signals on the g-th branch can be denoted as

$$r[t] = e^{-j2\pi f_0 \frac{mNG+Gn+g}{N}} (h[t] \otimes x[t] + w[t]) \tag{5.14}$$

where t=mNG+Gn+g, n=0, 1, …, N-1 and m=0,1,…, M-1; N is the size of DFT, and M means the number of adjoining DFTs for the calculation of the energy sensing metric; $h[q]$ (q=0, 1, …, Q) represents the channel impulse and $w[mNG+Gn+g]$ represents the zero mean Gaussian noise with variance σ^2. Then the G branches are added together and divided by G to generate the input of the m-th N-point DFT, which is given by

$$d_m[n] = \frac{1}{G} \sum_{g=0}^{G-1} r[mNG + Gn + g] \tag{5.15}$$

where $d_m[n]$ represents the signal after noise smoothing. The output of DFT is expressed as $Y_m[k]$, where k=0, 1, …, N-1. The narrow-band PU signal can be assumed as a phase continuous signal in one OFDM duration since slow symbol rate is assumed. Thus, we have

$$x[mNG+Gn+g]=x[mNG+Gn]e^{j2\pi f\frac{g}{N}}. \tag{5.16}$$

Substituting (5.14) and (5.16) into (5.15), we have $d_m[n]$ in (5.17)

$$\begin{aligned} d_m[n] &= \frac{1}{G}\sum_{g=0}^{G-1}(h[t]\otimes x[t]e^{-j2\pi f_0\frac{mNG+Gn+g}{N}}+w[t]e^{-j2\pi f_0\frac{mNG+Gn+g}{N}}) \\ &= \frac{1}{G}h[t]\otimes x[mNG+Gn]\sum_{g=0}^{G-1}e^{j2\pi f\frac{g}{N}}e^{-j2\pi f_0\frac{g}{N}}e^{-j2\pi f_0\frac{Gn}{N}}+\frac{1}{G}\sum_{g=0}^{G-1}w[mNG+Gn+g]e^{-j2\pi f_0\frac{g}{N}}e^{-j2\pi f_0\frac{Gn}{N}} \\ &= \frac{1}{G}h[t]\otimes x[mNG+Gn]\frac{1-e^{j\varphi G}}{1-e^{j\varphi}}e^{-j2\pi f_0\frac{Gn}{N}}+v[n] \end{aligned} \tag{5.17}$$

where $v[n]=\frac{1}{G}\sum_{g=0}^{G-1}w[mNG+Gn+g]e^{-j2\pi f_0\frac{g}{N}}e^{-j2\pi f_0\frac{Gn}{N}}$ represents zero mean Gaussian noise with variance $\sigma_v^2=\frac{\sigma^2}{G^2}\frac{1-e^{-j4\pi f_0\frac{G}{N}}}{1-e^{-j4\pi f_0\frac{1}{N}}}e^{-j2\pi f_0\frac{2Gn}{N}}$ and $\varphi=2\pi(f-f_0)\frac{1}{N}$ denotes the phase difference of the two adjacent samples of the primary signal. It can be deduced that the mean and variance of noise power $|v[n]|^2$ are $\mu_{S_0}=\sigma^2/G$ and $\sigma_{s0}^2=\sigma^4/G^2$, respectively. Thus, the probability of false alarm P_{fa} in (5.7) can be modified to (5.18).

$$P_{fa}=Q\left(\sqrt{M}\,\frac{T_{th}-\sigma^2/G}{\sigma^2/G}\right)=Q(\lambda). \tag{5.18}$$

The threshold T_{th} can then be calculated by (5.19) once λ is obtained from (5.18) with a predefined P_{fa}.

$$T_{th}=(\lambda\frac{1}{\sqrt{M}}+1)\frac{\sigma^2}{G}. \tag{5.19}$$

The energy sensing metric $T[k]$ is given by (5.5). The OFDM system decides that the primary signal on the subcarrier k is present according to the factor that the metric $T[k]$ is greater than the threshold T_{th}. Otherwise, the system decides there is no primary signal on the subcarrier k.

Same as that in Section 5.2, it is assumed that the signal power of $X[k]$ is P_k. Comparing (5.17) and (5.3), the SNR after the signal $d_m[n]$ can be deduced in (5.20) and the probability of detection

P_d for subcarrier k can be calculated by (5.10) with substituting $\hat{S}_k$ for S_k.

$$\hat{S}_k = \frac{1}{G}\left|\frac{1-e^{j\varphi G}}{1-e^{j\varphi}}\right|^2 \frac{\sigma_{h_k}^2 P_k}{\sigma^2} = \frac{1}{G}\frac{1-\cos(G\varphi)}{1-\cos(\varphi)}\frac{\sigma_{h_k}^2 P_k}{\sigma^2}. \tag{5.20}$$

Compared with the conventional ED, the proposed ED scheme can achieve the SNR gain β in (5.21).

$$\beta = \frac{1}{G}\frac{1-\cos(G\varphi)}{1-\cos(\varphi)} = \frac{1}{G}\left(\frac{\sin(G\varphi/2)}{\sin(\varphi/2)}\right)^2 \tag{5.21}$$

where $\varphi = 2\pi(f - f_0)\frac{1}{N}$ denotes the phase difference of the two adjacent samples of the primary signal. From (5.21), we can find that if the phase difference φ moves closer and closer to 0, the SNR gain will be approximate to G. The SNR gain gets smaller as the phase difference φ becomes larger. When SNR gain is equal to or less than 1 (i.e., $\beta \leq 0$ dB), there is no positive SNR gain and the SNR is actually decreased. To obtain positive SNR gain (i.e., $\beta > 0$ dB), the phase difference shall be less than a specified value. i.e., $|f\text{-}f_0|$ is limited to a specified value, where $|f\text{-}f_0|$ represents the frequency estimation error of the PU signal.

For the PU signal with multiple frequencies, it is assumed that the central frequency f_0 can be correctly estimated and is down-converted to the zero frequency position. Hence, the boundary frequency f_b will have the maximum estimation error. $|f_b\text{-}f_0|$ shall be less than a specified value to achieve the positive SNR gain. On the other hand, if the central frequency is not accurate, $|f_b\text{-}f_0|$ will become large, and the SNR gain obtained is reduced.

Compared with the conventional ED, the proposed NS-ED method oversampled the PU signal in the frequency domain. The symbol duration of the N-point DFT increases from NT to NTG by the proposed noise smoothing scheme, and the subcarrier spacing is reduced to $1/(NTG)$. Hence, the proposed ED can detect the signal that is located between two adjacent subcarriers. Accordingly, the bandwidth of PU signal that can be detected can also be reduced to $1/G$ of the CU bandwidth. Thus, the proposed ED is suitable for the detection of the narrowband PU signals. In addition, the proposed ED only needs additional noise smoothing process, which consists of one complex multiplier and G-1 complex adders. The average operator $1/G$ before DFT can

actually be merged into the calculation of metric $T(k)$ and threshold T_{th}.

For G=2, the SNR gain after noise smoothing can be simplified as

$$\beta_2 = 1+\cos\varphi \cdot \tag{5.22}$$

It shows that if the phase difference $|\varphi|$ between the two adjacent samples is less than $\pi/2$, the SNR is eventually increased. Otherwise, there is no SNR gain obtained. In other words, $|f-f_0|$ shall be less than $N/4$. When $f-f_0=0$, we can have the maximum SNR gain of 2 (i.e., 3dB). When $f-f_0=N/4$ or $-N/4$, we can have the minimum SNR gain of 1 (i.e., 0dB). If is $|f-f_0|$ is larger than $N/4$, the SNR gain is less than 1, i.e., the SNR is decreased.

For G=3 and G=4, the SNR after noise smoothing can be simplified as

$$\begin{aligned} \beta_3 &= \frac{(1+2\cos\varphi)^2}{3} \\ \beta_4 &= 2(\cos\varphi)^2(1+\cos\varphi) \end{aligned}. \tag{5.23}$$

It also shows that if $f-f_0=0$, we can have the maximum SNR gain of 3 (i.e., 4.77 dB) and 4 (i.e., 6 dB) for G=3 and G=4, respectively.

5.5 Simulation Results and Discussion

In the simulations, we assume that the CU signal is an OFDM signal, and DFT size N=64 and the sampling time is T. The PU signals are QPSK signals with normalized frequency f=0, 1, ..., 16. The QPSK symbol rate of the PU signal is far less than that of the CU signal. The sampled PU signal is passed through a quasi-static multipath channel. We assume that the channel has Q=8 linearly decaying multipath components with delays {0, T, 2T, 3T, 4T, 5T, 6T, 7T} and powers {8/36, 7/36, 6/36, 5/36, 4/36, 3/36, 2/36, 1/36}. The total power of the multipath components is 1. Hence, the variance of the channel $\sigma_{h,k}^2$ is 1 in (5.10). The received noised signal is then converted to frequency domain by N-point DFT. For all considered ED schemes, 500 continuous DFTs (i.e., M=500) are performed to calculate the spectrum sensing metric $T[k]$. The probability of false alarm P_{fa} is set to 0.1. The ED method described in Section 5.2 is referred to as conventional ED.

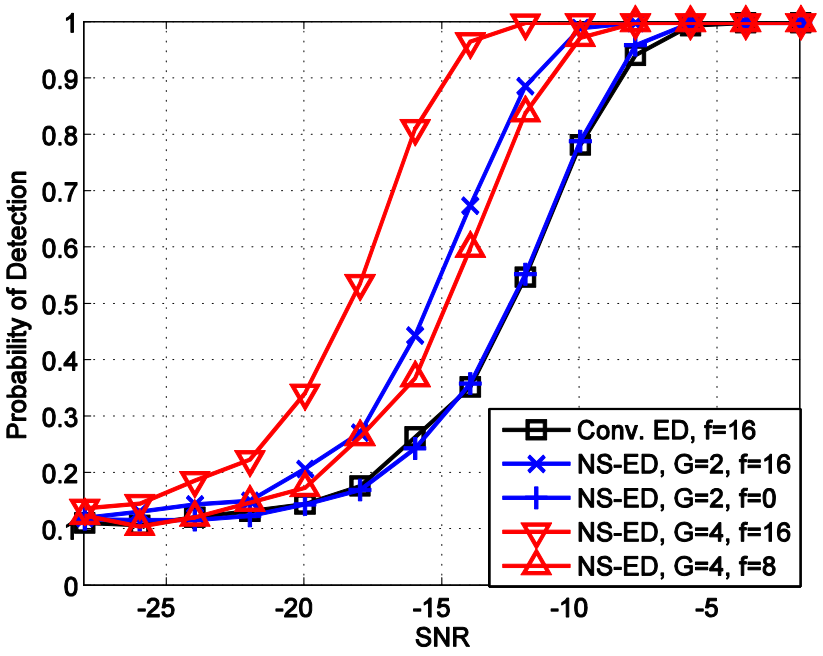

Fig. 5-4. PD versus SNR for the PU signals exactly on subcarriers.

If the estimated frequency is f_0=16, the PU signals after down-converting are exactly on the subcarriers of the OFDM system. The maximum estimation error $|f-f_0|$ is 16 and the minimum estimation is 0. The PD comparison between the conventional ED and the proposed NS-ED is shown in Fig. 5-4. If we choose G=2, compared with the conventional ED, the proposed NS-ED can achieve the maximum SNR gain of 3 dB for the frequency f=16 (with minimum estimation error) and the minimum SNR gain of 0 dB for f=0 (with maximum estimation error), respectively. In this case, the detectable frequency bandwidth is reduced to N/2 due to oversampling in frequency domain. If we choose G=4, the maximum SNR gain of 6 dB and the minimum gain of about 2 dB can be achieved for the PU signals with the frequency f=16 and f=8, respectively, which matches the equation (5.21) and (5.23). Accordingly, the frequency band that can be detected with positive SNR gain will be limited to 16 because it oversamples the PU signal in frequency domain and the detectable frequency bandwidth are reduce to 1/4 of the CU bandwidth.

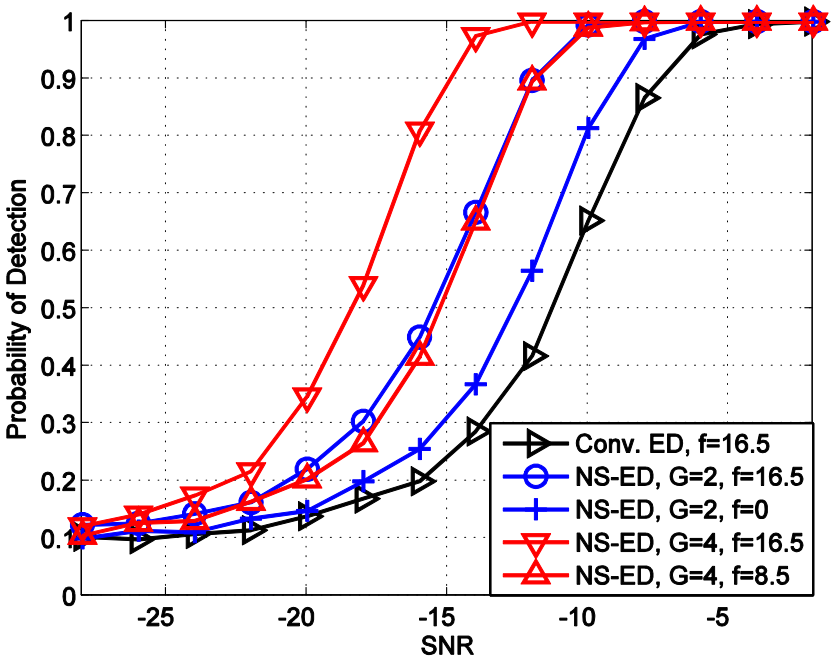

Fig. 5-5. PD versus SNR for the PU signals not exactly on subcarriers.

If the estimated frequency is f_0=15.5, the signals after down-converting are not exactly on the subcarriers of the OFDM system. In this case, the conventional ED cannot offer a good performance, while the proposed NS-ED can achieve a larger SNR gain, shown in Fig. 5-5, compared with that in the case that the signals are exactly on the subcarriers, shown in Fig. 5-4. For the PU signal with frequency f=16, the maximum SNR gain achieved is about 4.3 dB and 7.3 dB when G=2 and G=4, respectively. The minimum SNR gain is about 1.3 dB for f=0 and 4.3 dB for f=8 when G=2 and G=4, respectively. The main reason is that after oversampling in frequency domain, the PU signal is close to the subcarriers of the oversampled frequency domain. Hence, the SNR is improved by the proposed NS-ED, which leads to a higher PD. In this simulation, the PU signal is exactly on the subcarriers of the oversampled frequency domain, therefore a larger SNR gain can be achieved compared to the results shown in Fig. 5-4.

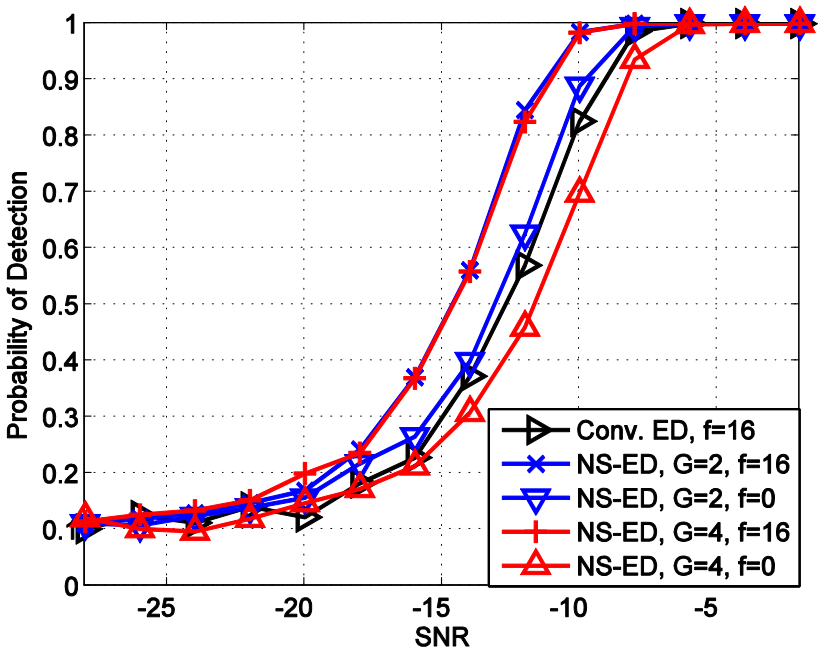

Fig. 5-6. PD versus SNR in the case of the PU signal with low symbol rate

The equations in Section 5.4 are based on the assumption that the PU signal has continuous phase in the duration of one OFDM symbol. i.e., the symbol rate of the PU signal shall be much slower than that of the CU signal. Otherwise, the phase of the PU signal is not continuous in some OFDM symbols, which may decrease the SNR gain. The curves in Fig. 5-6 show the PD performance for different ED methods when the PU signal's symbol rate (QPSK symbol) is 1/2 of the OFDM symbol rate of the CU signal. The PU signals consist of multiple frequencies with f = 0, 1, …, 16 and f_0=16. For G=2, each FTT symbol is interfered by the adjacent DFT symbol due to the multipath channel. For G=4, the PU signal changes its phase in each DFT symbol, which may greatly reduce the SNR gain. Hence, the SNR gain obtained is reduced. It can be found that our proposed NS-ED can still offer about 2 dB SNR gain for signal frequency f=16 when G=2 and G=4.

Finally we verify the close-form solution of PD for our proposed NS-ED method by simulations. We assume the PU signals are QPSK signal with integer frequencies and the symbol rate is much slower than that of the CU signal. The simulated PD is statistical result by using 2000 simulation runs with M=500. The close-form PD is calculated from equation (5.10) and (5.20). The results in Fig. 5-7 show the simulated PD (S-PD) and close-form PD (C-PD) curves of signals

with estimated frequency f_0=16 for the proposed ED with G=2 and 4. It can be found that for each frequency the simulated PD and the close-form PD almost overlap. The close-form solution can be used to represent our proposed NS-ED theoretically.

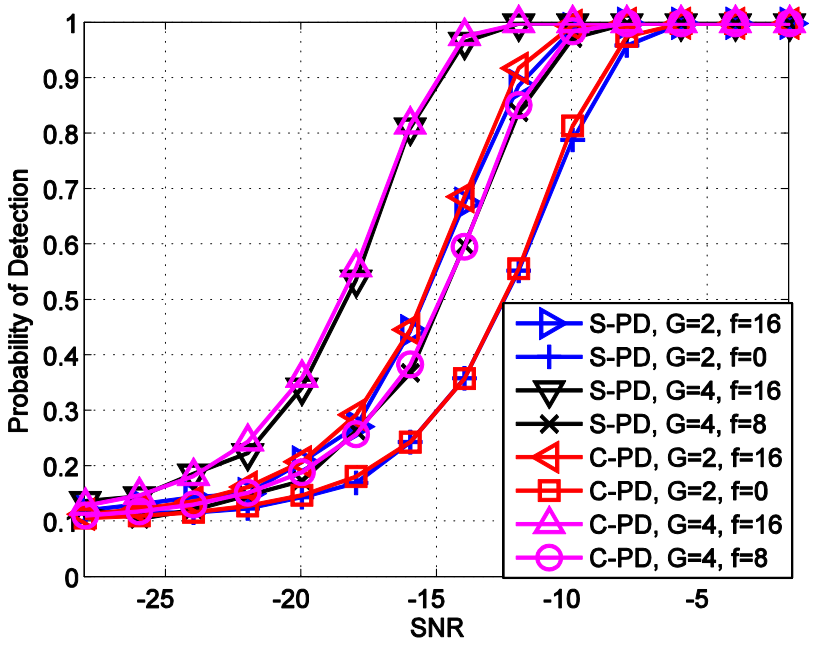

Fig. 5-7. The comparison between simulated PD and close-form PD

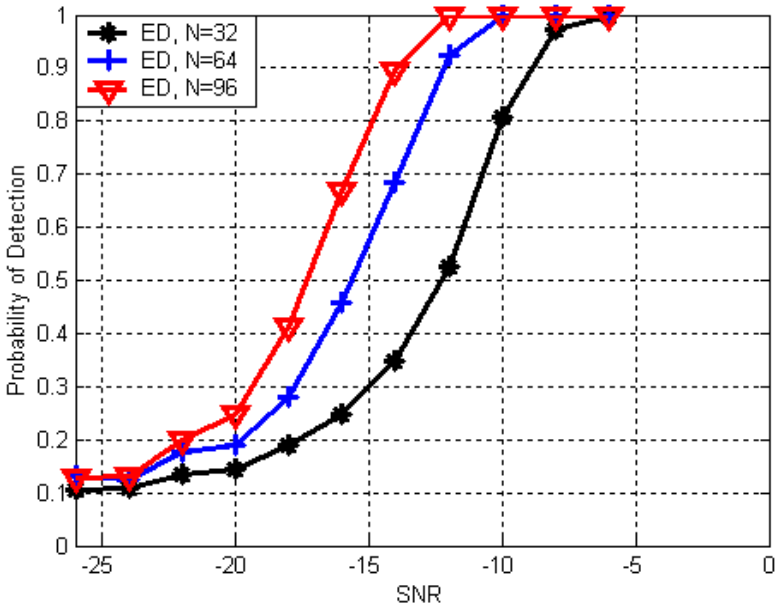

Fig. 5-8. PD versus SNR for different DFT size with PU signal exactly on bin 1.

The results in Fig. **5-8** show the probability of detection of the conventional ED with different DFT size N for the case that the PU signal is exactly on frequency bin 1 of the output of the 32-

point DFT (i.e., ε=1 and ξ=0 when DFT size equals to 32 in equation (5.13)). In this case, large DFT size can improve the performance of ED. However, it requires large computational complexity. If the PU signal is exactly on bin 1, about 3 dB and 4.7 dB SNR gain can be obtained when DFT size is doubled and tripled (e.g., N is increased from 32 to 64 and 96), respectively. The results match the analysis in Section 5.3.

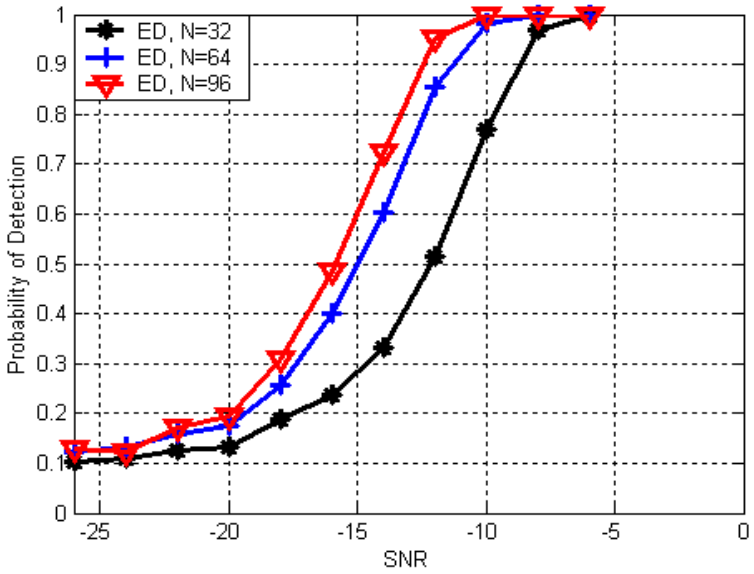

Fig. 5-9. PD versus SNR for different DFT size with PU signal not exactly on bin 1.

The results in Fig. **5-9** show the probability of detection of the conventional ED with different DFT size N for the case that the PU signal has frequency offset ξ=0.1 to bin 1 (i.e., ε=1 and $\xi\neq$0). In this case, large DFT size still can improve the performance of ED. However, the performance improvement is reduced due to the frequency offset. If the PU signal has frequency offset 0.1 to bin 1, about 2.5 dB and 3 dB SNR gain can be obtained when DFT size is doubled and tripled (e.g., N is increased from 32 to 64 and 96), respectively, which is smaller than that in the case shown in Fig. 5-8.

5.6 Conclusions

In this chapter, two schemes are considered to improve the performance of energy detection of narrow-band PU signal for cognitive radio systems. The first scheme is to use large DFT size for

ED. Increasing the DFT size not only improves the detection of the narrow-band signal located between two frequency bins, but also increases the probability of detection. In the case that the DFT size cannot be changed, we have proposed an improved ED scheme by using NS method to offer positive SNR gain for the OFDM system over a quasi-static multipath channel, and hence to improve the probability of detection. The signal is down-converted to zero frequency and then divided to G branches. The G branches of signals are added together and averaged to smooth the noise. Compared with the conventional ED, the maximum SNR gain achieved by the proposed NS-ED method is approximate to G. The proposed NS-ED method overcomes the difficulty in the detection of narrow-band signal to achieve a higher SNR gain by smoothing the noise in time domain without increasing the complexity. However, the SNR gains achieved by NS-ED for different frequencies are different and the bandwidth of the PU signal is limited to $1/G$ of the CU signal. In addition, the close-form solution of PD for our proposed ED under multipath channel is developed. The simulation results verify the SNR gains achieved by the proposed algorithms, and show that the close-form solution of PD matches the simulated PD very well.

6 Conclusions and Recommendations

6.1 Conclusions

Firstly, four types of equalizers including FDO-MMSE, FDO-DMMSE, FDO-NF and FDO-ZF equalizer have been proposed in this dissertation for different types of OFDM systems: ZP OFDM, ZP MC-CDMA, CP OFDM and CP MC-CDMA systems. The iterative FDO based equalizers have been designed for the cases that the OFDM symbol is interfered by the adjacent two OFDM symbols due to the multipath channel. The expression of the AI-BER performance for the four equalizers has been developed and verified by simulations. In addition, the BER performance of the four types of FDO based equalizers are compared in the various coded and uncoded MCM systems.

For ZP OFDM and ZP MC-CDMA systems, four FDO based equalizers, i.e., FDO-MMSE, FDO-DMMSE, FDO-NF and FDO-ZF equalizers are proposed in Chapter 3. The expression of the AI-BER performance of the FDO based equalizers is developed. All the four FDO based equalizers can offer better BER performance than the conventional ZF equalizer under different channel environment. The FDO-MMSE equalizer can offer the best BER performance, but the implementation is quite complex because it requires the calculation of matrix inverse. The FDO-ZF equalizer is easy to be implemented, but the BER performance of it is not as good as that of the FDO-MMSE, FDO-DMMSE and FDO-NF equalizers. One good feature of the FDO-ZF equalizer is that the BER performance can be improved by increasing OSF (i.e., DFT size). The FDO-DMMSE equalizer can offer the moderate BER performance with moderate complexity compared with the FDO-MMSE and FDO-ZF equalizers. To reduce the complexity of FDO-DMMSE equalizer, the FDO-NF equalizer with fixed noise variance is proposed, which can offer good BER performance similar to the FDO-DMMSE in the expected SNR range. It is a trade-off to select a suitable FDO based equalizer for a practical application. In the case that the channel delay is longer than the guard interval of the OFDM symbol. The iterative FDO based equalizers

are designed to achieve much better BER performance than the conventional equalizer. In order to reduce the ISI from the adjacent symbols, the SR method is proposed to be used before FDO based equalizers. The simulations are performed to verify the performance of the proposed equalizers. In addition, combining with channel coding such as convolutional encoder, the proposed FDO based equalizers can offer much better BER performance than the conventional ZF equalizer. Chapter 3 also compares the proposed FDO based equalizers in ZP OFDM and ZP MC-CDMA systems. The proposed FDO-ZF equalizer cannot show better BER performance in ZP MC-CDMA system than it in ZP OFDM system. However, the proposed FDO-MMSE, FDO-DMMSE and FDO-NF can achieve much better BER performance in ZP MC-CDMA system than they in ZP OFDM system.

Chapter 4 focuses on the FDO based equalizers for the CP OFDM and CP MC-CDMA systems, which is never studied in other literature. The novel two-stage iterative FDO-based receivers are proposed to improve the BER performance of CP OFDM systems by using SR method in multipath channel environment. The expression of the AI-BER is derived to accurately evaluate the BER performance of the proposed receivers. Simulations show that the BER performance of the proposed FDO-based receivers for CP OFDM is much better than that of the conventional equalizer and even slightly better than that of FDO-MMSE receiver for ZP OFDM when the residual CFO is small. Although the performance of the FDO-ZF receiver is not as good as that of the FDO-MMSE receiver, it’s still better than that of the conventional CP OFDM receiver. Moreover, it can be improved by increasing the oversampling rate. The proposed FDO-MMSE and FDO-ZF receivers can tolerate a larger frequency offset and Doppler frequency shift than the conventional receiver. It was also observed that for the proposed FDO-MMSE receiver, longer CP portion of the OFDM symbol can benefit the BER improvement. Furthermore, the proposed FDO-based receivers can tolerate large multipath delay, even when the path delay is larger than the CP length of OFDM. Although the IT-FDO-DMMSE and IT-FDO-NF receivers cannot offer better performance in CP OFDM system, they still can offer the moderate BER performance with moderate complexity in CP MC-CDMA systems compared with the IT-FDO-MMSE and IT-

FDO-ZF receivers. The IT-FDO-NF can obtain the similar BER performance to the IT-FDO-DMMSE in the expected SNR range by appropriately choosing the noise variance.

In addition, the BER performance of proposed four FDO based equalizers between the ZP MCM and CP MCM systems are compared by simulations. The iterative FDO based equalizers introduce more noise by the SR method in the CP systems, and the matrix diagonalization of the FDO-DMMSE and FDO-NF in the CP systems also introduces more noise than it in the ZP systems, which cause that the FDO-DMMSE, FDO-NF and FDO-ZF in the ZP MCM systems can have better BER performance than they in the CP MCM systems. However, the FDO-MMSE can take advantage of the CP part to improve the BER performance. In high SNR range, the effect of CP part can exceed the side-effect of the SR method, but in low SNR range, it may or may not counteract the side-effect of the SR method because the noise is increased. Hence, the FDO-MMSE can have slightly better BER performance in the uncoded CP systems than it in the uncoded ZP systems. However, it may not offer better BER performance in the coded CP systems than it in the coded ZP systems.

The BER performance of the proposed FDO based receivers between CP OFDM and CP MC-CDMA systems are compared by simulations. If the IT-FDO-MMSE, IT-FDO-DMMSE and IT-FDO-NF receivers are adopted, CP MC-CDMA system can achieve better BER performance than CP OFDM system due to the spreading codes. The BER curves of the three receivers in CP MC-CDMA system decline more quickly than they in CP OFDM with SNR increasing. However, if the IT-FDO-ZF and conventional ZF are adopted, CP OFDM can offer slightly better BER performance than CP MC-CDMA system.

Secondly, this dissertation has also considered the energy detection method for narrow-band PU signal in OFDM systems. The effect of DFT size on the probability of detection has been studied. The large DFT size has been proposed to improve the probability of detection for narrow-band signal. However, when DFT size is not able to change and the rough position of the narrow-band signal is known, an improved ED scheme by using NS method has been proposed to offer positive SNR gain for the OFDM system over a quasi-static multipath channel, and hence to

improve the probability of detection. The PU signal is down-converted to zero frequency and divided to *G* branches. The *G* branches are then added together and averaged to smooth the noise. Compared with the conventional ED, the maximum SNR gain achieved by the proposed NS-ED method is approximate to *G*. However, the SNR gains for different frequencies are different, and the bandwidth of the PU signal is limited to 1/*G* of the OFDM signal. In addition, the close-form solution of PD for our proposed ED under multipath channel is developed. The simulation results verify the SNR gains achieved by the proposed algorithms, and show that the close-form solution of PD matches the simulated PD very well.

6.2 Recommendations for Future Work

As a result of the research work undertaken for the present dissertation, several directions for future research are pointed out for real applications as we mention now.

- Obtaining the FDO based channel estimation algorithms to further improve the BER performance for ZP and CP OFDM systems.

  There are numerous literature that study the channel estimation for OFDM system [50]-[57]. However, all of them perform the channel estimation in the conventional frequency domain where the subcarriers are orthogonal to each other. In this case, the subchannel with power of zero will greatly reduce the BER performance of OFDM system and the noise cannot be efficiently suppressed by the MMSE method. In the thesis, we have already demonstrated that the FDO based receiver can achieve much better BER performance than conventional receiver. Accordingly with the pilot symbols or pilot subcarriers, it is possible to design an FDO based channel estimator with minimum MSE, and hence to further improve the BER performance of the system.

- Designing the FDO based equalizers for the uplink MC-CDMA systems to combat the severe multiple interference.

  It has been shown that the FDO based equalizers for the downlink MC-CDMA can tolerate large multiple interference and can improve the BER performance of the system.

It is reasonable that we use FDO combining with other equalization methods to improve the system performance. The basic uplink MC-CDMA structure is shown in Fig. 6-1.

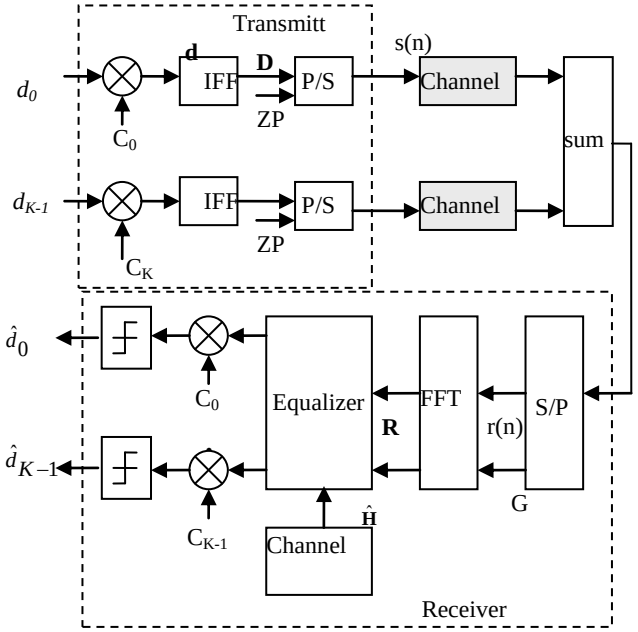

Fig. 6-1. The basic structure of uplink ZP MC-CDMA.

The received signal in time domain can be expressed as

$$\mathbf{r} = \mathbf{h_0} \otimes \mathbf{F}\mathbf{C_0} d_0 + \mathbf{h}_1 \otimes \mathbf{F}\mathbf{C}_1 d_1 + \cdots + \mathbf{h}_{N-1} \otimes \mathbf{F}\mathbf{C}_{N-1} d_{N-1} + \mathbf{v} \tag{6.1}$$

The received signal in frequency domain can be written as

$$\mathbf{R} = \mathbf{H_0}\mathbf{F}_{MN}\mathbf{F}_N^{-1}\mathbf{C_0} d_0 + \mathbf{H}_1\mathbf{F}_{MN}\mathbf{F}_N^{-1}\mathbf{C}_1 d_1 + \cdots + \mathbf{H}_{N-1}\mathbf{F}_{MN}\mathbf{F}_N^{-1}\mathbf{C}_{N-1} d_{N-1} + \mathbf{F}_M \mathbf{v} \tag{6.2}$$

The uplink MC-CDMA can be regarded as the summation of multiple downlink MC-CDMAs for multiple users. One of the difficulties to be solved is that the different users suffer from different fading channel, frequency offset and power amplitude. The FDO technique for the uplink MC-CDMA is expected to tolerate the large combined interference.

- Obtaining the iterative FDO based receivers for the OFDM system without guard intervals. As we know, the performance of OFDM system can be greatly reduced by ISI that caused by multipath channel. The feasible method to avoid ISI is to insert guard interval between

two OFDM symbols. However, the additional guard interval actually decreases the effective throughput of OFDM system. Therefore, some literature propose short guard interval or even no guard interval to maximize the system throughput. In this case, an effective ISI cancellation method shall be adopted to minimize the effect of ISI. However, the system performance is still not good enough for real applications. Hence, it is necessary to improve the performance of the equalizer to combat the heavy interference. The FDO based equalizers have been demonstrated their outperformance in this thesis. It is possible to combine with the methods of ISI cancellation and SR to improve the BER performance of the OFDM system without guard interval.

List of Publications

Journal Paper

- Yanxin Yan and Maode Ma, "SNR Improvement for Energy Detection of Narrow-band Signal in OFDM System," *IEEE communications letter*, vol. 18, iss. 11, pp. 1967-1970. Nov. 2014.

- Yanxin Yan, Yi Gong, Maode Ma and Qinghua Shi, "Iterative Frequency-Domain Fractionally Spaced Receiver for Zero-Padded MC-CDMA Systems," *IET communications*, vol. 8, iss. 17, pp. 2993-3000, Nov. 2014.

- Yanxin Yan and Maode Ma, "Novel Frequency-Domain Oversampling Receiver for CP MC-CDMA Systems," *IEEE communications letter*, accepted on 4-th Jan. 2015.

- Yanxin Yan, Yi Gong, Qinghua Shi and Maode Ma, "Two-Stage Frequency-Domain Oversampling Receiver for CP OFDM System," under major revision.

Conference Paper

- Yanxin Yan, Yi Gong, Yong Liang Guan and Liang Liu, "A frequency-domain oversampling detector for zero-padded MC-CDMA system," *ICICS* 2009,pp. 1639–1643. Dec. 2009
- Yanxin Yan, Yi Gong, "Energy Detection of Narrowband Signals in Cognitive Radio Systems," *IEEE Int Conf. Wireless Communications and Signal Processing (WCSP)*, pp.1-5. Oct. 2010

References

[1] J. Mitola and G.Q. Maguire, "Cognitive Radios: Making Software Radios More Personal," *IEEE Pers. Comm.*, vol. 6, no. 4, pp. 13-18, Aug. 1999.

[2] Chakravarthy, V.; Nunez, A.S.; Stephens, J.P.; Shaw, A.K.; Temple, M.A., "TDCS, OFDM, and MC-CDMA: A Brief Tutorial," *IEEE Comm. magazine*, vol. 43, pp. S11-S16, Sep. 2005.

[3] Apurva N. Mody. "Signal Acquisition and Tracking for Fixed Wireless Access Multiple Input Multiple Output Orthogonal Frequency Division Multiplexing". Thesis for PHD. Georgia Institute of Technology. Oct. 2004.

[4] A. Scaglione, G. B. Giannakis, and S. Barbarossa, "Redundant filterbank precoders and equalizers-Part I: Unification and optimal designs and Part II: Blind channel estimation, synchronization and direct equalization," *IEEE Trans. Signal Processing*, vol. 47, no. 7, pp. 1988–2022, Jul. 1999.

[5] B. Muquet, Z. Wang, G.B. Giannakis, M. de Courville and P. Duhamel, "Cyclic prefixing or zero padding for wireless multicarrier transmissions?" *IEEE Trans. Comm.*, vol. 50, no. 12, pp. 2136 – 2148, Dec. 2002.

[6] C. R. N. Athaudage and R. R. V. Angiras, "Sensitivity of FFT-equalised zero-padded OFDM systems to time and frequency synchronisation errors", *IEE Proc. Comm.*, vol. 152, no. 6, pp. 945-951, Dec. 2005.

[7] N. Yee, J. P. M. G. Linnartz, and G. Fettweis, "Multi-carrier CDMA in indoor wireless networks," in *Proc. PIMRC*, Sept. 1993, pp. 109-113.

[8] A. Chouly, A. Brajal, and S. Jourdan, "Orthogonal multicarrier techniques applied to direct sequence spread spectrum CDMA systems," in *Proc. GLOBECOM*, Nov. 1993, vol. 3, pp. 1723-1728.

[9] A.C. McCormick and E. A. Al-Susa, "Multicarrier CDMA for future generation mobile communication," *Electron. & Commun. Engineering Journal*, vol. 14, no. 2, pp. 52-60, Apr. 2002.

[10] Benvenuto N, Falconer D D, Tomasin S. "Single carrier modulation with nonlinear frequency domain equalization: An idea whose time has come - Again." *Proceedings of the IEEE,* vol. 98, no. 1, pp. 69-96, 2010.

[11] H.H. Seung, H.L. Jae, "An overview of peak-to-average power ratio reduction techniques for multicarrier transmission," *IEEE wireless comm.*, vol. 12, no. 2, pp. 56-65, Apr. 2005.

[12] M.T. Ahmed, J.Khalid, *et al*, "Bit Error Rate Comparison of OFDM and MC-CDMA systems," in *Proc. ICCSIT*, 2008. pp. 665-668.

[13] Deepshikha Garg and Fumiyuki Adachi, "Performance Comparison of Turbo-coded DS-CDMA, MC-CDMA and OFDM with Frequency-domain Equalization and Higher-level Modulation," in *Proc. IEEE VTC*, 2004. Vol. 3, pp. 2282-2286.

[14] S. Kaiser. "OFDM-CDMA versus DS-CDMA: Performance evaluation for fading channels," in *Proc. IEEE ICC*, 1995. pp 1722-1 726.

[15] S. Abeta. H. Atarashi, M. Sawahashi and F. Adachi, "Coherent Multicarrier DS-CDMA and MC-CDMA Broadband Packet Wireless Access," in *Proc. VTC,* May 2000, vol. 3, pp. 15-18.

[16] Yanxin Yan and Yi Gong, etc. "Joint Timing and Frequency Synchronization for IEEE 802.16 OFDM Systems,"in *Proc. IEEE Mobile WiMAX Symposium*, March 2007, pp. 17-21.

[17] Z. Wang and G. B. Giannakis, "Wireless multicarrier communications: where Fourier meets Shannon," *IEEE Signal Processing Mag.*, vol. 17, pp. 29-48, May 2000.

[18] Yuan-Pei Lin, See-May Phoong, P. P. Vaidyanathan, "Filter Bank Transceivers for OFDM and DMT Systems", *Cambridge University Press*, 2011, pp 142.

[19] N. Wang and S. D. Blostein, "Power loading for CP OFDM over frequency-selective fading channels," in *Proc. IEEE Globecom*, Dec. 2003, vol. 4, pp. 2305–2309.

[20] Jong-Bu Lim, *et al*, "Bandwidth-Efficient OFDM Transmission with Iterative Cyclic Prefix Reconstruction", *Journal of Comm. and Networks*, vol. 10, no. 3, pp 239-252, Sept. 2008.

[21] Park, Cheol-Jin ; Im, Gi-Hong H. "Efficient cyclic prefix reconstruction for coded OFDM systems", *IEEE Comm. Letters*, vol. 8, no. 5, pp.274-276, May 2004.

[22] N. Yee and J.-P. Linnartz, "Controlled equalization of multi-carrier CDMA in an indoor

Rican fading channel," in *Proc. IEEE VTC*, June 1994, pp. 1665-1669.

[23] S. Kaiser, "On the performance of different detection techniques for OFDM-CDMA in fading channels," in *Proc. IEEE GLOBECOM*. Nov. 1995, pp.2059-2063.

[24] J-F. Helard, J.-Y. Baudais, and J. Citerne, "Linear MMSE detection technique for MC-CDMA," *IEE Electron. Lett*., vol. 36, no. 7, pp. 665-666, Mar. 2000

[25] A. Conti, "MC-CDMA bit error probability and outage minimization through partial combining," *IEEE Comm. Lett*., vol. 9, no. 12, pp.1055-1057, Dec. 2005.

[26] Fotopoulou, E.; Paliouras, V. and Thanos Stouraitis, "A Frequency-Domain Interpolation Implementation for OFDM Transmitters," in *Proc. ISWPC*, May 2008, pp: 628-632.

[27] B. Hombs and J. S. Lehnert, "Multiple-access interference suppression for MC-CDMA by frequency-domain oversampling," *IEEE Trans. Commun*., vol. 53, no. 4, pp. 677-686, Apr. 2005.

[28] S. Qinghua, et al., "Fractionally spaced frequency-domain MMSE receiver for OFDM systems," *IEEE Trans. Veh. Technol.*, vol. 59, no. 9, pp. 4400–4407, Nov. 2010.

[29] Z.-H. Wang, S. Zhou, J. Catipovic, and P. Willett, "Asynchronous Multiuser Reception for OFDM in Underwater Acoustic Communications," *IEEE Trans. Wireless Comm.*, vol. 12, no. 3, pp. 1050-1061, Mar. 2013.

[30] Z.-H.Wang, S. Zhou, G. B. Giannakis, C. R. Berger, and J. Huang, "Frequency-Domain Oversampling for Zero-Padded OFDM in Underwater Acoustic Communications," *IEEE Journal of Oceanic Engineering*, vol. 37, no. 1, pp. 14 - 24, Jan. 2012.

[31] Tepedelenli ́oglu, Cihan; Challagulla, Ravikanth, "Low-Complexity Multipath Diversity Through Fractional Sampling in OFDM", *IEEE Trans. Signal Processing*, vol. 52, no. 11, pp 3104-3116, Nov. 2004.

[32] Nishimura, H.; *et al*, "Non-uniform sampling point selection in orthogonal frequency division multiplexing receiver with fractional sampling", *IET communications*, vol. 5, no. 4, pp 554-562, Mar. 2011.

[33] Y.-S. Lee and B.-S. Seo, "OFDM receivers using oversampling with rational sampling

ratios," *IEEE Trans. Consumer Electron.*, vol. 55, no. 4, pp. 1765-1770, Nov. 2009.

[34] M. Sharif, M. Gharavi-Alkhansari, and B. H. Khalaj, "On the peak-to-average power of OFDM signals based on oversampling," *IEEE Trans. Commun.*, vol. 51, no. 1, pp. 72-78, Jan. 2003.

[35] B. Chen and H. Wang, "Blind estimation of OFDM carrier frequency offset via oversampling," *IEEE Trans. Signal Process.*, vol. 52, no. 7, pp. 2047- 2057, July 2004.

[36] Qinghua Shi，Karasawa, Y.，Ying Wang, "Blind Channel and Frequency Offset Estimation for OFDM via Frequency-Domain Oversampling," in *Proc. IEEE WiCOM*, Sept. *2010*,pp. 23-25.

[37] S.M.Kay, "Fundamentals of Statistical Signal Processing: Detection Theory." Englewood Cliffs, NJ: Prentice-Hall, 1998, vol.2.

[38] W. A. Gardner, "Exploitation of spectral redundancy in cyclostationary signals," *IEEE Signal Process. Mag.*, vol. 8, no. 2, pp. 14–36, Apr. 1991.

[39] N. Han, S. H. Shon, J. O. Joo, and J. M. Kim, "Spectral correlation based signal detection method for spectrum sensing in IEEE 802.22 WRAN systems," in *Proc. Int. Conf. Advanced Communication Technology*, Feb. 2006, vol. 3, pp. 1766-1770.

[40] A. Sonnenschein and P. M. Fishman, "Radiometric detection of spread spectrum signals in noise of uncertainty power," *IEEE Trans. Aerosp. Electron. Syst.*, vol. 28, no. 3, pp. 654–660, Jul. 1992.

[41] A. Sahai and D. Cabric, "Spectrum sensing: Fundamental limits and practical challenges," in *Proc. IEEE Int. Symp. New Frontiers in Dynamic Spectrum Access Networks (DySPAN)*, Nov. 2005.

[42] H. Urkowitz, "Energy detection of unknown deterministic signals," *Proc. IEEE*, vol. 55, no. 4, pp. 523–531, Apr. 1967.

[43] Parthapratim De and Ying-Chang Liang, "Blind Spectrum Sensing Algorithms for Cognitive Radio Networks," *IEEE Trans. on VT*, vol. 57, no. 5, Sep. 2008

[44] F.F. Digham, M. Alouini and M.K. Simon, "On the Energy Detection of Unknown Signals

Over Fading Channels," *IEEE Trans. Commun*. vol. 55, no. 1, pp. 21-24. Jan. 2007.

[45] S. P. Herath, N. Rajatheva, C. Tellambura, "Energy Detection of Unknown Signals in Fading and Diversity Reception," *IEEE Trans. Commun*. Vol. 59, No. 9, pp. 2443-2453, Sep. 2011

[46] M. L B, F.Casadevall, "Improved energy detection spectrum sensing for Cognitive Radio," *IET comm*. vol. 6, no. 8, pp. 785-796, May 2012.

[47] Di He, Yingpei Lin, Chen He, and Lingge Jiang, "A Novel Spectrum-Sensing Technique in Cognitive Radio Based on Stochastic Resonance," *IEEE Trans. Veh. Tech*. vol. 59, no. 4, pp 1680- 1688. May 2010.

[48] S. M. Mishra, R. W. Brodersen, S. T.Brink and R. Mahadevappa, "Detect and Avoid: An Ultra-Wideband/WiMAX Coexistence Mechanism," *IEEE Communications Magazine*, vol. 45, no. 6, pp. 68-75. Jun. 2007.

[49] Z. Wang and G.B.Giannakis, "Linearly precoded or coded OFDM against wireless channel fades?" in Proc. *IEEE Third Workshop on Signal Processing Advances for Wireless Communications* (SPAWC '01). Mar. 2001, pp. 267-270.

[50] C. Tellambura, M. Parker, Y. J. Guom, S. Shepherd, and S. Barton, "Optimal sequences for channel estimation using discrete Fourier transform techniques," *IEEE Trans. Commun.*, vol. 47, no. 2, pp. 230–238, Feb. 1999.

[51] J. van de Beek, O. Edfors, M. Sandell, S.Wilson, and P. Borjesson, "On channel estimation in OFDM systems," in *Proc. IEEE Vehicular Technology Conf.*, vol. 2, Chicago, IL, July 1995, pp. 815–819.

[52] O. Edfors, M. Sandell,J. J. van de Beek, S. K. Wilson, and P. O. Brjesson, "OFDM Channel Estimation by Singular Value Decomposition," *IEEE Trans. Commun.*, vol. 46, no. 7, pp. 931-939, Jul. 1998.

[53] M. Hsieh and C.Wei, "Channel Estimation for OFDM Systems Based on Comb-type Pilot Arrengement in Frequency Selective Fading Channels," *IEEE Trans. Consumer Electron*., vol. 44, no. 1, pp. 217-225, Feb. 1998.

[54] Y. Li, L. J. Cimini, Jr., and N. R. Sollenberger, “Robust channel estimation for OFDM systems with rapid dispersive fading channels,” *IEEE Trans. Commun.*, vol. 46, no. 7, pp. 902–915, Jul. 1998.

[55] S. Roy and C. Li, “A subspace blind channel estimation method for OFDM systems without cyclic prefix," *IEEE Trans. Wireless Commun*., vol. 1, no. 4, pp. 572-579, Oct. 2002.

[56] Colieri, S.; Ergen, M.; Puri, A.; Bahai A , “A study of channel estimation in OFDM systems,” in *Proc. IEEE 56th Vehicular Technology Conference*, 2002, vol.2, pp. 894 – 898

[57] M. Sandell and O. Edfors, “A comparative study of pilot-based channel estimators for wireless OFDM,” Lulea Univ. of Technol., Lulea, Sweden, *Research Rep. TULEA* 1996.

[58] Baoguo Yang, K.B. Letaief, R.S. Cheng and Zhigang Cao, “Windowed DFT based pilot-symbol-aided channel estimation for OFDM systems in multipath fading channels,” in *Proc. IEEE VTC*, May 2000, vol. 2, pp 1480-1484.

[59] Yanxin Yan, Yi Gong, “Energy Detection of Narrowband Signals in Cognitive Radio Systems,” in *Proc. IEEE Int Conf. Wireless Communications and Signal Processing (WCSP)*, Oct. 2010. pp.1-5.

[60] Haiyun Tang, “Some Physical Layer Issues of Wide-band Cognitive Radio Systems,” in *Proc. IEEE Int. Symp. New Frontiers in Dynamic Spectrum Access Networks (DySPAN)*, Dec. 2005. pp 151-159.

Appendix: Matlab Codes

The following is the matlab code used to simulate the proposed FDO equalizers. Some parameters and variables may need to be modified for each simulation.

```
function [ber, ber_user]=fdo_ofdm(total_num_sym, snr_range, OSF, enable_CC, enable_zp_ofdm, fo, ...
   near_far_factor, user_range, fd, MMSE_EN, FDO_MMSE_EN, SR_MMSE_EN, SR_DIA_EN, ...
   SR_ZF2_EN, SR_ZF4_EN, SR_ZF8_EN, ...
   num_path, path_int, Max_iter, Enable_MC_CDMA);
%
% Copyright (C) 2015 Yanxin Yan
% This code was designed by Yanxin Yan for his PhD degree @ Nanyang Technological University.
%
% You can use or modify it for your personal purpose, but WITHOUT ANY WARRANTY.
% Some paramters and variables may need modification for successfully simulation.
% For technical discussion, please contact the author: yany0011@ntu.edu.sg
%
% Inputs:
% total_num_sym: Number of OFDM symbols for simulation.
% snr_range    : snr range, e.g. 4:2:14
% OSF          : Oversampling factor, e.g. 40/32
% enable_CC    : = 1, enable convolutional code. =0, disable
% enable_zp_ofdm:   =1, using zero padding OFDM. =0, using CP OFDM.
% fo           : Frequency offset normalised with subcarrier spacing.
% near_far_factor:   near-far effect. =1 means without near-far effect. =2 means 1/3 users with power*2
% user_range   : number of users. Please set to N.
% fd           : normalizsed Doppler frequency shift
% MMSE_EN      : =1 Enable use MMSE
% FDO_MMSE_EN  : =1 Enable FDO MMSE
% SR_MMSE_EN   : =1 Enable FDO MMSE with symbol reconstruction (SR)
% SR_DIA_EN    : =1 Enable Diagonal FDO MMSE with SR.
% SR_ZF2_EN    : =1 Enable FDO zero-forcing with oversampling rate = 2.
% SR_ZF4_EN    : =1 Enable FDO zero-forcing with oversampling rate = 4.
% SR_ZF8_EN    : =1 Enable FDO zero-forcing with oversampling rate = 8.
% num_path     : number of multipath.
% path_int     : integer, represents interval between two paths.
% Max_iter     : The maximum iteration number when SR is used.
% Enable_MC_CDMA: =1 Enable MC-CDMA.

fid = fopen('run.log', 'a');

temp_str=sprintf('start sim at: \t%s', datestr(now));
disp(temp_str);
fprintf(fid, '%s\n', temp_str);

global modobj demodobj;

single_user = 0;  %% 0-add all users. otherwise, which user is used. e.g =2, user 2 is used.
```

```
N = 64;              %% FFT size, number of subcarriers
%N = 256;           %% FFT size, number of subcarriers    % for TVT paper
GI = N/8;           %% 1/4 guard interval
Nsym = N + GI;      %% size of OFDM symbol
Ns = N+GI;
Mt = 1;             %% Number of Tx antennas
Mr = 1;             %% Number of Rx antennas
M = 8;              %% Max constellation bit number
SF = N;             %% spread factor. spreading length.
mod_type = 1;       %% modulation type. 1-QPSK, 2-16QAM, 3-64QAM
  modobj=modem.qammod('M', 4^mod_type, 'InputType', 'Bit');
  demodobj=modem.qamdemod(modobj, 'OutputType', 'Bit', 'DecisionType', 'Hard Decision');
num_subc = N;       %% number of subcarriers for data.

if nargin < 8; user_range = N;  end
if nargin < 9; fd = 0.00; end     %set doppler frequency offset.
if nargin < 1
    snr_range = 100;           %9:4:33;  %% SNR range
    total_num_sym = 2000;      %% number of OFDM symbols
    OSF = 2;                   %% oversampling factor in frequency domain.
    enable_CC=1;               %% enable convolutional coding.
    fo = 0.00;                 %% Frequency offset in multiple of subcarrier spacing.
    enable_zp_ofdm = 0;        %% =1: prefix=zero. =0: use Cyclic prefix.
    near_far_factor = 1;       % no near far effect
elseif nargin < 5
    error('Not enough input arguments!');
end

if nargin < 10; MMSE_EN=0; end       %Enable OLA_MMSE
if nargin < 11; FDO_MMSE_EN=1; end   %Enable OLA_MMSE
if nargin < 12; SR_MMSE_EN=1; end    %Enable OLA_MMSE
if nargin < 13; SR_DIA_EN=1; end     %Enable Diag MMSE
if nargin < 14; SR_ZF2_EN=0; end     %Enable ZF, OSF=2
if nargin < 15; SR_ZF4_EN=0; end     %Enable ZF, OSF=4
if nargin < 16; SR_ZF8_EN=0; end     %Enable ZF, OSF=8
if nargin < 17; num_path = GI; end
if nargin < 18; path_int = 1; end
if nargin < 19; Max_iter=5; end      %
if nargin < 20; Enable_MC_CDMA=1; end   %Enable 1: MC-CDMA or 0: OFDM

SR_ZF1_EN=0;         %enable zf.
OLA_INI_EN = 1;      % 1: step 1 uses OLA equ.  0: step 1 uses fdfs method.
if MMSE_EN == 0
    MMSE_INI_EN = 0;
else
    MMSE_INI_EN = 1;
end

enable_chann_esti = 0;  %enable channel estimation.

%Enable_MC_CDMA = 1;    % 1: MC_CDMA, 0: OFDM.

Enable_Doppler = (fd ~= 0);
%Max_iter = 3;
if single_user ~= 0;
    num_user = 1;
else
    num_user = N;
end;
```

```
temp_str = [sprintf('MC-CDMA-EN=%d, ', Enable_MC_CDMA) sprintf('num_sym=%d, ', total_num_sym) sprintf('snr=') sprintf('%d ', snr_range) ...
    sprintf('osf=%f, cc=%d, zp=%d, fo=%f, near-far=%d, fd=%d, N=%d, GI=%d, SF=%d\n', ...
        OSF, enable_CC, enable_zp_ofdm, fo, near_far_factor, fd, N,GI, SF) ...
    sprintf('users=') sprintf('%d ', user_range) sprintf('path num=%d, path intv=%d ', num_path, path_int) ...
    sprintf('OLA_INI_EN=%d, Max_iter=%d, MMSE_INI_EN=%d', OLA_INI_EN, Max_iter, MMSE_INI_EN)];
disp(temp_str);

fprintf(fid, '%s\n', temp_str);

%num_path = GI;
%path_int = 2;
PD = (num_path-1)*path_int+1;
if (enable_zp_ofdm == 1)
   Npd = N+PD;
else
   Npd = N+GI+PD;
end
BypassChannel = 0;  %% =1: without channel, =0: with channel.

%if enable_zp_ofdm ~= 1; OSF = 1; end  %% for CP, OSF is not applicable.

if enable_CC==1; code_rate = 0.5; else code_rate = 1; end

PP1=ones(1, N-round(N/3)*2);
PP2=near_far_factor*ones(1, round(N/3));
PP3=1/near_far_factor*ones(1,round(N/3));
PP = [PP1 PP2 PP3];

%% generate walsh codes
if (Enable_MC_CDMA==1)
   SC = hadamard(N)/sqrt(N);  % MC-CDMA
   SC1 = hadamard(SF)/sqrt(SF);
   numSC=N/SF;
   SC = zeros(N,N);
   for k=1:numSC
      SC((k-1)*SF+1:k*SF, (k-1)*SF+1:k*SF) = SC1;
   end
else
   SC = eye(N);              % OFDM
end

F = exp(1j*2*pi* (0:N-1).' * (0:N-1) /N)/sqrt(N);
G = exp(-1j*2*pi* (0:N-1).' * (0:N-1) /N)/sqrt(N);
G_NsN=exp(-1j*2*pi*(0:Ns-1).'*(0:N-1)/Ns)/sqrt(Ns);
G_Ns =exp(-1j*2*pi*(0:Ns-1).'*(0:Ns-1)/Ns)/sqrt(Ns);
G_N2 = exp(-1j*2*pi*(0:N*2-1).'*(0:N*2-1)/N/2)/sqrt(N*2);
G_N4 = exp(-1j*2*pi*(0:N*4-1).'*(0:N*4-1)/N/4)/sqrt(N*4);
G_N8 = exp(-1j*2*pi*(0:N*8-1).'*(0:N*8-1)/N/8)/sqrt(N*8);
G_Npd =exp(-1j*2*pi*(0:Npd-1).'*(0:Npd-1)/Npd)/sqrt(Npd);
G_NpdN=exp(-1j*2*pi*(0:Npd-1).'*(0:N-1)/Npd)/sqrt(Npd);
G_N1 =exp(-1j*2*pi*(0:N).'*(0:N)/(N+1))/sqrt(N+1);

gamma_nn = G*G';
gamma_ns = G_Ns*G_Ns';
gamma_npd = G_Npd*G_Npd';
gamma_n2 = G_N2(:, 1:Npd)*G_N2(:, 1:Npd)';
```

```
gamma_n4 = G_N4(:, 1:Npd)*G_N4(:, 1:Npd)';
gamma_n8 = G_N8(:, 1:Npd)*G_N8(:, 1:Npd)';
gamma_n1 = eye(N+1);

if single_user
   SC_U = zeros(N,N); SC_U(:, single_user)=SC(:, single_user);
   %SC_U  = SC;
else
   SC_U = SC;
end

   GF_nn  =G(:, 1:N) * F * SC_U;
   GF2_nn  = eye(N); %G(:, 1:N) * F *F'*G(:, 1:N)';  %GF_nn * GF_nn';
if enable_zp_ofdm
   GF_nsn  =G_Ns(:, 1:N) * F * SC_U;
   GF_npdn = G_Npd(:, 1:N) * F *SC_U;
   GF_n2n = G_N2(:, 1:N) *F *SC_U;
   GF_n4n = G_N4(:, 1:N) *F *SC_U;
   GF_n8n = G_N8(:, 1:N) *F *SC_U;

   GF2_nsn  = G_Ns(:, 1:N) * F *F'*G_Ns(:, 1:N)';  %GF_nsn * GF_nsn';
   GF2_npdn = G_Npd(:, 1:N) * F * F'*G_Npd(:, 1:N)'; %GF_npdn * GF_npdn';

   GF2_n2n = G_N2(:, 1:N) * G_N2(:, 1:N)';  %  FDFS-ZF
   GF2_n4n = G_N4(:, 1:N) * G_N4(:, 1:N)';
   GF2_n8n = G_N8(:, 1:N) * G_N8(:, 1:N)';
   GF_pinv_GF2_n2n = GF_n2n' * pinv(GF2_n2n);
   GF_pinv_GF2_n4n = GF_n4n' * pinv(GF2_n4n);
   GF_pinv_GF2_n8n = GF_n8n' * pinv(GF2_n8n);
   GF_pinv_GF2_npdn = GF_npdn' * pinv(GF2_npdn);
else
   Fsc = F*SC_U;
   GF_n1n  = G_N1 * [Fsc(N, :); Fsc];
   GF_nsn  = G_Ns * [Fsc(N-GI+1:N, :); Fsc];
   GF_nsn_zp  = G_Ns(:, 1:N) * Fsc;
   GF_npdn = G_Npd(:, 1:Npd) * [Fsc(N-GI+1:N, :); Fsc; zeros(Npd-Ns, N)];
   GF_n2n = G_N2(:, 1:N*2) *[Fsc(N-GI+1:N, :); Fsc; zeros(N*2-Ns, N)];
   GF_n4n = G_N4(:, 1:N*4) *[Fsc(N-GI+1:N, :); Fsc; zeros(N*4-Ns, N)];
   GF_n8n = G_N8(:, 1:N*8) *[Fsc(N-GI+1:N, :); Fsc; zeros(N*8-Ns, N)];
   GF_n2n_zp = G_N2(:, 1:N*2) *[Fsc; zeros(N*2-N, N)];
   GF_n4n_zp = G_N4(:, 1:N*4) *[Fsc; zeros(N*4-N, N)];
   GF2_n2n_zp = GF_n2n_zp * GF_n2n_zp';
   GF2_n4n_zp = GF_n4n_zp * GF_n4n_zp';

   Fsc = F*SC;
   GF2_n1n  = G_N1(:, 1:N+1) * [Fsc(N, :); Fsc] * [Fsc(N, :); Fsc]'*G_N1(:, 1:N+1)';  %GF_nsn1 * GF_nsn1';
   GF2_nsn  = G_Ns(:, 1:Ns) * [Fsc(N-GI+1:N, :); Fsc] * [Fsc(N-GI+1:N, :); Fsc]'*G_Ns(:, 1:Ns)';  %GF_nsn *
GF_nsn';
   GF2_nsn_zp = GF_nsn_zp * GF_nsn_zp';
   GF2_npdn = G_Npd(:, 1:Npd) *[Fsc(N-GI+1:N, :); Fsc; zeros(Npd-Ns, N)] * ...
         [Fsc(N-GI+1:N, :); Fsc; zeros(Npd-Ns, N)]'*G_Npd(:, 1:Npd)'; %GF_npdn * GF_npdn';

   GF2_n2n = (G_N2(:, 1:N*2) *[Fsc(N-GI+1:N, :); Fsc; zeros(N*2-Ns, N)] * ...
         [Fsc(N-GI+1:N, :); Fsc; zeros(N*2-Ns, N)]'*G_N2(:, 1:N*2)');
   GF2_n4n = (G_N4(:, 1:N*4) *[Fsc(N-GI+1:N, :); Fsc; zeros(N*4-Ns, N)] * ...
         [Fsc(N-GI+1:N, :); Fsc; zeros(N*4-Ns, N)]'*G_N4(:, 1:N*4)');
   GF2_n8n = (G_N8(:, 1:N*8) *[Fsc(N-GI+1:N, :); Fsc; zeros(N*8-Ns, N)] * ...
         [Fsc(N-GI+1:N, :); Fsc; zeros(N*8-Ns, N)]'*G_N8(:, 1:N*8)');
   GF_pinv_GF2_n2n = GF_n2n' * pinv(GF2_n2n);
```

```
    GF_pinv_GF2_n4n = GF_n4n' * pinv(GF2_n4n);
    GF_pinv_GF2_n8n = GF_n8n' * pinv(GF2_n8n);
    GF_pinv_GF2_npdn = GF_npdn' * pinv(GF2_npdn);
end

%% channel profile. delay = 0, 1T, 2T, 3T, 4T, ...
hn_len = (num_path-1)*path_int+1;  % path delay.
multipath=zeros(1,hn_len);
path_pow = (num_path:-1:1)/sum(num_path:-1:1);    %linear
%path_pow = exp(-1:-1:-num_path) / sum(exp(-1:-1:-num_path));  %exponential[0.6323 0.2326 0.0856 0.0315 0.0116
0.0043 0.0016 0.0006]

multipath(1:path_int:hn_len) = sqrt(path_pow);

tau = (0:num_path-1)*path_int;
pdb = 10*log10(path_pow);
if (Enable_Doppler)
    chan_dop = rayleighchan(1, 1/N*fd, tau, pdb);
end

%%% start loop for users.

randn('state', 0);
rand('state', 0);
rand_state =0;
%randint(1, 2, [0 1], rand_state); %% reset state to 0;
rng('default');         %initial random generator for randi

%%% ============================== start TX   ========================
num_sym=total_num_sym;

msg_bits = num_sym * mod_type * 2 * code_rate;  %% message bits per user.
msg_coded = zeros(N, msg_bits/code_rate);
msg = zeros(N, msg_bits);
%% generate tx of different users, and add together.
for loop_user = 1:N
    msg(loop_user,:) = randi([0 1], 1, msg_bits);
    msg(loop_user,end-5:end) = [0 0 0 0 0 0];     %% force end state to zero.

    %%% convolutional encoder
    if enable_CC ==1
        trellis = poly2trellis(7, [133 171]);
        [msg_coded_1 end_state] = convenc(msg(loop_user,:), trellis);
        msg_coded(loop_user, :) = msg_coded_1;
    else
        msg_coded_1 = msg(loop_user,:);
        trellis = 0;
    end

%%% modulation
    msg_mod(loop_user, :) = modulate(modobj, msg_coded(loop_user,:).').';
end % end loop_user

txd_frame = zeros(1, (N+GI)*num_sym+PD);

channel = zeros(num_sym, hn_len);

txf = F*SC*diag(PP)*msg_mod;    % select users to send
```

```
if enable_chann_esti
   pilot_dat_f = msg_mod(:,1);
   pilot_dat=  F*pilot_dat_f;  % fixed pilot symbol for channel estimation.
   txd_pilot_frame = zeros(num_sym, Ns+hn_len-1);
end

for k=1:num_sym


%%% ============================== pass to channel ======================
%%% apply channel per symbol.
   if BypassChannel;
      len_chan = 1;
      channel(k, 1) = 1;
   else
      len_chan = hn_len;
      channel(k, :) = multipath .* ...
         (randn(1, len_chan) + 1j*randn(1,len_chan))*sqrt(0.5);
   end % end bypass channel
   Nsch = Ns+len_chan-1;

   if enable_zp_ofdm
      tx_sig = [txf(:,k).' zeros(1,GI+len_chan)];
   else
      tx_sig =[txf(N-GI+1:N, k).' txf(:, k).' zeros(1, len_chan)];
   end

   if Enable_Doppler
      tx_sym_ch = filter(chan_dop, tx_sig(1:Ns+len_chan-1));
      channel(k, 1:path_int:hn_len) = chan_dop.PathGains(1, :);
   else
      tx_sym_ch = conv(channel(k, 1:len_chan), tx_sig(1:Ns));
   end

   % add frequency offset.
   % tx_sym_ch = tx_sym_ch .* exp(1j*2*pi*(1:length(tx_sym_ch))*(fo)/N); % frequency offset
   tx_sym_ch = tx_sym_ch .* exp(1j*2*pi*(1-N/8:length(tx_sym_ch)-N/8)*(fo)/N); % frequency offset. CP=N/4. align
with CP=N/8

   if (k==1)
     txd_frame(1:Nsch) = tx_sym_ch(1:Nsch);
   else
     txd_frame((k-1)*Ns+1:(k-1)*Ns+Nsch) = txd_frame((k-1)*Ns+1:(k-1)*Ns+Nsch)+tx_sym_ch(1:Nsch);
   end

   if(enable_chann_esti)
      if (enable_zp_ofdm)
         pilot_sym=[pilot_dat.' zeros(1, GI+len_chan)];
      else
         pilot_sym=[pilot_dat(N-GI+1:N).' pilot_dat.' zeros(1, len_chan)];
      end
      if Enable_Doppler
         tx_pilot_ch = filter(chan_dop, pilot_sym(1:Ns+len_chan-1));
      else
         tx_pilot_ch = conv(channel(k, 1:len_chan), pilot_sym(1:Ns));
      end
      tx_pilot_ch = tx_pilot_ch .* exp(1j*2*pi*(1:length(tx_sym_ch))*(fo)/N);

      txd_pilot_frame(k, 1:Nsch) = tx_pilot_ch;
```

```
    end

end  % end k symbol

ber_ola = zeros(1, length(snr_range));
ber_ola_mmse = zeros(1, length(snr_range));
ber_fdfs = zeros(1, length(snr_range));
ber_fdo1 = zeros(1, length(snr_range));
ber_fdfs_diag0 = zeros(1, length(snr_range));
ber_fdfs_sr = zeros(Max_iter, length(snr_range), 3);
ber_fdfs_diag = zeros(Max_iter, length(snr_range), 8, 3);
ber_fdfs_diag2 = zeros(Max_iter, length(snr_range));
ber_fdfs_diag4 = zeros(Max_iter, length(snr_range));
ber_fdfs_diag8 = zeros(Max_iter, length(snr_range));
ber_fdfs_zf = zeros(Max_iter, length(snr_range), 4); %(iter, snr_idx, osf_idx);

ber_code_ola = zeros(1, length(snr_range));
ber_code_ola_mmse = zeros(1, length(snr_range));
ber_code_fdfs = zeros(1, length(snr_range));
ber_code_fdo1 = zeros(1, length(snr_range));
ber_code_fdfs_diag0 = zeros(1, length(snr_range));
ber_code_fdfs_sr = zeros(Max_iter, length(snr_range), 3);
ber_code_fdfs_diag = zeros(Max_iter, length(snr_range), 8, 3);
ber_code_fdfs_zf = zeros(Max_iter, length(snr_range), 4); %(iter, snr_idx, osf_idx);

berc_fdfs_diag = zeros(8, length(snr_range), 3); %snr, var_idx, osf_idx
berc_fdfs_sr = zeros(3, length(snr_range));  %snr, var_idx
berc_fdfs_zf = zeros(4, length(snr_range)); %(osf_idx, snr_idx);

ber_user_ola = zeros(N, length(snr_range));
ber_user_ola_mmse = zeros(N, length(snr_range));
ber_user_fdfs = zeros(N, length(snr_range));
ber_user_fdfs_diag0 = zeros(N, length(snr_range));
ber_user_fdfs_sr = zeros(N, length(snr_range), Max_iter, 3);
ber_user_fdfs_diag = zeros(N, length(snr_range), Max_iter, 8, 3);
ber_user_fdfs_diag2 = zeros(N, length(snr_range), Max_iter);
ber_user_fdfs_diag4 = zeros(N, length(snr_range), Max_iter);
ber_user_fdfs_diag8 = zeros(N, length(snr_range), Max_iter);
ber_user_fdfs_zf = zeros(N, length(snr_range), Max_iter, 4); %(:, snr_idx, iter, osf_idx);

ber_code_user_ola = zeros(N, length(snr_range));
ber_code_user_ola_mmse = zeros(N, length(snr_range));
ber_code_user_fdfs = zeros(N, length(snr_range));
ber_code_user_fdfs_diag0 = zeros(N, length(snr_range));
ber_code_user_fdfs_sr = zeros(N, length(snr_range), Max_iter, 3);
ber_code_user_fdfs_diag = zeros(N, length(snr_range), Max_iter, 8, 3);
ber_code_user_fdfs_zf = zeros(N, length(snr_range), Max_iter, 4); %(:, snr_idx, iter, osf_idx);

snr_idx=0;
for snr = snr_range
   snr_idx = snr_idx + 1;
%    noise = N/num_user/(10^(snr/10));
   noise = 2*N/num_user/(10^(snr/10));  %the signal power=2, correct noise power

   % To reduce simulation time
   switch snr_idx
      case {1}
         num_sym=total_num_sym/8;
      case {2}
```

```
        num_sym=total_num_sym/4;
    case {3}
        num_sym=total_num_sym/1;
    case {4}
        num_sym=total_num_sym;
    case {5, 6}
        num_sym=total_num_sym;
    case {7, 8}
        num_sym=total_num_sym;
end
temp_str = sprintf('num_sym        = %d', num_sym);
disp(temp_str);
fprintf(fid, '%s\n', temp_str);


%%% add AWGN noise
snr_offset=0;
if enable_zp_ofdm                    %CP and ZP OFDM have the same noise variance
    snr_offset = 10*log10(N/Nsym);     %%compensate for zero-padding post-fix.
end
snr_offset = snr_offset + 10*log10(num_user/N);
rx_sig = awgn(txd_frame, snr+snr_offset, 'measured', 0);
%rx_sig = txd_frame;

%%%============================== start receiving ======================
% channel estimation
channel_est = zeros(num_sym, N);
for k=1:num_sym
    if (enable_chann_esti)
        if enable_zp_ofdm
            chan_sym = txd_pilot_frame(k, 1:N) + [txd_pilot_frame(k, N+1:N+GI) zeros(1, N-GI)];
        else
            chan_sym = txd_pilot_frame(k, GI+1:N+GI);
        end
        chan_sym_f = fft(chan_sym, N)/sqrt(N);
        Hn = chan_sym_f./pilot_dat_f.';
        channel_user = (F*Hn.')./sqrt(N);
        channel_est(k,:) = channel_user;
    end
end

for  k=1:num_sym
    channel_user = channel(k, :);

    if (enable_chann_esti)
        Hn = fft(channel_est(k,:), N);
    else
        Hn = fft(channel_user, N);
    end
    DHn = diag(Hn);
    inv_DHn = diag(1./Hn);

    % ola
    if enable_zp_ofdm
        rx_sig_sym = rx_sig((k-1)*Ns+1: (k-1)*Ns+N) + ...
                [rx_sig((k-1)*Ns+N+1: (k-1)*Ns+Ns) zeros(1, N-GI)];
    else
        rx_sig_sym = rx_sig((k-1)*Ns+GI+1: (k-1)*Ns+Ns);
    end
```

```
    rx_fn = fft(rx_sig_sym, N)/sqrt(N);


    whn = SC_U'*inv_DHn;
    rx_ola(:, k) = whn*rx_fn.';

    % ola-mmse
    if (MMSE_EN==1)
       phi=DHn*GF2_nn*DHn'+gamma_nn*noise;
       pinv_phi=pinv(phi);
       svalue=0;
       while(isfinite(pinv_phi(1,1))==0)  % add small value to avoid infinite value
          svalue=svalue+1e-10;
          pinv_phi= pinv(phi+ svalue);
       end
       whn = GF_nn' * DHn' * pinv_phi;
       % whn = GF_nn' * DHn' * pinv(DHn*GF2_nn*DHn'+gamma_nn*noise);
       rx_ola_mmse(:,k)=whn*rx_fn.';
    end


  end
  [ber_ola(snr_idx)  ,  ber_user_ola(:,snr_idx),  ber_code_ola(snr_idx),  ber_code_user_ola(:,snr_idx)  ] =
err_cal(rx_ola  , num_sym, mod_type, code_rate, N, enable_CC, msg, trellis, msg_coded);
  temp_str = ([sprintf('BER_ola  = [') sprintf('%g ',ber_ola) sprintf('];')]);
  disp(temp_str);
  fprintf(fid, '%s\n', temp_str);
  temp_str = ([sprintf('BER_code_ola  = [') sprintf('%g ',ber_code_ola) sprintf('];')]);
  disp(temp_str);
  fprintf(fid, '%s\n', temp_str);

  if (MMSE_EN==1)
  [ber_ola_mmse(snr_idx)  ,  ber_user_ola_mmse(:,snr_idx),  ber_code_ola_mmse(snr_idx)  ,
ber_code_user_ola_mmse(:,snr_idx) ] = err_cal(rx_ola_mmse  , num_sym, mod_type, code_rate, N, enable_CC, msg,
trellis, msg_coded);
  temp_str=([sprintf('BER_ola_mmse  = [') sprintf('%g ',ber_ola_mmse) sprintf('];')]);
  disp(temp_str);
  fprintf(fid, '%s\n', temp_str);
  temp_str=([sprintf('BER_code_ola_mmse  = [') sprintf('%g ',ber_code_ola_mmse) sprintf('];')]);
  disp(temp_str);
  fprintf(fid, '%s\n', temp_str);
  end

  if (FDO_MMSE_EN==1)
  for k=1:num_sym
  %% proposed detection.
    if (enable_chann_esti)
       channel_user = channel_est(k,:);
    else
       channel_user = channel(k, :);
    end
    Hns=fft(channel_user, Ns);
    DHns = diag(Hns);


    % fdo-mmse
    rx_sig_sym = rx_sig((k-1)*Ns+1: (k-1)*Ns+Ns);
    rx_fns = fft(rx_sig_sym, Ns) / sqrt(Ns);
```

```
        phi=DHns*GF2_nsn*DHns'+gamma_ns*noise; %add small value to avoid NAN in pinv()
        pinv_phi=pinv(phi);
        svalue=0;
        while(isfinite(pinv_phi(1,1))==0)
            svalue=svalue+1e-10;
            pinv_phi= pinv(phi+ svalue);
        end
        wh_nsn = GF_nsn' * DHns' * pinv_phi;
        rx_fdfs(:, k) = wh_nsn * rx_fns.';

        %fdo-diag
        phi_inv=diag(1./diag(phi .* eye(Ns)));
        wh_nsn = GF_nsn' * DHns' * phi_inv;
        rx_fdfs_diag(:, k) = wh_nsn * rx_fns.';

    end % k

    [ber_fdfs(snr_idx) , ber_user_fdfs(:,snr_idx), ber_code_fdfs(snr_idx) , ber_code_user_fdfs(:,snr_idx) ] = err_cal(rx_fdfs , num_sym, mod_type, code_rate, N, enable_CC, msg, trellis, msg_coded);
    temp_str=([sprintf('BER_fdfs = [') sprintf('%g ',ber_fdfs) sprintf('];')]);
    disp(temp_str);
    fprintf(fid, '%s\n', temp_str);
    temp_str=([sprintf('BER_code_fdfs = [') sprintf('%g ',ber_code_fdfs) sprintf('];')]);
    disp(temp_str);
    fprintf(fid, '%s\n', temp_str);

    [ber_fdfs_diag0(snr_idx) , ber_user_fdfs_diag0(:,snr_idx), ber_code_fdfs_diag0(snr_idx) , ber_code_user_fdfs_diag0(:,snr_idx)] = err_cal(rx_fdfs_diag , num_sym, mod_type, code_rate, N, enable_CC, msg, trellis, msg_coded);
    temp_str=([sprintf('BER_fdfs_diag = [') sprintf('%g ',ber_fdfs_diag0) sprintf('];')]);
    disp(temp_str);
    fprintf(fid, '%s\n', temp_str);
    temp_str=([sprintf('BER_code_fdfs_diag = [') sprintf('%g ',ber_code_fdfs_diag0) sprintf('];')]);
    disp(temp_str);
    fprintf(fid, '%s\n', temp_str);
    end

    if OLA_INI_EN == 1
        if (MMSE_INI_EN==1)
            rx_sr = rx_ola_mmse;
            rx_sr_d = rx_ola_mmse;
            rx_sr2 = rx_ola_mmse;
            rx_sr4 = rx_ola_mmse;
            rx_sr8 = rx_ola_mmse;
        else
            rx_sr = rx_ola;
            rx_sr_d = rx_ola;
            rx_sr2 = rx_ola;
            rx_sr4 = rx_ola;
            rx_sr8 = rx_ola;
        end
    else
        rx_sr = rx_fdfs;
        rx_sr_d = rx_fdfs_diag;
        rx_sr2 = rx_fdfs_diag;
        rx_sr4 = rx_fdfs_diag;
        rx_sr8 = rx_fdfs_diag;
    end
```

```
    %wh = zeros(N, Npd, num_sym);
    if (fd < 0.0001 && fo < 0.0001)  % i.e., no fd and fo.
%       var_list = [2*noise noise 0.5*noise]; %test for different variance
        var_list = noise;
    else
        var_list = noise;
    end

    var_cof = eye(Npd);
    Hnpd_c = zeros(num_sym, Npd);
    be=zeros(1, num_sym);
    var_idx=0;
    for var = var_list
        var_idx= var_idx+1;

    if OLA_INI_EN == 1
        if (MMSE_INI_EN==1)
            rx_sr = rx_ola_mmse;
        else
            rx_sr = rx_ola;
        end
    else
        rx_sr = rx_fdfs;
    end
    if (SR_MMSE_EN==1)     % FDO-MMSE, SR - sym reconstruction
    for iter = 1: Max_iter
      for k=1:num_sym

            if (enable_chann_esti)
                channel_user = channel_est(k,:);
                rx_sig_sym_sr = sym_cal(rx_sig, rx_sr, k, channel_est, F, SC, Npd, Ns, GI, num_sym, enable_zp_ofdm);
            else
                channel_user = channel(k, :);
                rx_sig_sym_sr = sym_cal(rx_sig, rx_sr, k, channel, F, SC, Npd, Ns, GI, num_sym, enable_zp_ofdm);
            end
            rx_fnpd = fft(rx_sig_sym_sr, Npd)/sqrt(Npd);

            if iter == 1 && var_idx==1
                Hnpd = fft(channel_user, Npd);
                Hnpd_c(k,:) = Hnpd;
            else
                Hnpd = Hnpd_c(k,:);
            end
                DHnpd = diag(Hnpd);

                % MMSE
                phi=(DHnpd*GF2_npdn*DHnpd'+gamma_npd*var*var_cof);   %add small value 1e-12 to avoid NAN in
pinv().
                %phi_0=(DHnpd*GF_npdn)'*(DHnpd*GF_npdn)+eye(N)*var;    % equivalent equation: reduce matrix
dimension to N
                pinv_phi=pinv(phi);
                svalue=0;
                while(isfinite(pinv_phi(1,1))==0)
                    svalue=svalue+1e-10;
                    pinv_phi= pinv(phi+ svalue);
                end
                wh_npdn = GF_npdn' * DHnpd' * pinv_phi;
                %wh_npdn_0 = pinv(phi_0) * (DHnpd*GF_npdn)';          % equivalent equation: reduce matrix dimension to
N
```

```
        rx_fdfs_sr(:,k) = wh_npdn * rx_fnpd.';

        %calculate BER
        if iter == 1
          phi=wh_npdn*DHnpd*GF_npdn;%  HD_Lideal*GF_ln;
          aa = diag(phi);
          sft = sum(real(phi).^2+imag(phi).^2, 2) - real(aa).^2;
          bb = wh_npdn*G_Npd;
          var_bb = sum(real(bb).^2+imag(bb).^2, 2) ...
          + sum(real(bb(1:PD-GI)).^2 + imag(bb(1:PD-GI)).^2, 2) ...
          + sum(real(bb(N+1:Npd)).^2 + imag(bb(N+1:Npd)).^2, 2); % estimate reconstructure error
%           var_bb = sum(real(bb).^2+imag(bb).^2, 2) ; %assume all noise virances are same.
          be(k)=mean(qfunc(real(aa)./sqrt(var_bb*noise/2 + sft)));
        end

      end
      if iter == 1
        %save('mc_cdma_wh_npdn.mat', '-mat', 'wh');
        berc_fdfs_sr(var_idx, snr_idx) = mean(be);
        temp_str=([sprintf('BERC_fdfs_sr_%1.2d = [', var) sprintf('%g ',berc_fdfs_sr(var_idx, :)) sprintf('];')]);
        disp(temp_str);
        fprintf(fid, '%s\n', temp_str);
      end
      rx_sr = rx_fdfs_sr(:, :);     % update equalized data for reconstruction.

      if (sum(sum(~isfinite(rx_sr))) )
        pause;
      end

      [ber_fdfs_sr(iter, snr_idx, var_idx), ber_user_fdfs_sr(:, snr_idx, iter), ber_code_fdfs_sr(iter, snr_idx, var_idx),
ber_code_user_fdfs_sr(:, snr_idx, iter)] = ...
        err_cal(rx_fdfs_sr(:,:)   , num_sym, mod_type, code_rate, N, enable_CC, msg, trellis, msg_coded);
      temp_str=([sprintf('BER_fdfs_sr_%1.2d        = [', var) sprintf('%g ',ber_fdfs_sr(iter, :, var_idx)) sprintf('];')]);
      disp(temp_str);
      fprintf(fid, '%s\n', temp_str);
    end  % for iter
    for iter=1: Max_iter
      temp_str=([sprintf('BER_code_fdfs_sr_%1.2d        = [', var) sprintf('%g ',ber_code_fdfs_sr(iter, :, var_idx))
sprintf('];')]);
      disp(temp_str);
      fprintf(fid, '%s\n', temp_str);
    end
    end % if(SR_MMSE_EN
    end % for var

    %diag, Npd
    osf_idx=1; osf_val=1;
    with_cp = 0;  % without CP
      if with_cp==1 || enable_zp_ofdm==1
        GF1 = GF_npdn; GF2 = GF2_npdn; gamma_n = gamma_npd; ND=Npd;    Gv=G_Npd;       % OFDM with CP
      else
        GF1 = GF_nsn_zp; GF2=GF2_nsn_zp; gamma_n = gamma_ns; ND = Ns;   Gv=G_Ns;      % OFDM without CP
      end
      var_cof = eye(ND);
    var_idx = 0;
    Hnpd_c = zeros(num_sym, ND);

    if (fd < 0.0001 && fo < 0.0001)  % i.e., no fd and fo.
```

```
    var_list = [noise 0.001 0.003 0.007 0.016 0.032];
  else
    var_list = [noise 0.003 0.032];
  end
  for var = var_list
  if OLA_INI_EN == 1
    if (MMSE_INI_EN==1)
      rx_sr_d = rx_ola_mmse;
    else
      rx_sr_d = rx_ola;
    end
  else
    rx_sr_d = rx_fdfs_diag;
  end
    var_idx= var_idx+1;

  %wh = zeros(N, Npd, num_sym);
  if (SR_DIA_EN == 1)
  for iter = 1: Max_iter
    % FDO-DMMSE, osf = 2,
      for k=1:num_sym
        if (enable_chann_esti)
          channel_user = channel_est(k, :);
          rx_sig_sym_sr = sym_cal(rx_sig, rx_sr_d, k, channel_est, F, SC, Npd, Ns, GI, num_sym, enable_zp_ofdm,
with_cp);
        else
          channel_user = channel(k, :);
          rx_sig_sym_sr = sym_cal(rx_sig, rx_sr_d, k, channel, F, SC, Npd, Ns, GI, num_sym, enable_zp_ofdm,
with_cp);
        end
        rx_sym2 = fft(rx_sig_sym_sr, ND)/sqrt(ND);

        if iter==1 && var_idx==1
          Hnpd = fft(channel_user, ND);
          Hnpd_c(k,:)=Hnpd;
        else
          Hnpd = Hnpd_c(k,:);
        end
          DHnpd = diag(Hnpd);
        if enable_zp_ofdm
% wh_npdn = GF_npdn' .* repmat((diag(DHnpd') .* (1./diag(DHnpd.*DHnpd'+gamma_npd*var))).', N, 1);
          wh_npdn = GF1' .* repmat((diag(DHnpd') .* (1./diag(DHnpd.*DHnpd'+gamma_n*var*var_cof + (1e-
8)))).', N, 1);
        else
%           wh_npdn = GF_npdn' * DHnpd' * diag(1./diag(DHnpd*GF2_npdn*DHnpd'+gamma_npd*noise));
          wh_npdn = GF1' .* repmat((conj(Hnpd) .* (1./diag( repmat(Hnpd.', 1, ND).*GF2.*repmat(conj(Hnpd),
ND,1)+gamma_n*var + (1e-8) )).'), N, 1);
        end
        rx_fdfs_diag(:,k) = wh_npdn * rx_sym2.';

        %FDO MMSE BER calculation equation
        if iter == 1
          phi=wh_npdn*DHnpd*GF1;%  HD_Lideal*GF_ln;
          aa = diag(phi);
          sft = sum(real(phi).^2+imag(phi).^2, 2) - real(aa).^2;
          bb = wh_npdn*Gv;
%           var_bb = sum(real(bb).^2+imag(bb).^2, 2) ...
%           + sum(real(bb(1:PD-GI)).^2 + imag(bb(1:PD-GI)).^2, 2) ...
%           + sum(real(bb(N+1:Npd)).^2 + imag(bb(N+1:Npd)).^2, 2); % estimate reconstructure error
```

```
            var_bb = sum(real(bb).^2+imag(bb).^2, 2) ; %assume all noise virances are same.
            be(k)=mean(qfunc(real(aa)./sqrt(var_bb*noise/2 + sft)));
        end

    end
    if iter == 1
        %save('mc_cdma_wh_n2n.mat', '-mat', 'wh');
        berc_fdfs_diag(var_idx, snr_idx, osf_idx) = mean(be);
        temp_str=([sprintf('BERC_fdfs_diag%d_%1.2d = [', osf_val, var) sprintf('%g ',berc_fdfs_diag(var_idx, :, osf_idx)) sprintf('];')]);
        disp(temp_str);
        fprintf(fid, '%s\n', temp_str);
    end
    rx_sr_d = rx_fdfs_diag(:, :);

    if (sum(sum(~isfinite(rx_sr_d))) )
        pause;
    end

    [ber_fdfs_diag(iter, snr_idx, var_idx, osf_idx), ber_user_fdfs_diag(:, snr_idx, iter, var_idx, osf_idx), ber_code_fdfs_diag(iter, snr_idx, var_idx, osf_idx), ber_code_user_fdfs_diag(:, snr_idx, iter, var_idx, osf_idx)] = ...
        err_cal(rx_fdfs_diag(:,:), num_sym, mod_type, code_rate, N, enable_CC, msg, trellis, msg_coded);
    temp_str=([sprintf('BER_fdfs_diag%d_%1.2d = [', osf_val, var) sprintf('%g ',ber_fdfs_diag(iter, :, var_idx, osf_idx)) sprintf('];')]);
    disp(temp_str);
    fprintf(fid, '%s\n', temp_str);
  end
  for iter=1: Max_iter
    temp_str=([sprintf('BER_code_fdfs_diag%d_%1.2d = [', osf_val, var) sprintf('%g ',ber_code_fdfs_diag(iter, :, var_idx, osf_idx)) sprintf('];')]);
    disp(temp_str);
    fprintf(fid, '%s\n', temp_str);
  end
  end
  end  % end for var


  %----- Normal FDO, with variance = 0:   ZF1, ZF2, ZF4, ZF8
  osf_idx=0;
  for osf_val = [1 2 4 8]
    if osf_val == 1
      GF1 = GF_npdn; GF3 = GF_pinv_GF2_npdn; gamma_n = gamma_npd; ND=Npd;GN=G_Npd;
      var_cof = eye(Npd);       elseif osf_val == 2
      GF1 = GF_n2n; GF3 = GF_pinv_GF2_n2n; gamma_n = gamma_n2; ND=N*2; GN=G_N2;
    elseif osf_val == 4
      GF1 = GF_n4n; GF3 = GF_pinv_GF2_n4n; gamma_n = gamma_n4; ND=N*4; GN=G_N4;
    else  % ==8
      GF1 = GF_n8n; GF3 = GF_pinv_GF2_n8n; gamma_n = gamma_n8; ND=N*8; GN=G_N8;
    end
    osf_idx=osf_idx+1;

    if OLA_INI_EN == 1
      if (MMSE_INI_EN==1)
        rx_sr2 = rx_ola_mmse;
      else
        rx_sr2 = rx_ola;
      end
    else
      rx_sr2 = rx_fdfs_diag;
```

```
    end

  if (SR_ZF1_EN == 1 && osf_val==1 || SR_ZF2_EN == 1 && osf_val == 2 || SR_ZF4_EN && osf_val == 4 ||
SR_ZF8_EN && osf_val==8)
    for iter = 1: Max_iter
      for k=1:num_sym

        if (enable_chann_esti)
          channel_user = channel_est(k,:);
          rx_sig_sym_sr = sym_cal(rx_sig, rx_sr2, k, channel_est, F, SC, Npd, Ns, GI, num_sym, enable_zp_ofdm);
        else
          channel_user = channel(k,:);
          rx_sig_sym_sr = sym_cal(rx_sig, rx_sr2, k, channel, F, SC, Npd, Ns, GI, num_sym, enable_zp_ofdm);
        end
        rx_sym2 = [rx_sig_sym_sr zeros(1, 2*N-Npd)];
        rx_sym2 = fft(rx_sig_sym_sr, ND)/sqrt(ND);

          Hn2 = fft(channel_user, ND);
          DHn2 = diag(Hn2);

          wh = GF3 .* repmat(1./Hn2, N, 1);
          rx_fdfs_zf1(:,k) = wh * rx_sym2.';

          if iter == 1
            phi=wh*DHn2*GF1;%  HD_Lideal*GF_ln;
            aa = diag(phi);
            sft = sum(real(phi).^2+imag(phi).^2, 2) - real(aa).^2;
            bb = wh*GN;
            var_bb = sum(real(bb).^2+imag(bb).^2, 2) ...
            + sum(real(bb(1:PD-GI)).^2 + imag(bb(1:PD-GI)).^2, 2) ...
            + sum(real(bb(N+1:Npd)).^2 + imag(bb(N+1:Npd)).^2, 2); % estimate reconstructure error
 %            var_bb = sum(real(bb(:, 1:Npd)).^2+imag(bb(:, 1:Npd)).^2, 2) ; %assume all noise virances are same.
get 1 column.
            be(k)=mean(qfunc(real(aa)./sqrt(var_bb*noise/2 + sft)));
          end
      end
      if iter == 1
        %save('mc_cdma_wh_n2n.mat', '-mat', 'wh');
        berc_fdfs_zf(osf_idx, snr_idx) = mean(be);
        temp_str=([sprintf('BERC_fdfs_zf%d = [', osf_val) sprintf('%g ',berc_fdfs_zf(osf_idx, :)) sprintf('];')]);
        disp(temp_str);
        fprintf(fid, '%s\n', temp_str);
      end

      rx_sr2 = rx_fdfs_zf1(:, :);

      if (sum(sum(~isfinite(rx_sr2))) ) dbstep 1; end

      [ber_fdfs_zf(iter, snr_idx, osf_idx), ber_user_fdfs_zf(:, snr_idx, iter, osf_idx), ber_code_fdfs_zf(iter, snr_idx,
osf_idx), ber_code_user_fdfs_zf(:, snr_idx, iter, osf_idx)] = ...
        err_cal(rx_fdfs_zf1(:,:), num_sym, mod_type, code_rate, N, enable_CC, msg, trellis, msg_coded);
      temp_str=([sprintf('BER_fdfs_zf%d = [', osf_val) sprintf('%g ',ber_fdfs_zf(iter, :, osf_idx)) sprintf('];')]);
      disp(temp_str);
      fprintf(fid, '%s\n', temp_str);
    end
    for iter=1: Max_iter
      temp_str=([sprintf('BER_code_fdfs_zf%d      = [', osf_val) sprintf('%g ',ber_code_fdfs_zf(iter, :, osf_idx))
sprintf('];')]);
      disp(temp_str);
```

```
            fprintf(fid, '%s\n', temp_str);
        end
      end
    end %end of osf_idx

temp_str=(sprintf('end snr=%02d at:\t%s',snr, datestr(now)));
disp(temp_str);
fprintf(fid, '%s\n', temp_str);

end %% end snr

temp_str=(sprintf('Total users: %d ', num_user)) ;
disp(temp_str);
fprintf(fid, '%s\n', temp_str);
if (near_far_factor ~= 1)
    if num_user >= 10; user = 10; else user = num_user; end;
    temp_str=(sprintf('BER for first %d users: ', user));
    disp(temp_str);
    fprintf(fid, '%s\n', temp_str);
    temp_str=(sprintf('%g ', sum(ber_user_ola(1:user,:), 1)/user));
    disp(temp_str);
    fprintf(fid, '%s\n', temp_str);
end

data_base_name = sprintf('result_zp_ofdm_%d_%d_%s.mat', num_path, path_int, date);
save(data_base_name);

temp_str=(sprintf('End sim at: \t%s', datestr(now)));
disp(temp_str);
fprintf(fid, '%s\n', temp_str);

temp_str=(sprintf('End of Simulation ==========================================')) ;
disp(temp_str);
fprintf(fid, '%s\n', temp_str);

fclose(fid);

function y = demod_1s(x);
global demodobj;
    lenx = length(x);
    y=demodulate(demodobj, x);

function y = mod_1s(x);
global modobj
    lenx = length(x);
    y=modulate(modobj, x);

function [ber, ber_user, ber_code, ber_code_user] = err_cal(x, num_sym, mod_type, code_rate, N, enable_CC, msg,
trellis, msg_coded);
    %% demodulation
global demodobj;
    dem_rx = (demodulate(demodobj, x.')).';

    %uncoded ber
    code_rate = 1;
    tt =msg_coded(:, 1:num_sym*mod_type*2) - dem_rx;
    err_bits = sum(sum(tt.^2,2));
    ber = err_bits/(N*num_sym * mod_type * 2 * code_rate);
    ber_user = sum(tt.^2,2)/(num_sym * mod_type * 2 * code_rate);
```

```
    %coded BER
    code_rate=0.5;
    tb_len = 32; %%max([floor(length(dem_rx)/2) 10]);
    for k=1:N
       dec_rx(k,:) = vitdec(dem_rx(k,:), trellis, tb_len , 'trunc', 'hard');
    end
    tt =(msg(:, 1:num_sym*mod_type) - dec_rx);
    err_bits = sum(sum(tt.^2,2));
    ber_code = err_bits/(N*num_sym * mod_type * 2 * code_rate);
    ber_code_user = sum(tt.^2,2)/(num_sym * mod_type * 2 * code_rate);

function rx_sig_sym_sr = sym_cal(rx_sig, rx_sr, k, channel, F, SC, Npd, Ns, GI, num_sym, enable_zp_ofdm, with_cp);
    if nargin < 12; with_cp=1; end
    if enable_zp_ofdm
       if k==1
          rx_sym_pre = zeros(1, Npd);
       else
          abs_rx_sr =ones(Ns-GI, 1);  %abs(rx_sr(:, k-1))*sqrt(2)/2;     % for near-far effect
          dat_cal = (mod_1s(demod_1s(rx_sr(:, k-1))).*abs_rx_sr);
          rx_sym_pre = conv([(F*SC*dat_cal).' zeros(1, GI)], channel(k-1, :));
       end
       if k==num_sym
          rx_sym_post = zeros(1, Npd);
       else
          abs_rx_sr = ones(Ns-GI, 1);     %abs(rx_sr(:, k+1))*sqrt(2)/2;     % for near-far effect
          dat_cal = (mod_1s(demod_1s(rx_sr(:, k+1))).*abs_rx_sr);
         rx_sym_post = conv([(F*SC*dat_cal).' zeros(1, GI)], channel(k+1, :));
       end
       if Npd > Ns
          rx_sig_sym_sr = [rx_sig((k-1)*Ns+1: (k-1)*Ns+Npd-Ns) - rx_sym_pre(Ns+1:Npd) ...
                rx_sig((k-1)*Ns+Npd-Ns+1 : (k-1)*Ns+Ns) ...
                rx_sig((k-1)*Ns+Ns+1: (k-1)*Ns+Npd) - rx_sym_post(1:Npd-Ns) ];
       else
          rx_sig_sym_sr = rx_sig((k-1)*Ns+1: (k-1)*Ns+Npd);
       end
    else   % CP OFDM
       F_Ns = [F(Ns-2*GI+1:Ns-GI, :); F]; % F(N-GI+1 : N)

       rx_sym_pre = zeros(1, Npd);
       rx_sym_cur = zeros(1, Npd);
       if k~=1
          abs_rx_sr =ones(Ns-GI, 1);  %abs(rx_sr(:, k-1))*sqrt(2)/2;     % for near-far effect
          dat_cal = (mod_1s(demod_1s(rx_sr(:, k-1))).*abs_rx_sr);
          rx_sym_pre(1:Npd-1) = conv([(F_Ns*SC*dat_cal).'], channel(k-1, :));
          if with_cp == 0
              dat_cal = (mod_1s(demod_1s(rx_sr(:, k))).*abs_rx_sr);
             rx_sym_cur(1:Npd-1) = conv([(F_Ns*SC*dat_cal).'], channel(k, :));
          end
       end
       rx_sym_post = zeros(1, Npd);
       if k~=num_sym
          abs_rx_sr = ones(Ns-GI, 1); %abs(rx_sr(:, k+1))*sqrt(2)/2;     % for near-far effect
          dat_cal = (mod_1s(demod_1s(rx_sr(:, k+1))).*abs_rx_sr);
          rx_sym_post = conv([(F_Ns*SC*dat_cal).'], channel(k+1, :));
       end
       if with_cp == 1
          rx_sig_sym_sr = [rx_sig((k-1)*Ns+1: (k-1)*Ns+Npd-Ns) - rx_sym_pre(Ns+1:Npd) ...
                rx_sig((k-1)*Ns+Npd-Ns+1 : (k-1)*Ns+Ns) ...
```

```
            rx_sig((k-1)*Ns+Ns+1: (k-1)*Ns+Npd) - rx_sym_post(1:Npd-Ns)];
    else
        %rx_sig_gi = rx_sig((k-1)*Ns+1: (k-1)*Ns+GI) - [rx_sym_pre(Ns+1:Npd) zeros(1, Ns+GI-Npd)];
        %          (rx_sig((k-1)*Ns+Ns-GI+1 : (k-1)*Ns+Ns) + rx_sig_gi)/2
        rx_sig_sym_sr = [rx_sig((k-1)*Ns+GI+1: (k-1)*Ns+GI+Npd-Ns) - rx_sym_cur(Ns+1:Npd) ...
            rx_sig((k-1)*Ns+GI+Npd-Ns+1 : (k-1)*Ns+Ns-GI) ...
            rx_sig((k-1)*Ns+Ns-GI+1 : (k-1)*Ns+Ns) ...
            rx_sig((k-1)*Ns+Ns+1: (k-1)*Ns+Npd) - rx_sym_post(1:Npd-Ns)];
    end
end
```